What moves wasting muscle?

Cancer cachexia; treatment, targets and translation

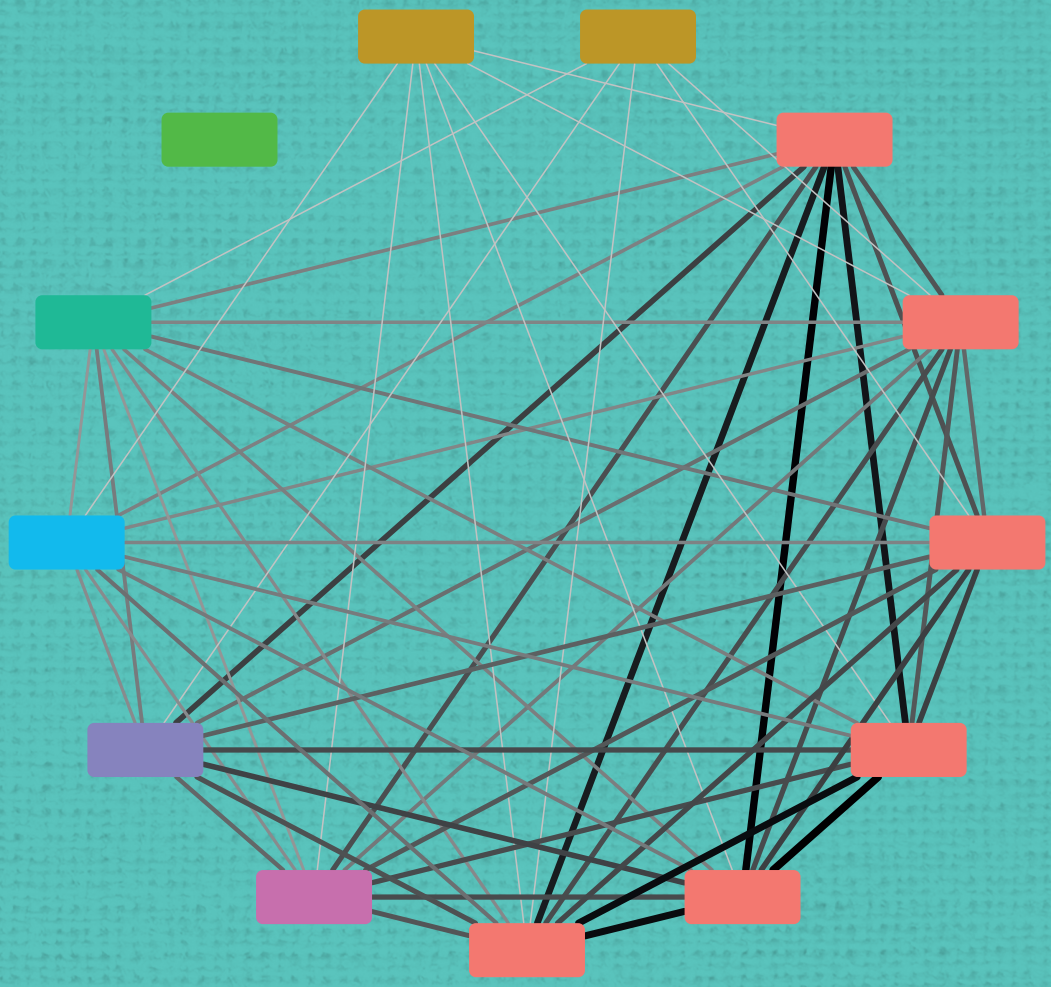

Rogier L. C. Plas

Propositions

1. Cachexia prevention and treatment should be based on functional analysis of muscle quality, not merely on muscle mass.
   (this thesis)

2. Molecular biology analysis is crucial to select the most appropriate animal model for cachexia research.
   (this thesis)

3. The principles of FAIR data sharing enabling collaboration and data integration are fundamental to advance scientific research.

4. Within 10 years, artificial intelligence will outsmart humans and will be able to cure any cancer.

5. Competition in academia is counterproductive.

6. A PhD trajectory is the perfect time to start a family.

7. The best way to save our planet is by introducing a basic income funded by CO_2 tax.

Propositions belonging to the thesis, entitled

What moves wasting muscle? Cancer cachexia; treatment, targets and translation

Rogier L.C. Plas

Wageningen, 10th December 2019

What moves wasting muscle?

Cancer cachexia; treatment, targets and translation

Rogier L. C. Plas

Thesis Committee

Promotors

Prof. Dr Renger F. Witkamp
Professor of Nutritional Biology and Health
Wageningen University and Research

Prof. Dr Ellen Kampman
Professor of Nutrition and Disease
Wageningen University and Research

Co-promotor

Dr Klaske van Norren
Associate Professor, Nutritional Biology
Wageningen University and Research

Other members

Prof. Dr A.H. Kersten, Wageningen University & Research
Prof. Dr C.M.L. van Herpen, Radboud University, Nijmegen
Dr R.C.J. Langen, Maastricht University
Dr R.T. Jaspers, VU University, Amsterdam

This research was conducted under the auspices of the Graduate School VLAG (Advanced studies in Food Technology, Agrobiotechnology, Nutrition and Health Sciences).

What moves wasting muscle?

Cancer cachexia; treatment, targets and translation

Rogier Leendert Charles Plas

Thesis

submitted in fulfilment of the requirements for the degree of doctor
at Wageningen University
by the authority of the Rector Magnificus,
Prof. Dr A.P.J. Mol,
in the presence of the
Thesis Committee appointed by the Academic Board
to be defended in public
on Tuesday 10 December 2019
at 11.00 a.m. in the Aula

Rogier L.C. Plas

What moves wasting muscle?
Cancer cachexia; treatment, targets and translation
140 Pages

PhD thesis, Wageningen University, Wageningen, the Netherlands (2019)
With references, with summary in English
ISBN: 978-94-6395-158-6
DOI: https://doi.org/10.18174/502585

Table of Contents

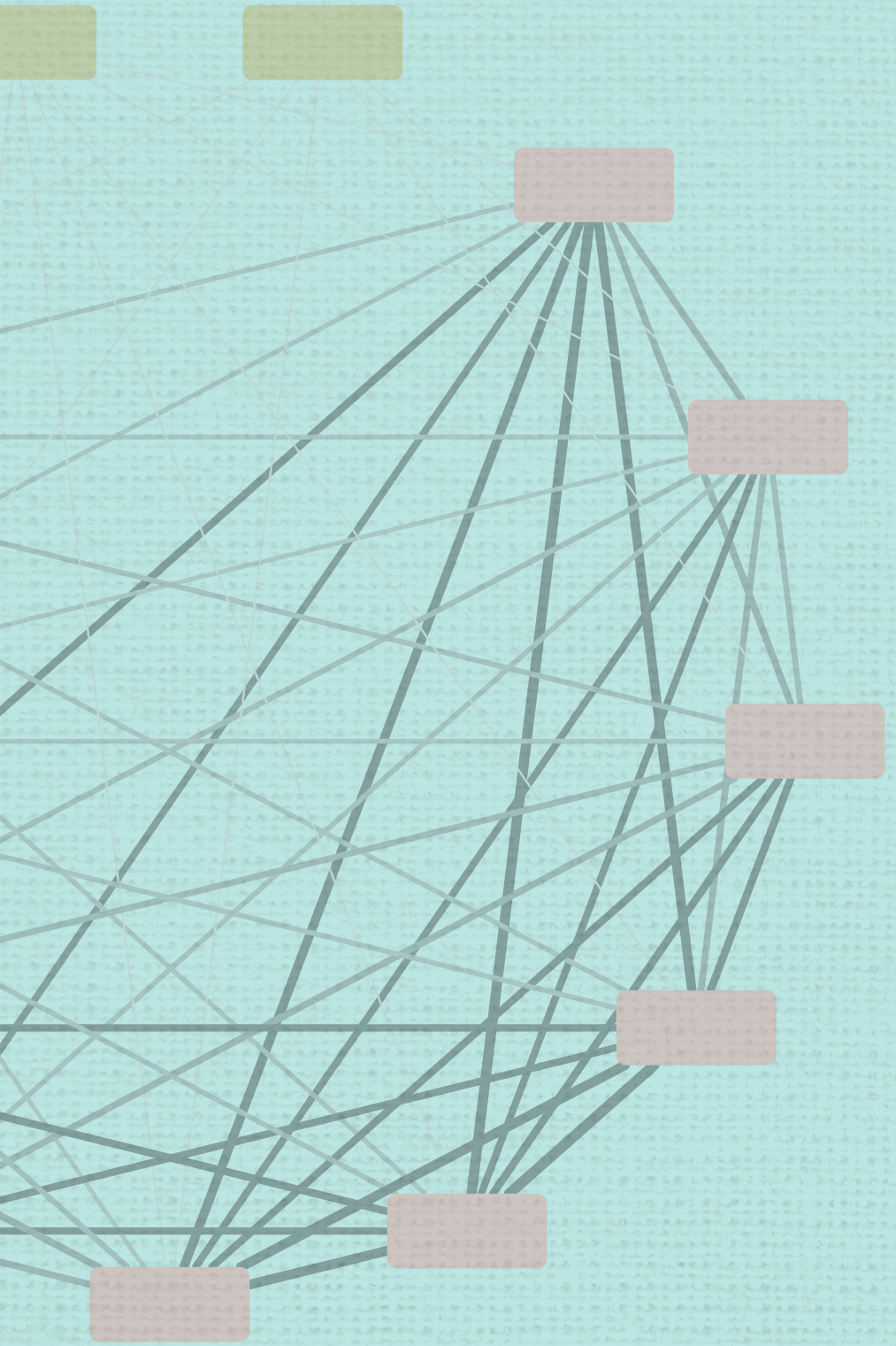

Chapter 1

General Introduction

Cancer Cachexia – definition, prevalence and consequences

Cachexia is a complex multi-factorial syndrome driven by metabolic changes with or without a reduction in food intake, including elevated energy expenditure, excess catabolism and inflammation. The term is derived from the Greek words κακός (kakós, bad) and ἕξις (héxis, condition). The condition can include weight loss, muscle atrophy, fatigue and anorexia. As a consequence, it can contribute to functional impairment, treatment-related complications, reduced quality of life and cancer-related mortality[1]. Cachexia affects multiple organs and tissues, including the central nervous system, skeletal and cardiac muscles and adipose tissue[2]. A considerable degree of cross-talk between these tissues and organs clearly complicates the disorder (figure 1.1)[2]. Therefore, cancer cachexia is defined 'multifactorial syndrome characterised by an ongoing loss of skeletal muscle mass (with or without loss of fat mass) that cannot be fully reversed by conventional nutritional support and leads to progressive functional impairment'. The internationally accepted criteria for diagnosis of cachexia are >5% weight loss or BMI<20 with >2% weight loss or sarcopenia with >2% weight loss[1].

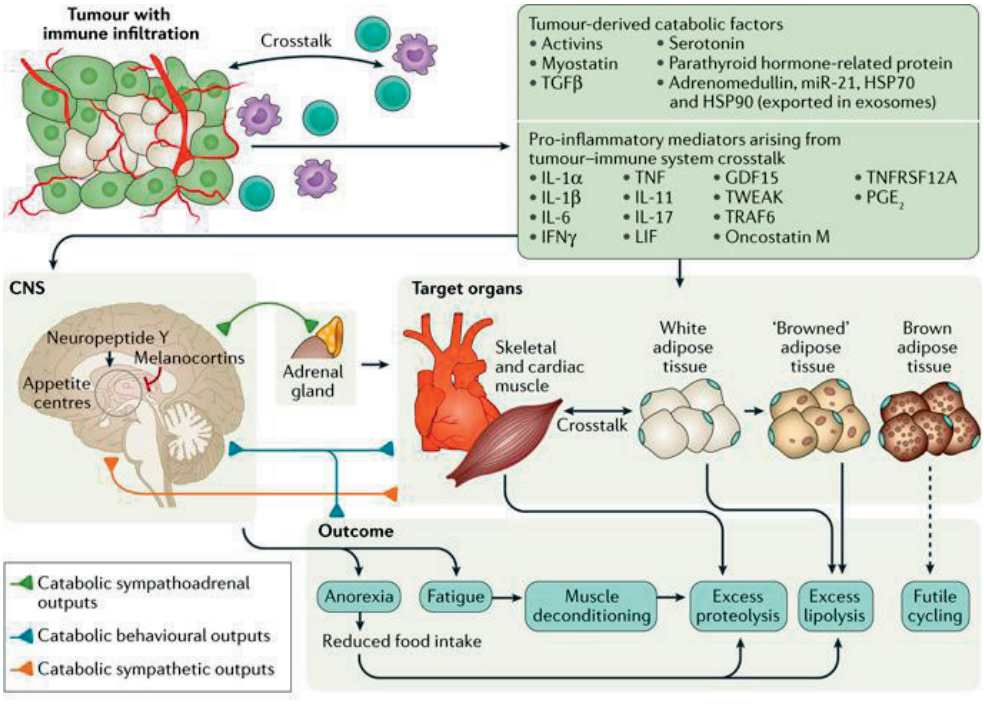

Figure 1.1 *– Crosstalk between different organs in cancer-associated cachexia. Reprinted by permission from Springer Nature: [NATURE REVIEWS DISEASE PRIMERS] (Cancer-associated cachexia, Baracos et al. Nat. Rev. Dis. Prim.* ***4,*** *17105), Copyright © (2018)[2].*

Despite its impact and contribution to the disease burden, clinicians do not always disentangle cachexia from the underlying disease as a specific syndrome. This hampers accurate estimation of its prevalence to some extent. From specific cachexia prevalence studies we do know that cachexia is more prevalent in some cancer types than in others. Prevalence appears to be highest in pancreatic cancer patients, with over 75% of patients affected, while prostate cancer patients show lowest prevalence with less than 15% of patients affected[3]. In colorectal cancer patients, prevalence is close to 50%[2]. Since having a low BMI is one of the criteria for cachexia diagnosis, the increasing prevalence of obesity in the population complicates cachexia diagnosis, in particular during the initial stages. At the same time, several studies underline the importance of timely diagnosis as this leaves more options to delay the process[1]. Surprisingly, the presence of obesity over the time-course of cancer is associated with both increased and decreased risk factors. Prior to diagnosis, a high BMI increases the risk of several cancer types, whereas post-diagnosis, a high BMI is often associated with a decreased risk of poor outcomes like mortality in cancer[4,5]. This is sometimes referred to as the obesity paradox and nicely captured by Brown et al. [2019] in figure 1.2.

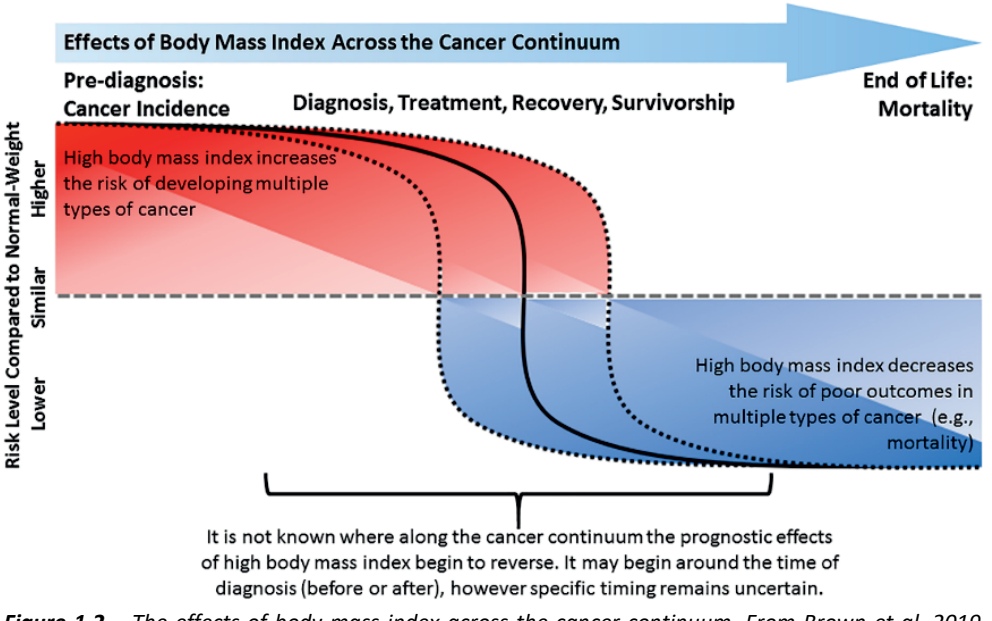

Figure 1.2 *– The effects of body mass index across the cancer continuum. From Brown et al. 2019, Copyright © 2019 Brown et al. Journal of Cachexia, Sarcopenia and Muscle published by John Wiley & Sons Ltd on behalf of the Society on Sarcopenia, Cachexia and Wasting Disorders*[4].

Medical imaging techniques like CT and MRI allow to measure skeletal muscle mass in patients with different BMI's[6–8]. Moreover, by using skeletal muscle radio density, also known as muscle attenuation, and quantification of intramuscular fat, an indication of muscle quality can be obtained[9,10]. Independently of a patient's BMI, a decreased skeletal muscle mass and a reduced muscle attenuation, as measured in a CT scan, have been associated with increased risks of mortality, complications in surgery, chemotherapy related toxicities, a reduced physical functioning and quality of life[11,12]. However, different tumour types show different associations between body composition parameters and risk factors previously mentioned, warranting repetition of studies in different cohorts with different outcome measures.

Treatment – Multimodal containing: *Nutrition, Exercise and Drugs*

The multi-organ and multi-factorial characteristics of cachexia make it a complex syndrome to prevent or treat. In line with this, effective treatment strategies are currently unavailable. General consensus exists about the need to approach the disorder from a multi-modal perspective, consisting of nutrition, exercise and pharmacological intervention components(Figure 1.3)[13]. Main targets that should be addressed are the anorexia and the metabolic disturbances that together lead to a negative energy balance[13]. For effective treatment, several elements should be present, together aiming to stimulate appetite, shift the anabolic-catabolic balance and reduce inflammation[13,14]. To stimulate appetite, different medicinal compounds are in use, including ghrelin stimulants and -analogues, corticosteroids and progestins[13]. The use of medicinal cannabinoids is also increasingly proposed to stimulate appetite in cachexia treatment[14]. To stimulate anabolism, nutrition should be high in energy and provide sufficient protein, up to 1.5 g/kg/day[15]. To reduce inflammatory activity, many specific drugs are in use targeting for instance cytokines released by- or in response to the tumour[13]. Moreover, synergistic effects of pharmaceutical and nutritional intervention also deserve more attention[16]. Specific nutrients, including n-3 polyunsaturated fatty acids, are increasingly considered of interest for cachexia treatment since these have shown to exert positive effects like reduction of inflammation while showing little to no side-effects[17]. Moreover, micronutrient abnormalities can occur due to changed food intake, disturbed metabolism, drug use and/or change in daily activity[15]. However, evidence for efficacy of specifically targeting micronutrient deficiencies or accumulation is low[15]. Last but not least, physical exercise is considered an important element of cachexia treatment, as it assists in improving muscle anabolism, reducing fatigue and systemic inflammation and improving strength. Both resistance and endurance type of exercise have been shown to potentially improve the quality of life of cachectic patients[18].

However, the frequent presence of fatigue and muscle weakness in cachectic patients sometimes makes exercise treatment difficult[19]. Therefore, easily accessible training modalities should be considered for cachectic patients.

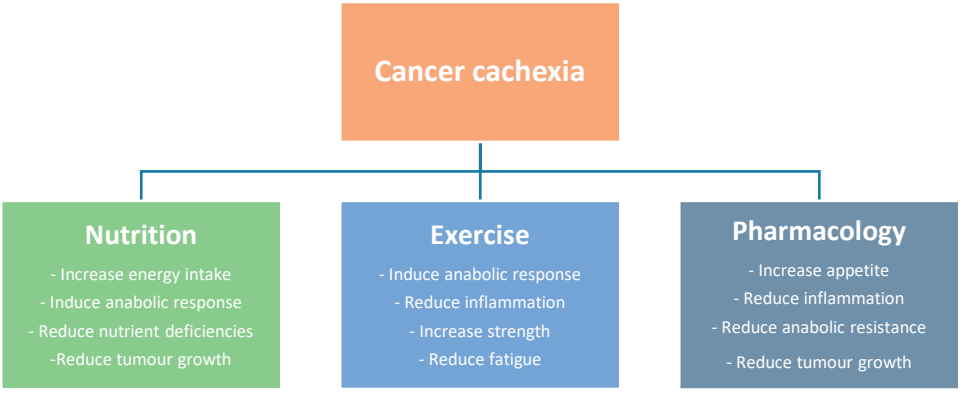

Figure 1.3 *– Overview of multi-modal treatment regime targeting different aspects of cachexia.*

Preclinical studies – can we model cachexia?

Most experimental treatments are first tested in animal models before they can be applied in human patients. To simulate human cancer cachexia, different types of animal models exist, mostly in mice and rats[20]. The traditional and most common models, e.g. C26 carcinoma, Lewis lung carcinoma or Walker 256 carcinoma, use direct injection of *in vitro* cultured tumour cells[21–23]. These are usually injected subcutaneously in the flank or intra-muscular in a mouse or rat where they grow into a solid tumour. More advanced are models induced in animals carrying genetic modifications causing spontaneous tumours[24]. These models are considered closer to the human situation since tumours occur for instance as a pancreatic adenocarcinoma[24]. Other models where tumours grow at organ specific sites use adenoviruses to induce tumour development[25]. The most recent so called xenograft models use human tumour cells injected orthotopically to develop a tumour at an organ specific site to mimic the original tumour host tissue and microenvironment. This has already been performed successfully using human leukemia[26], ovarian cancer[27], bladder cancer[28] and pancreatic cancer[29,30] cells. However, these xenograft models require immunodeficient mice which is a great limitation considering the inflammatory nature of cachexia. In all models used, validity and translation ability to human patients requires attention. To this end, analysis of their resemblance to the human situation on a molecular level can provide relevant insights.

Many studies, both preclinical and clinical, focus on gene expression and post-translational processes important in the development of cachexia. Meta-analyses and systematic reviews have been performed on differences and commonalities of molecular processes between mice and men[31,32]. These indicate that due to the complexity of the disease in which many pathways are involved, animal models can never fully mimic human cachexia. Moreover, different pathways can be involved in different types of cancer and different patients. Given these limitations, molecular pathway analysis in animal models of cancer cachexia can be instrumental to understand and study mechanisms, to generate hypotheses and to develop intervention strategies.

Thesis outline

This thesis aims to add to the current knowledge on the impact of cancer cachexia, possible treatment targets and translation of results from mouse to human in the complex condition of cancer cachexia. The effects of two important treatment modalities (nutrition and exercise) are studied in a widely used cancer cachexia mouse model. In addition, the influence of the tumour on muscle gene expression is compared between commonly used mouse models and human patients to advance insight into the possible translation of pre-clinical studies to a clinical setting.

In **chapter 2**, the association between body composition and side-effects of chemotherapy treatment is investigated in colorectal cancer patients receiving a combination of capecitabine and oxaliplatin. The amount of muscle and fat tissue was determined in a single slice of a CT scan and associated with deviations from the standard treatment protocol. In **chapter 3 and 4**, two treatment modalities for cancer cachexia are studied. In **chapter 3**, the effect of nutrition enriched with high protein, fish-oil and free leucine on calcium homeostasis in C26 tumour bearing mice was tested. **Chapter 4** describes an animal experiment where the same type of C26 tumour bearing mice are subjected to whole body vibration training. To assess the translatability of results obtained in mice experiments to the human situation, **chapter 5** contains a comparison of publically available whole genome gene expression data sets of different mice experiments and human datasets. The final **chapter 6** is a general discussion summarizing the results from this thesis and giving guidance to future research into cancer cachexia.

References

1. Fearon, K. *et al.* Definition and classification of cancer cachexia: an international consensus. *Lancet Oncol.* **12,** 489–95 (2011).
2. Baracos, V. E., Martin, L., Korc, M., Guttridge, D. C. & Fearon, K. C. H. Cancer-associated cachexia. *Nat. Rev. Dis. Prim.* **4,** 17105 (2018).
3. Baracos, V. E., Martin, L., Korc, M., Guttridge, D. C. & Fearon, K. C. H. Cancer-associated cachexia. *Nat. Rev. Dis. Prim.* **4,** 1–18 (2018).
4. Brown, J. C., Cespedes Feliciano, E. M. & Caan, B. J. The evolution of body composition in oncology-epidemiology, clinical trials, and the future of patient care: facts and numbers. *J. Cachexia. Sarcopenia Muscle* (2019). doi:10.1002/jcsm.12379
5. Martin, L. *et al.* Diagnostic criteria for the classification of cancer-associated weight loss. *J. Clin. Oncol.* **33,** 90–99 (2015).
6. Mitsiopoulos, N. *et al.* Cadaver validation of skeletal muscle measurement by magnetic resonance imaging and computerized tomography Cadaver validation of skeletal muscle measurement by magnetic resonance imaging and computerized tomography. *J. Appl. Physiol.* **85,** 115–122 (1998).
7. Mourtzakis, M. *et al.* A practical and precise approach to quantification of body composition in cancer patients using computed tomography images acquired during routine care. *Appl. Physiol. Nutr. Metab.* **33,** 997–1006 (2008).
8. Prado, C. M. M., Birdsell, L. A. & Baracos, V. E. The emerging role of computerized tomography in assessing cancer cachexia. *Curr. Opin. Support. Palliat. Care* **3,** 269–75 (2009).
9. Addison, O., Marcus, R. L., Lastayo, P. C. & Ryan, A. S. Intermuscular fat: A review of the consequences and causes. *International Journal of Endocrinology* **2014,** 1–11 (2014).
10. Goodpaster, B. H. *et al.* Attenuation of skeletal muscle and strength in the elderly: The Health ABC Study. *J. Appl. Physiol.* **90,** 2157–2165 (2001).
11. Martin, L. *et al.* Cancer cachexia in the age of obesity: Skeletal muscle depletion is a powerful prognostic factor, independent of body mass index. *J. Clin. Oncol.* **31,** 1539–1547 (2013).
12. Baracos, V. E., Mazurak, V. C. & Bhullar, A. S. Cancer cachexia is defined by an ongoing loss of skeletal muscle mass. *Ann. Palliat. Med.* **8,** 3–12 (2019).
13. Argilés, J. M., López-Soriano, F. J., Stemmler, B. & Busquets, S. Novel targeted therapies for cancer cachexia. *Biochem. J.* **474,** 2663–2678 (2017).
14. Mattox, T. W. Cancer Cachexia: Cause, Diagnosis, and Treatment. *Nutr. Clin. Pract.* **32,** 599–606 (2017).
15. Arends, J. *et al.* ESPEN guidelines on nutrition in cancer patients. *Clin. Nutr.* **36,** 11–48 (2017).
16. Witkamp, R. F. & van Norren, K. Let thy food be thy medicine….when possible. *Eur. J. Pharmacol.* **836,** 102–114 (2018).
17. Gorjao, R. *et al.* New Insights on the Regulation of Cancer Cachexia By N-3 Polyunsaturated Fatty Acids. *Pharmacol. Ther.* (2018). doi:10.1016/j.pharmthera.2018.12.001
18. Hardee, J. P., Counts, B. R. & Carson, J. A. Understanding the Role of Exercise in Cancer Cachexia Therapy. *Am. J. Lifestyle Med.* **13,** 46–60 (2017).

19. Bowen, T. S., Schuler, G. & Adams, V. Skeletal muscle wasting in cachexia and sarcopenia: molecular pathophysiology and impact of exercise training. *J. Cachexia. Sarcopenia Muscle* **6,** 197–207 (2015).
20. Ballaro, R., Costelli, P. & Penna, F. Animal models for cancer cachexia. *Curr. Opin. Support. Palliat. Care* 281–287 (2016). doi:10.1097/SPC.0000000000000233
21. Blackwell, T. A. *et al.* A Transcriptomic Analysis of the Development of Skeletal Muscle Atrophy in Cancer-Cachexia in Tumor-Bearing Mice. *Physiol. Genomics* (2018). doi:10.1152/physiolgenomics.00061.2018
22. van Dijk, M. *et al.* Improved muscle function and quality after diet intervention with leucine-enriched whey and antioxidants in antioxidant deficient aged mice. *Oncotarget* **7,** 17338–17355 (2016).
23. Schiessel, D. L. *et al.* α-Linolenic Fatty Acid Supplementation Decreases Tumor Growth and Cachexia Parameters in Walker 256 Tumor-Bearing Rats. *Nutr. Cancer* **67,** 839–846 (2015).
24. Gilabert, M. *et al.* Pancreatic cancer-induced cachexia is Jak2-dependent in mice. *J. Cell. Physiol.* **229,** 1437–1443 (2014).
25. Goncalves, M. D. *et al.* Fenofibrate prevents skeletal muscle loss in mice with lung cancer. *Proc. Natl. Acad. Sci.* **115,** E743 LP-E752 (2018).
26. Krombholz, C. F. *et al.* Long-term serial xenotransplantation of juvenile myelomonocytic leukemia recapitulates human disease in Rag2-/-γc-/- mice. *Haematologica* **101,** 597–606 (2016).
27. Pin, F. *et al.* Growth of ovarian cancer xenografts causes loss of muscle and bone mass: a new model for the study of cancer cachexia. *J. Cachexia. Sarcopenia Muscle* **9,** 685–700 (2018).
28. Chen, M. C., Chen, Y. L., Lee, C. F., Hung, C. H. & Chou, T. C. Supplementation of magnolol attenuates skeletal muscle atrophy in bladder cancer-bearing mice undergoing chemotherapy via suppression of FoxO3 activation and induction of IGF-1. *PLoS One* **10,** 1–15 (2015).
29. Shukla, S. K. *et al.* Silibinin-mediated metabolic reprogramming attenuates pancreatic cancer-induced cachexia and tumor growth. *Oncotarget* **6,** 41146–41161 (2015).
30. Delitto, D. *et al.* Human pancreatic cancer xenografts recapitulate key aspects of cancer cachexia. *Oncotarget* **8,** 1177–1189 (2016).
31. Widner, D. B., Files, D. C., Weaver, K. E. & Shiozawa, Y. Preclinical and clinical studies on cancer-associated cachexia. *Front. Biol. (Beijing).* **13,** 11–18 (2018).
32. Mueller, T. C., Bachmann, J., Prokopchuk, O., Friess, H. & Martignoni, M. E. Molecular pathways leading to loss of skeletal muscle mass in cancer cachexia - can findings from animal models be translated to humans? *BMC Cancer* **16,** 75 (2015).

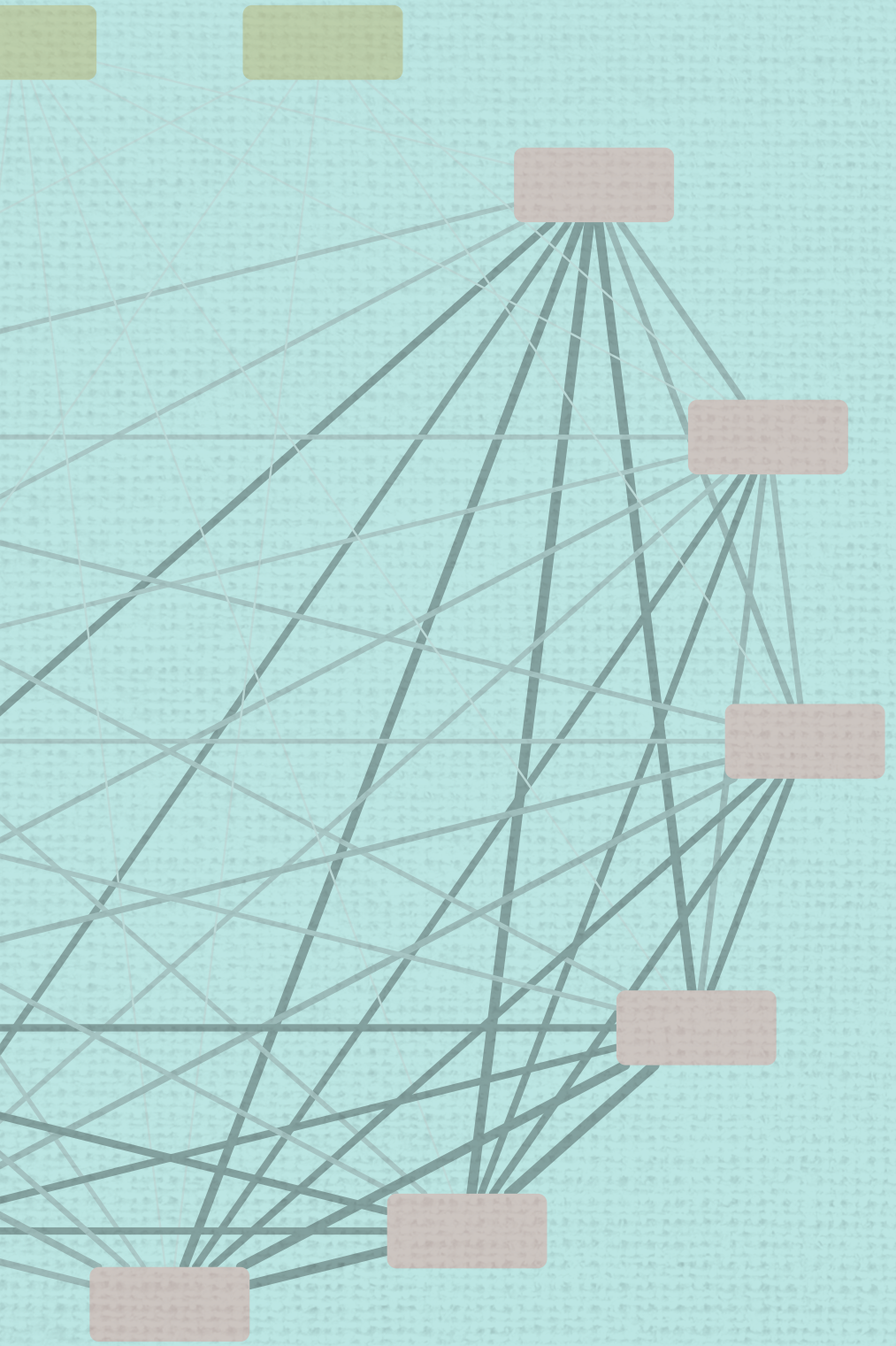

Chapter 2

Side-effects related to adjuvant CAPOX treatment for colorectal cancer are associated with intermuscular fat area, not with total skeletal muscle or fat, a retrospective observational study

Rogier L.C. Plas
Klaske van Norren
Harm van Baar
Carla van Aller
Maarten de Bakker
Nadia Botros
Renger F. Witkamp
Annebeth Haringhuizen
Ellen Kampman
Renate Winkels

Published in Journal of Cachexia, Sarcopenia Muscle - Clinical Reports (2018)
DOI: https://dx.doi.org/10.17987/jcsm-cr.v3i1.46

Abstract

Background: Chemotherapeutic treatment is regularly accompanied by side-effects. Hydrophilic chemotherapeutics such as capecitabine and oxaliplatin (CAPOX), often used in colorectal cancer treatment, predominantly accumulate in non-adipose tissues. From this we hypothesized that body composition and fat infiltration in the muscle (muscle attenuation and intermuscular-adipose-tissue [IMAT] content) are associated with chemotherapy-induced toxicities.

Methods: In this retrospective observational study, we collected data from 115 colorectal cancer patients receiving adjuvant CAPOX chemotherapy between 2006 and 2015. Information on cancer characteristics were obtained from the Netherlands Cancer Registry. Diagnostic CT scans were retrieved to assess cross-sectional areas of skeletal muscle and adipose tissue at the third lumbar vertebrae. Information on dose-limiting toxicity [DLT] and relative administered dose (as % of BSA-based-planned-dose) were retrieved from medical charts. Associations between body composition, muscle quality and chemotherapy-induced toxicities were determined using Cox-regression and linear-regression analyses.

Results: We found that DLT incidence was 90% in our cohort: 50% had their dose reduced, 30% their next cycle postponed, 4% a full treatment stop and 6% was hospitalized at their first DLT. Most common were reductions in oxaliplatin dose whilst keeping the capecitabine dose constant. Cox regression analysis indicated no association between body composition or muscle quality and DLT during the first treatment cycle or time to the first DLT. Multiple linear regression showed that higher IMAT-index and IMAT muscle percentage were associated with a lower relative administered dose of oxaliplatin.

Conclusions: In conclusion; only IMAT, not skeletal or fat area was associated with dose-limiting toxicities among these CRC patients who received CAPOX treatment.

Abbreviations

BSA	body surface area	**LBM**	lean body mass
CAPOX	capecitabine and oxaliplatin	**MA**	muscle attenuation
CRC	colorectal cancer	**SAT**	subcutaneous adipose tissue
DLT	dose limiting toxicity	**SM**	skeletal muscle
FU	fluorouracil	**SMI**	skeletal muscle index
HU	Houndsfield units	**TAT**	total adipose tissue
IMAT	intermuscular adipose tissue	**VAT**	visceral adipose tissue

Introduction

Surgical removal of the tumour is the standard treatment of colorectal cancer (CRC). Depending on the stage of cancer, this may be followed by adjuvant chemotherapy. The therapeutic window of most drugs used in adjuvant therapy is very narrow making underdosing (leading to poor antitumor effects) and overdosing (leading to toxicities) common problems[1]. Severe adverse drug reactions can necessitate dose reduction, postponement of the next treatment cycle, hospitalization or even termination of treatment.

Most CRC patients on chemotherapy receive a combination of different drugs, usually a fluorouracil (FU) based and platinum based drug (e.g. capecitabine and oxaliplatin (CAPOX)). Capecitabine is a highly water-soluble pro-drug which is enzymatically metabolized into the anti-metabolite fluorouracil (FU) in the body[2]. This conversion is performed by thymidine phosphorylase found in several tumour tissues at relatively high levels. The cytotoxic effects of FU are due to incorporation of its metabolites into the DNA and RNA or inhibition of thymidine synthesis (crucial for DNA synthesis)[2]. Oxaliplatin is a platinum coordination complex, which undergoes a series of spontaneous, non-enzymatic conversions in the body. It can form several reactive species which form complexes with amino acids, proteins, DNA and other macromolecules in plasma and tissues[3]. Platinum-DNA adducts disrupt DNA replication and transcription[4]. In clinical practice, the chemotherapeutic dose is based on a patient's body surface area (BSA, calculated with the Mosteller[5] formula: [$BSA\ (m^2) = \sqrt{height\ (cm)\ x\ weight\ (kg)/3600}$]). As can be seen from this formula, only height and weight are used as input, and body composition is not taken into account. Considering the pharmacokinetic determinants of capecitabine and oxaliplatin (i.e. water solubility and binding to amino acids, proteins and DNA), it is expected that both will distribute mainly over the lean body (fat-free) compartments of the patient. Therefore, not taking skeletal muscle mass into account, could lead to under- or overdosing.

Body composition can be determined by measuring the total surface area of muscle, visceral fat, subcutaneous fat and intermuscular fat in a single slice CT scan analysis at L3 level[6]. Commonly, muscle mass is expressed as skeletal muscle index (SMI [cm^2/m^2]; muscle surface area indexed for length)[6]. Shen et al. reported that single slice CT scan tissue areas at L3 level are a good indicator for whole body fat and muscle volume as determined by MRI[7]. Mourtzakis et al. found that CT derived muscle surface at L3 was strongly related to whole-body fat free mass measured by DXA making it possible to estimate lean body mass (LBM)[6]. Previous research suggests an association between a low muscle mass and a decreased survival rate in colorectal cancer patients[8]. Moreover, low lean body mass or muscle mass have been associated with a higher risk of chemotherapy-induced toxicities in

colorectal cancer patients[9–12]. In these studies different methods to assess lean body mass were used and for these different outcomes, different cut-off points for low lean mass were used. The study of Jung[10], for example, focussed on the cross-sectional area of the psoas muscle instead of the more common measurement of abdominal muscles at L3 level. Additionally these studies included patients with different diseases and therapeutic backgrounds. For example, the study of Barrett[9] included metastatic colorectal cancer patients, while others focussed on patients with a primary colorectal tumour[10–12]. Some studies included patients on 5-FU-based chemotherapy[10,12], while others included patients on multiple different treatment regiments[9,11]. Despite the differences in design of the studies, outcomes confirm each-other and therefore, there is an overall consensus that low SMI is prognostic of chemo-therapy induced toxicity outcomes[13]. However, most studies focus on SMI or lean body mass only, without taking the fat mass, or muscle to fat ratio into account. Moreover, no study has been performed to assess the association between low muscle mass and toxicities in CRC patients receiving adjuvant CAPOX treatment.

Besides skeletal muscle mass, fat infiltration in the muscle might influence adjuvant chemotherapy. Fat infiltration can be assessed by studying the radio density of muscle tissue (muscle attenuation), which is considered a measure of intramyocellular lipid droplets in the muscle[14], and by assessing intermuscular adipose tissue areas[6] (IMAT) using CT scans. Low muscle attenuation was found to be associated with poor prognosis in metastatic renal cell carcinoma[15]. It was also found to be associated with high-grade adverse events during immunotherapy treatment in metastatic melanoma patients[16]. Moreover, IMAT has been shown to be associated with an altered systemic inflammatory response in patients with primary operable CRC[17]. At this moment the role of low muscle attenuation or IMAT has not been studied in the context of CAPOX induced toxicities.

Therefore, the aim of the current study was to investigate the association between body composition, muscle attenuation and IMAT content and chemotherapy-induced toxicities in a retrospective cohort among colorectal cancer patients receiving adjuvant CAPOX treatment. Moreover, we aimed to get insight into the prognostic relevance of treatment toxicities for the patient. Therefore, the secondary aim of this study was to explore whether high dose reductions or an early stop of the treatment were associated with survival.

Methods

Patient characteristics/inclusion

Patients treated with chemotherapy for CRC were selected from all CRC patients treated in hospital Gelderse Vallei (Ede, The Netherlands), a peripheral mid-sized hospital, located centrally in the Netherlands, between June 2006 and July 2015. Information on cancer location, stage and treatment were obtained from the Netherlands Cancer Registry, data on chemotherapy toxicity and survival were extracted from medical records. Inclusion criteria were: adjuvant treatment with CAPOX chemotherapy; availability of abdominal CT scan made within 100 days before start of chemotherapy treatment; and availability of toxicity data. Patients were excluded from the study if their treatment was stopped prematurely without experiencing toxicities or if the patient did not receive the standard chemotherapeutic dose due to a dihydropyrimidine dehydrogenase deficiency (a key enzyme involved in the metabolism of capacetabine) (n=8) or comorbidities. A large part of the patients was excluded from the cohort as they did not receive chemotherapy treatment because of the stage of their cancer (n = 1351, 77%). Of the 410 CRC patients who received CAPOX treatment, 168 were excluded because they had a palliative or neo-adjuvant treatment regime, 106 were excluded for missing data, 13 for an early stop of treatment without toxicities and 8 for deviating treatment without toxicities. As a result, we included 115 patients in this retrospective study (figure 2.1).

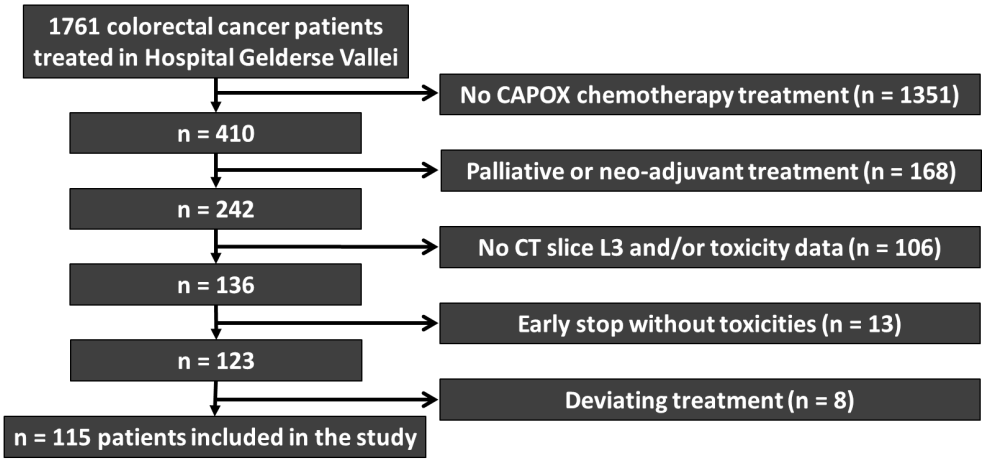

Figure 2.1 – *Flow-chart of colorectal cancer patients, from hospital Gelderse Vallei (Ede, The Netherlands), included in this retrospective study.*

Treatment protocol

The CAPOX dose that was administered was based on the BSA calculated with the Mosteller formula[5]. The treatment protocol consisted of eight cycles of 21 days. On day 1, patients were planned to receive 130 mg/m^2 of oxaliplatin. On day 1 to day 14, patients were planned to receive 1000 mg/m^2 of capecitabine twice daily, and from day 15 to 21 patients had a resting period.

Body composition

Cross-sectional areas of skeletal muscle and fat tissue were determined in single slice CT scans (made for diagnostic purposes) at the third lumbar vertebra (L3) as described by others[6]. Image analysis software was used for the analysis of the CT slices (SliceOmatic version 5.0, Tomovision). Different tissue areas were characterised based on Hounsfield units (HU)[6]; HU of -190 to -30 represent intermuscular adipose tissue (IMAT) and subcutaneous adipose tissue (SAT), -150 to -50 visceral adipose tissue (VAT), and -29 to 150 skeletal muscle tissue (SM). Muscle attenuation (MA) was determined by taking the mean HU in the entire skeletal muscle area at the third lumbar vertebra. Total adipose tissue (TAT) was defined as IMAT + VAT + SAT. SM and IMAT were indexed by height (in m^2) and named skeletal muscle index (SMI) and IMAT index, respectively. Furthermore, the following relative values were calculated: Muscle percentage (SM area as a percentage of total area of SM + TAT at L3 level) and IMAT muscle percentage (IMAT area as a percentage of muscle + IMAT area at L3 level). BSA divided by the LBM was used as measure for the chemotherapeutic dose per kg LBM at the start of the treatment. Whole lean body mass was determined using the following formula[6]: $LBM\ (kg) = (SM \times 0.3) + 6.06$. Sarcopenia was determined using sex and BMI specific cut-offs which have been shown to be significantly negatively associated with mortality in patients with solid tumours determined by Martin et al. (i.e. 41 cm^2/m^2 for women, 43 cm^2/m^2 for men with a BMI < 25 kg/m^2 and 53 cm^2/m^2 for men with a BMI ≥ 25 kg/m^2)[18]. CT-scans were analysed by 3 different researchers who were trained to quantify muscle mass, intermuscular adipose tissue, visceral adipose tissue and subcutaneous adipose tissue at the L3 level. The inter-observer variation was 1.43% for SM, 6.15% for IMAT, 4.74% for VAT and 2.82% for SAT.

Chemotherapy-induced toxicities and survival

Side-effects and survival data were extracted from patients' medical records. Administered dose, deviation from treatment cycle and chemotherapeutic side effects were scored for each treatment cycle. Toxicities per chemotherapy cycle were defined as dose limiting toxicity (DLT) if there was: 1) dose reduction, 2) cycle delay, 3) cycle stop or 4)

hospitalization because of side-effects. From these data we defined our output parameters: 1) First cycle DLT, which is a DLT during/resulting from the first cycle of chemotherapy 2) time to first DLT (expressed in cycles) and 3) the total relative administered dose of oxaliplatin and capecitabine (total administered dose as % of the BSA-based planned dose). A low total relative administered dose implies that the patient experienced more frequent, or more severe toxicities compared to a high relative administered dose. Survival was defined as time between start of chemotherapy treatment and date of death. Patients with no record of death were censored on October 20, 2016.

Data-analysis

Prevalence ratios were calculated to assess the association between body composition and DLT (yes/no) using the Cox regression model with time as a fixed variable. Hazard ratios were calculated to assess the association between body composition and the time to the first dose-limiting toxicity using the Cox regression model with time expressed as the number of treatment cycles. Regression coefficients were calculated to assess the association between body composition and relative administered dose using a multiple linear regression model. All body composition parameters were assessed as continuous variables. In addition, BMI and sarcopenia were included as categorical variables. A separate model was constructed for each body composition parameter. Next to the separate models, we also made a multivariate model containing all CT-scan derived measures.

To explore the effect of dose reduction on survival, hazard ratios were calculated for patients receiving less than the median relative administered dose vs those receiving the median dose or more, using Cox regression.

For all analyses, the factors age and gender were added to each model-based on associations found in literature[19]. Moreover, factors BMI and tumour stage were tested for possible confounding.

Results

Patients' characteristics and toxicity incidence

Slightly more men than women were included in the study (54%) (Table 2.1). The mean age at CRC diagnosis was 61.9 years (± 9.4 SD). The majority of the patients were diagnosed with tumour stage III (84%). There were no patients with tumour stage I receiving chemotherapy; tumour stage II and IV were present in 9% and 7% of the study population, respectively. More than half of the patients were overweight [BMI 25-29] or obese [BMI>30] (57%) at diagnosis.

Patient Characteristics	Total	DLT cycle 1	No DLT cycle 1
Number of patients	**115**	**26**	**89**
Age	**61.9 ± 9.4**	**64.4 ± 9.4**	**61.2 ± 9.4**
Sex			
Male	**62 [54]**	**14 [54]**	**48 [54]**
Female	**53 [46]**	**12 [46]**	**41 [46]**
Tumour stage (n [%])			
Stage I	**0 [0]**	**0 [0]**	**0 [0]**
Stage II	**10 [9]**	**3 [12]**	**7 [8]**
Stage III	**97 [84]**	**22 [85]**	**75 [84]**
Stage IV	**8 [7]**	**1 [4]**	**7 [8]**
Cancer site (n [%])			
Colon	**105 [91]**	**25 [96]**	**80 [90]**
Rectum	**10 [9]**	**1 [4]**	**9 [10]**
BMI (n [%])			
Underweight	**2 [2]**	**0 [0]**	**2 [2]**
Normal weight	**48 [42]**	**11 [42.3]**	**37 [42]**
Overweight	**44 [38]**	**11 [42.3]**	**33 [37]**
Obese	**21 [18]**	**4 [15.4]**	**17 [19]**
Sarcopenia (n [%])			
Non Sarcopenic	**75 [65]**	**19 [73]**	**56 [63]**
Sarcopenic	**40 [35]**	**7 [27]**	**33 [37]**
Sarcopenic Overweight (n [%])			
Non Sarcopenic/Non Overweight	**30 [26]**	**8 [31]**	**22 [25]**
Non Sarcopenic/Overweight	**45 [39]**	**11 [42]**	**34 [38]**
Sarcopenic/Non Overweight	**20 [17]**	**3 [12]**	**17 [19]**
Sarcopenic/Overweight	**20 [17]**	**4 [15]**	**16 [18]**
Skeletal Muscle Index (cm^2/m^2)	**47.3 ± 7.8**	**47.9 ± 7.0**	**47.1 ± 8.1**
TAT Surface (VAT+SAT+IMAT, cm^2)	**353.8 ± 171.2**	**357.7 ± 173.4**	**352.6 ± 171.5**
Muscle Percentage (%)	**32.7 ± 14.4**	**33.3 ± 16.6**	**32.5 ± 13.8**
BSA / LBM (cm^2/kg)	**399.9 ± 62.3**	**392.8 ± 54.3**	**402.0 ± 64.6**
Muscle Attenuation (HU)	**35.0 ± 7.8**	**34.2 ± 8.3**	**35.3 ± 7.7**
IMAT Index (cm^2/m^2)	**4.9 ± 3.4**	**5.7 ± 4.1**	**4.7 ± 3.2**
IMAT Muscle Percentage (%)	**9.2 ± 5.5**	**10.3 ± 5.8**	**8.9 ± 5.4**

Table 2.1 *– Patient characteristics*

DLT incidence was high with 90% of all patients experiencing a DLT (figure 2.2 A). Half of the patients (50%) had their dose reduced, 30% had their next cycle postponed, 4% had a full treatment stop and 6% was hospitalized because of side-effects at their first DLT. The relative administered dose of capecitabine and oxaliplatin varied greatly between patients (figure 2.2 B). Most commonly, oxaliplatin was reduced, less often capecitabine. In some instances, capecitabine dosis was even increased slightly leading to relative administered doses of > 100%. However, it has to be noted that these relative doses cannot be seen as completely independent outcome measures since a full stop leads to a low relative administered dose of both drugs. Unfortunately, we were not able to determine whether such a stop was caused by toxicities by either one or both of the drugs. In the analyses of relative administered dose, we therefore only focussed on oxaliplatin. In none of the performed analyses, BMI or tumour stage affected the outcome of the analysis, therefore all models were only adjusted for sex and age.

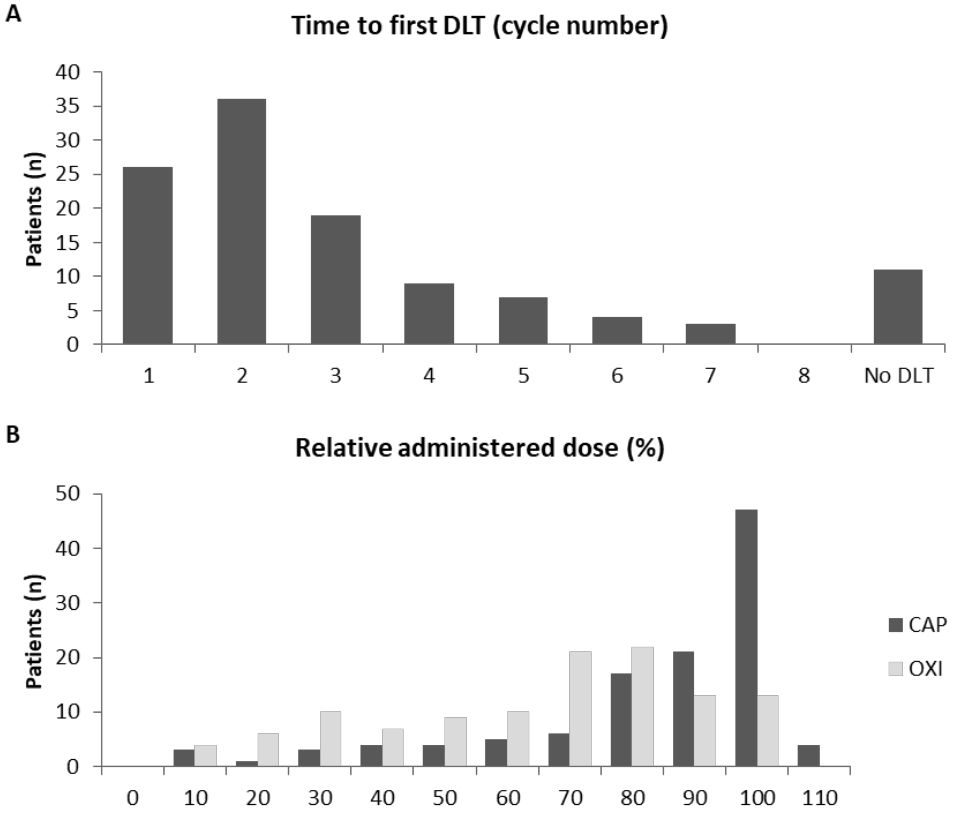

Figure 2.2 *– [**A**] number of people experiencing first DLT per cycle. [**B**] Number of people receiving relative administered dose rounded to the closest 10th percent point (as a percentage of BSA based planned dose).*

Dose limiting toxicities in the first cycle of chemotherapy, and time to first DLT

None of the indicators of body composition were associated with DLT during the first cycle of chemotherapy, as indicated by the prevalence ratios in table 2.2. Moreover, the hazard ratios in table 2.2 show that none of the indicators of body composition was associated with time to first DLT. These indicators included BMI, the body composition parameters SMI and muscle percentage, the muscle fat infiltration parameters MA and IMAT and the dose per lean body mass.

Dose limiting toxicities expressed as the relative administered dose

Muscle percentage, IMAT index and IMAT muscle percentage were log transformed to comply with assumptions of the regression analysis. Regression coefficients indicated that a higher IMAT index was associated with a lower relative administered dose of oxaliplatin both in the model with only the IMAT index, as well as in the multivariate model containing all CT-scan derived body composition variables. A higher IMAT muscle percentage was associated with a lower relative administered dose of oxaliplatin. No associations were observed for any of the other parameters and relative administered dose of oxaliplatin (table 2.3).

For visualisation of the results, two heat-map plots were produced. The first one shows the relative administered dose of oxaliplatin plotted against BMI and SMI. The figure shows scattered data indicating no relation between plotted parameters (figure 2.3 A). The second plot shows the relative administered dose plotted against BMI and IMAT muscle percentage, showing a clear pattern over the IMAT-SM percentage axis illustrating the association found with the multiple linear regression (figure 2.3 B).

Dose reductions and survival

Two groups were made for the survival analysis; patients receiving equal or more than the median relative administered dose (71.7%) of oxaliplatin (n=60) and patients receiving less than the median administered dose (n=55). In these subgroups, survival was 76.7% (n=46) and 74.5% (n=41), respectively. Mean follow up time was 58.0 months (± 27.2 SD) and 48.7 months (± 28.8 SD), respectively. No association was found for a dose below median versus a dose equal or above median and overall survival (adjusted HR 1.08, 95% CI: 0.48 - 2.40).

	First Cycle DLT			Time to first DLT		
Variable	PR	(95% CI)		HR	(95% CI)	
BMI	1.00	0.91	1.10	1.01	0.97	1.06
Skeletal Muscle Index (cm^2/m^2)	1.02	0.96	1.08	1.01	0.98	1.04
TAT Surface (VAT+SAT+IMAT, cm^2)	1.00	1.00	1.00	1.00	1.00	1.00
Muscle Percentage (%)	1.01	0.98	1.04	1.00	0.98	1.01
BSA / LBM (cm^2/kg)	1.00	0.99	1.00	1.00	1.00	1.00
Muscle Attenuation (HU)	1.00	0.95	1.06	1.00	0.97	1.02
IMAT Index (cm^2/m^2)	1.03	0.93	1.15	1.04	0.98	1.10
IMAT Muscle Percentage (%)	1.02	0.95	1.10	1.03	0.99	1.07
BMI						
Underweight	*n<1*			0.35	0.05	2.56
Normal weight	*ref*			*ref*		
Overweight	1.17	0.50	2.74	0.89	0.57	1.40
Obese	0.85	0.27	2.72	0.97	0.57	1.67
Sarcopenia						
No	*ref*			*ref*		
Yes	0.67	0.28	1.60	1.14	0.76	1.72
Sarcopenic Overweight (n [%])						
Non Sarcopenic/Non Overweight	*ref*			*ref*		
Non Sarcopenic/Overweight	0.91	0.34	2.44	0.93	0.54	1.61
Sarcopenic/Non Overweight	0.52	0.13	2.02	1.07	0.57	2.02
Sarcopenic/Overweight	0.78	0.23	2.60	1.12	0.60	2.08

Multivariate	TOTAL			TOTAL		
Variable	PR	(95% CI)		HR	(95% CI)	
Skeletal Muscle Index (cm^2/m^2)	1.01	0.95	1.08	1.00	0.97	1.03
VAT Surface (cm^2)	1.00	1.00	1.01	1.00	1.00	1.00
SAT Surface (cm^2)	1.00	0.99	1.01	1.00	1.00	1.00
Muscle Attenuation (HU)	1.05	0.91	1.22	1.05	0.96	1.14
IMAT Index (cm^2/m^2)	0.75	0.23	2.41	1.01	0.98	1.04

Table 2.2 *– Association between body composition parameters and first cycle DLT or time to first DLT. Prevalence and Hazards ratios (including 95% CI) determined using COX Proportional Hazards modelling, adjusting for sex and age.*

	Relative Administered Dose OXI		
Variable	B	(95% CI)	
BMI	-0.38	-1.43	0.67
Skeletal Muscle Index (cm^2/m^2)	-0.18	-0.84	0.48
TAT Surface (VAT+SAT+IMAT, cm^2)	-0.02	-0.04	0.01
Muscle Percentage (%)⁺	12.77	-15.95	41.49
BSA / LBM (cm^2/kg)	0.04	-0.06	0.14
Muscle Attenuation (HU)	0.11	-0.51	0.73
IMAT Index (cm^2/m^2)⁺	*-17.04**	*-32.62*	*-1.45*
IMAT Muscle Percentage (%)⁺	*-17.92**	*-35.64*	*-0.21*
BMI			
Underweight	22.08	-11.34	55.49
Normal weight	*ref.*		
Overweight	1.51	-8.25	11.28
Obese	4.26	-7.96	16.49
Sarcopenia			
No	*ref.*		
Yes	1.19	-7.87	10.26
Sarcopenic Overweight (n [%])			
Non Sarcopenic/Non Overweight	*ref.*		
Non Sarcopenic/Overweight	3.99	-7.49	15.47
Sarcopenic/Non Overweight	4.80	-9.01	18.68
Sarcopenic/Overweight	2.44	-11.05	15.92
Multivariate Variable			
Skeletal Muscle Index (cm^2/m^2)	0.11	-0.60	0.82
VAT Surface (cm^2)	-0.01	-0.08	0.05
SAT Surface (cm^2)	0.02	-0.04	0.09
Muscle Attenuation (HU)	-0.64	-1.48	0.20
IMAT Index (cm^2/m^2)⁺	*-30.89**	*-56.65*	*-5.14*

Table 2.3 *– Association between body composition parameters and the relative administered dose of oxaliplatin. Beta's (including 95% CI) determined using the Multiple Linear Regression model. All betas were adjusted for sex and age. ⁺Data is log-transformed *p<0.05*

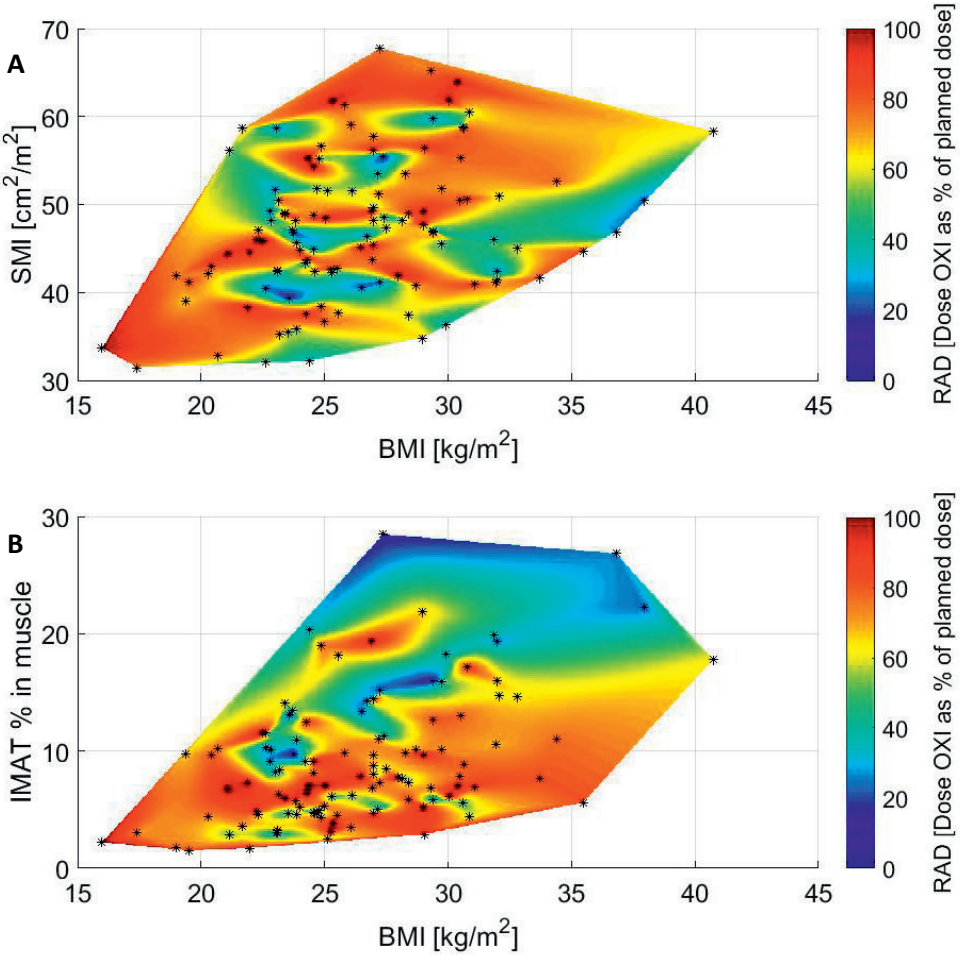

Figure 2.3 *– heat map indicating the relative administered dose plotted against [**A]** SMI/BMI and [**B**. IMAT-SM Percentage/BMI. Asterisks indicate patients. Figure **A** shows a clearly scattered pattern whereas in figure **B** a gradient can be seen on the y-axis.*

Discussion

In this study we found no association between either low skeletal muscle mass, or relatively low skeletal muscle mass (relative to amount of fat) and CAPOX-induced toxicities. However, we found that during the course of their treatment program, patients with more intermuscular fat received a significantly lower percentage of the planned dose of oxaliplatin. This dose was planned based on the BSA of the patient at the start of treatment. This means that in our study, patients with more IMAT were likely to experience more often dose reduction or curtailment of their chemotherapy.

In this study, the incidence of toxicity was very high: 90% of patients apparently experienced serious side-effects. We found no associations between body composition and chemotherapy-induced toxicities during the first cycle of the treatment or the time to first DLT. Often, oxaliplatin dose was reduced whilst maintaining the capecitabine dose constant. To get an indication of the consequence of dose reductions or early stop of the treatment, we studied the association between the relative administered dose of oxaliplatin and survival rate. No significant association between receiving a dose lower than the median relative administered dose and survival rate was observed.

Unlike previous studies, we did not find an association between low skeletal muscle mass and chemotherapy-induced toxicities in colorectal cancer patients[9–12]. There are three factors that may explain this discrepancy; 1) treatment protocol, 2) measurement/analysis methods and 3) population. Regarding 1), Treatment protocol; patients in this retrospective study received a combination of capecitabine and oxaliplatin, whereas some previously published studies applied other chemotherapeutics [10,12] or included multiple treatment strategies[9,11]. Possibly, the association between SMI and chemotherapy-induced toxicities is stronger in these other chemotherapeutic treatments than in the CAPOX treatment used in our study. With respect to 2), measurement/analysis methods: we abstracted toxicity data from medical records; in these records severity of side-effects was not systematically scored. As we did not have this information, we decided to focus on the information that was systematically recorded in the medical records including dose reduction, postponement or termination of treatment or hospitalization information. In our study, toxicity incidence was very high (91%) compared to studies (max 61.3%[12]) that did find an association between muscle mass and chemotherapy-induced toxicities in colorectal cancer patients. Possibly this is due to our way of toxicity recording; we recorded all DLT's where in other studies mild toxicities leading to small dose reductions or postponements might not be included. Furthermore, for determining muscle mass, not all studies use the same variable. In some studies, only the psoas muscle[10] was measured not taking the full muscle surface into account. Moreover, many studies use sarcopenia cut-

offs to compare sarcopenic with non sarcopenic patients. Therefore, to make it possible to compare our results to these studies we used cut-off points available in literature[18]. The cut-off values used are determined in a Northern American population and might not be adequate for a Dutch population. However, patient characteristics in this study (age, BMI and body composition parameters) are similar to those in our study making this the most reliable cut-offs available. Another factor is that not all previous studies have used the same covariates to correct for potential confounding. Some use no correction for confounding, whereas others correct for multiple factors including tumour stage or obesity. We adjusted for sex and age in all our models based on previous findings published in literature[19]. Nevertheless, adjustment for additional confounding did not importantly affect our regression estimates. Regarding 3) study population; in our study, we included only patients receiving adjuvant chemotherapy who were predominantly classified as stage III colorectal cancer patients. This deviates from some other studies where predominantly[11] or only[9] stage IV colorectal cancer patients were included. Maybe the associations across different cancer stages differ. It is likely that patients classified stage IV will more often have cachexia where a decreased muscle mass is often accompanied by a general poor condition. Moreover, populations used in cited studies are Northern American, French and South Korean. Populations may differ in their physical fitness resulting from differences in lifestyle habits. Fitness may also be reflected by IMAT but this parameter was not commonly reported in earlier studies. To conclude, there are some differences between our study and the cited studies that might explain why we did not find an association between muscle mass and toxicities in our population. However, the exact cause for this difference in findings remains unclear.

Low muscle attenuation is associated with excess fat deposition in the tissue[20]. This has been shown to be independently associated with poor survival rates in a large cohort of patients with solid tumours of the lung and gastrointestinal tract[18]. However, in our study we did not find an association of muscle attenuation with chemotherapy-induced toxicities. To the best of our knowledge the association between IMAT and chemotherapy-induced toxicities has not been described earlier. In literature, IMAT is associated with adverse clinical outcomes like insulin resistance, loss of muscle strength and mobility dysfunction[21]. Possibly, the explanation for our finding that patients with more IMAT are prone to more frequent/more severe toxicities might be that having a high IMAT content is a generic marker for poor health indicative for patients who are less able to cope with the impact of the treatment.

In our study we had limited statistical power to study the association between dose-limitations and survival, and we did not find indications that dose-limitation was associated with higher mortality. Previous research suggests that early discontinuation of

FU-based chemotherapy is associated with increased mortality rate for stage III colorectal cancer patients (n=3,733)[22]. Another study indicates a trend that discontinuation of CAPOX treatment in an elderly colorectal cancer population is associated to lower crude 3-year recurrence-free and overall survival (n=191)[23]. However, these studies are not directly comparable to our study since we used a different measure for chemotherapy compliance as mentioned earlier.

Our study is the first to examine the association between the relative muscle mass (relative to fat mass) and fat infiltration in the muscle and CAPOX induced toxicities in colorectal cancer patients. This was done in a retrospective study with a homogeneous patient group. We only included colorectal cancer patients with the same treatment policy and dosing strategy. Due to the retrospective nature of the study, we had to work with data that were available in medical records. Although toxicity data were not scored in a standardized way in those records, the toxicity parameters used in our study (DLT and relative administered dose) are based on objective data (dosing, treatment timing and hospitalization), which will not be affected by the way they are reported. Strength of our outcome parameters is that these indicate several different aspects of the toxicities experienced by patients; 1) toxicity in the first cycle 2) the number of toxicities experienced at different points in the treatment (time to first DLT) and 3) the severity of toxicities (relative administered dose). Body composition was determined using L3 single slice CT scan analysis. CT scans are considered as the golden standard for body composition analysis, and L3 skeletal muscle tissue and total adipose tissue are strongly correlated with respectively LBM and total fat mass[7]. Moreover, a study on cadaver material showed a highly significant correlation between the amount of IMAT measured by CT scan and the actual amount of IMAT[24].

In conclusion, we could not confirm our hypothesis that relatively low skeletal muscle mass (relative to amount of fat) is associated with chemotherapy-induced toxicities in a retrospective study of CRC patients receiving adjuvant CAPOX treatment. At the same time, we did find that patients with more IMAT were more likely to receive a lower relative administered dose of oxaliplatin. In exploratory analyses, receiving a lower relative administered dose however was not associated with a decreased survival rate. If these results are confirmed in prospective studies, measurement of IMAT may emerge as a diagnostic tool indicating patients who are at increased risk of toxicities.

Acknowledgements

We thank L. Homans from the hospital Gelderse Vallei for her help in getting access to anonymized patient data. This study was in part supported by Nutricia Research.

References

1. Felici, A., Verweij, J. & Sparreboom, A. Dosing strategies for anticancer drugs: The good, the bad and body-surface area. *Eur. J. Cancer* **38,** 1677–1684 (2002).
2. Walko, C. M. & Lindley, C. Capecitabine: A review. *Clinical Therapeutics* **27,** 23–44 (2005).
3. Graham, M. A. *et al.* Clinical pharmacokinetics of oxaliplatin: A critical review. *Clin. Cancer Res.* **6,** 1205–1218 (2000).
4. Graham, J., Muhsin, M. & Kirkpatrick, P. Fresh from the pipeline: Oxaliplatin. *Nat. Rev. Drug Discov.* **3,** 11–12 (2004).
5. Mosteller. R.D. Simplified Calculation of Body Suface Area. *N. Engl. J. Med.* **317,** 1098 (1987).
6. Mourtzakis, M. *et al.* A practical and precise approach to quantification of body composition in cancer patients using computed tomography images acquired during routine care. *Appl. Physiol. Nutr. Metab.* **33,** 997–1006 (2008).
7. Shen, W. *et al.* Total body skeletal muscle and adipose tissue volumes: estimation from a single abdominal cross-sectional image. *J. Appl. Physiol.* **97,** 2333–8 (2004).
8. Shachar, S. S., Williams, G. R., Muss, H. B. & Nishijima, T. F. Prognostic value of sarcopenia in adults with solid tumours: A meta-analysis and systematic review. *Eur. J. Cancer* **57,** 58–67 (2016).
9. Barret, M. *et al.* Sarcopenia is linked to treatment toxicity in patients with metastatic colorectal cancer. *Nutr. Cancer* **66,** 583–9 (2014).
10. Jung, H.-W. *et al.* Effect of muscle mass on toxicity and survival in patients with colon cancer undergoing adjuvant chemotherapy. *Support. Care Cancer* **23,** 687–694 (2015).
11. Ali, R. *et al.* Lean body mass as an independent determinant of dose-limiting toxicity and neuropathy in patients with colon cancer treated with FOLFOX regimens. *Cancer Med.* **5,** 607–16 (2016).
12. Prado, C. M. M. *et al.* Body composition as an independent determinant of 5-fluorouracil-based chemotherapy toxicity. *Clin. Cancer Res.* **13,** 3264–3268 (2007).
13. Hopkins, J. J. & Sawyer, M. B. Expert Review of Clinical Pharmacology A Review of Body Composition and Pharmacokinetics in Oncology A Review of Body Composition and Pharmacokinetics in Oncology. *Expert Rev. Clin. Pharmacol. ISSN* **2433,** 1–10 (2017).
14. Aubrey, J. *et al.* Measurement of skeletal muscle radiation attenuation and basis of its biological variation. *Acta Physiol.* **210,** 489–497 (2014).
15. Antoun, S. *et al.* Skeletal muscle density predicts prognosis in patients with metastatic renal cell carcinoma treated with targeted therapies. *Cancer* **119,** 3377–3384 (2013).
16. Daly, L. E. *et al.* The impact of body composition parameters on ipilimumab toxicity and survival in patients with metastatic melanoma. *Br. J. Cancer* **116,** 310–317 (2017).
17. Malietzis, G. *et al.* Low Muscularity and Myosteatosis Is Related to the Host Systemic Inflammatory Response in Patients Undergoing Surgery for Colorectal Cancer. *Ann. Surg.* **263,** 320–325 (2015).
18. Martin, L. *et al.* Cancer cachexia in the age of obesity: Skeletal muscle depletion is a

powerful prognostic factor, independent of body mass index. *J. Clin. Oncol.* **31,** 1539–1547 (2013).

19. Stein, B. N. *et al.* Age and sex are independent predictors of 5???fluorouracil toxicity. Analysis of a large scale phase III trial. *Cancer* **75,** 11–17 (1995).
20. Goodpaster, B. H., Kelley, D. E., Thaete, F. L., He, J. & Ross, R. Skeletal muscle attenuation determined by computed tomography is associated with skeletal muscle lipid content. *J. Appl. Physiol.* **89,** 104–110 (2000).
21. Addison, O., Marcus, R. L., Lastayo, P. C. & Ryan, A. S. Intermuscular fat: A review of the consequences and causes. *International Journal of Endocrinology* **2014,** 1–11 (2014).
22. Neugut, A. I. *et al.* Duration of adjuvant chemotherapy for colon cancer and survival among the elderly. *J. Clin. Oncol.* **24,** 2368–2375 (2006).
23. van Erning, F. N. *et al.* Recurrence-free and overall survival among elderly stage III colon cancer patients treated with CAPOX or capecitabine monotherapy. *Int. J. Cancer* **140,** 224–233 (2017).
24. Mitsiopoulos, N. *et al.* Cadaver validation of skeletal muscle measurement by magnetic resonance imaging and computerized tomography Cadaver validation of skeletal muscle measurement by magnetic resonance imaging and computerized tomography. *J. Appl. Physiol.* **85,** 115–122 (1998).

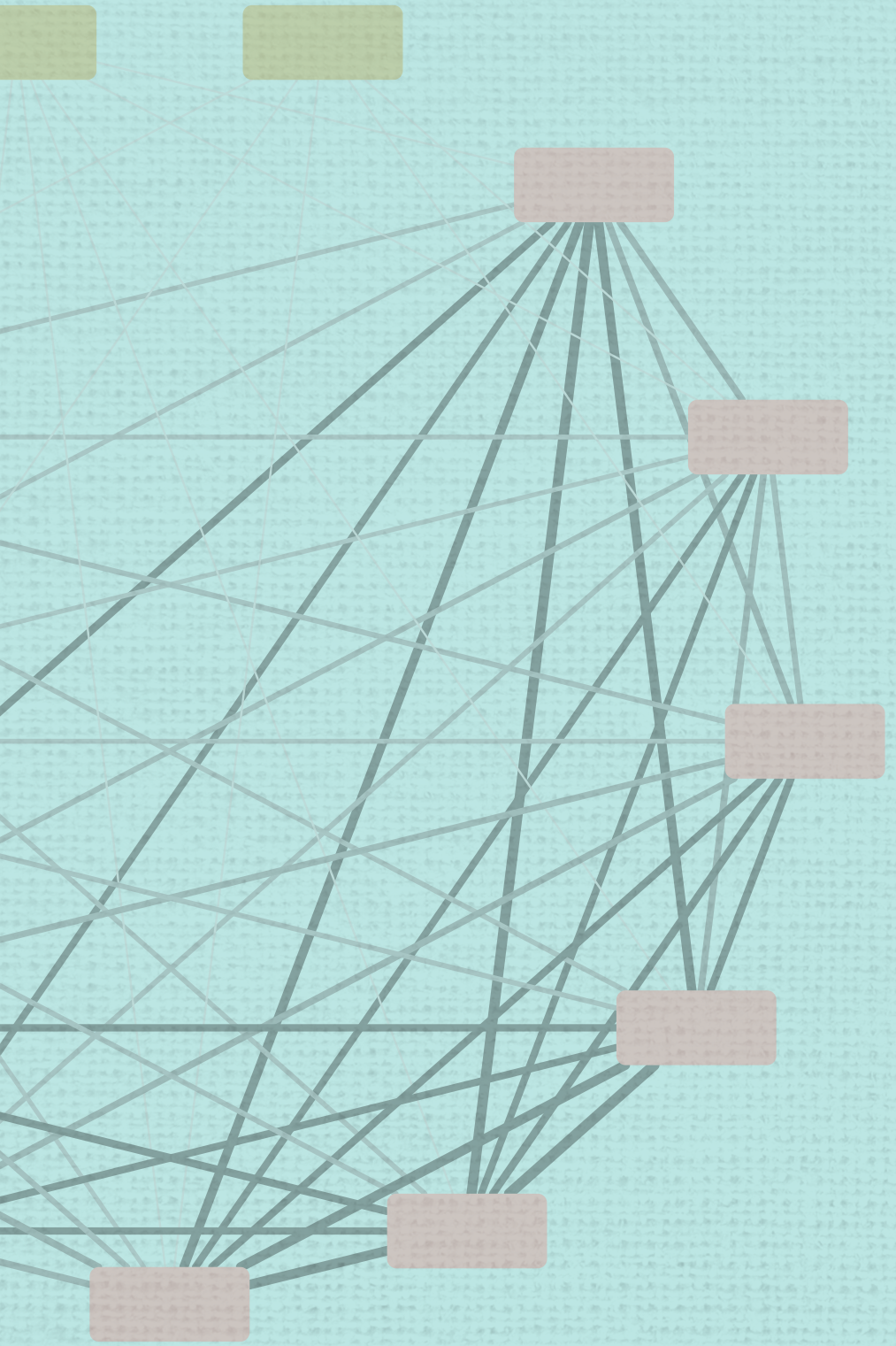

Chapter 3

A diet rich in fish oil and leucine ameliorates hypercalcemia in tumour-induced cachectic mice

Rogier L.C. Plas
Mieke Poland
Joyce Faber
Josep Argilès
Miriam van Dijk
Alessandro Laviano
Jocelijn Meijerink
Renger F. Witkamp
Ardy van Helvoort
Klaske van Norren

Published in International Journal of Molecular Sciences (2019)
DOI: https://doi.org/10.3390/ijms20204978

Abstract

Background Dietary supplementation with leucine and fish-oil rich in omega-3 fatty acids docosahexaenoic-acid (DHA) and eicosapentaenoic-acid (EPA) has previously been shown to reduce cachexia-related outcomes in C26 tumour-bearing mice. To further explore associated processes and mechanisms we investigated changes in plasma Ca^{2+}-levels, the involvement of parathyroid hormone related protein (PTHrP), and its possible interactions with cyclooxygenase-type 2 (COX-2).

Methods CD2F1 mice were subcutaneously inoculated with C26 adenocarcinoma cells or sham treated and divided in: (1) controls, (2) tumour-bearing controls, and (3) tumour-bearing receiving experimental diets. After 20 days, body and organ masses and total plasma Ca^{2+}-levels were determined. Furthermore, effects of DHA, EPA and Leucine on production of PTHrP were studied in cultured C26 cells.

Results The combination of Leucine and fish-oil reduced tumour-associated hypercalcemia. Plasma Ca^{2+} levels negatively correlated with carcass mass and multiple organ masses. DHA was able to reduce PTHrP production by C26 cells *in vitro*. Results indicate that this effect occurred independently of COX-2 inhibition.

Conclusion Our results suggest that cancer-related hypercalcemia may be ameliorated by a nutritional intervention rich in leucine and fish-oil. The effect of fish-oil possibly relates to a DHA-induced reduction of PTHrP excretion by the tumour.

Abbreviations

COX-2	cyclooxygenase-type 2
CXB	celecoxib
DHA	docosahexaenoic-acid
EPA	eicosapentaenoic-acid
IL-6	interleukin 6
PGE-2	prostaglandin E2
PTHrP	parathyroid hormone related protein
SNC	specific nutritional combination

Introduction

Cancer-related hypercalcemia is seen in up to 30% of patients with malignancies[1]. Very often, this is accompanied by increased bone resorption[2]. Calcium plays a vital role in many different physiological functions, for example in the contraction of all muscle cell types and neuronal signalling. In healthy individuals, the plasma concentration of calcium is tightly regulated by the interplay of parathyroid hormone (PTH), vitamin D and calcitonin[2]. In patients with malignant disorders, calcium balance is often disrupted, reflected by elevated calcium plasma levels[1]. Calcium is partly bound to albumin and its plasma levels are either expressed as albumin corrected levels (common in clinical practice) or as total Ca^{2+} levels (free + bound). Hypercalcemia is defined in patients as mild for levels between 10.5 and 11.9 mg/dL (2.6-2.9 mmol/l), as moderate between 12 and 13.9 mg/dL (3.0-3.4 mmol/l) and as severe above 14 mg/dL (3.5 mmol/l) serum total Ca^{2+} [1,3]. Main cause of malignancy-related hypercalcemia is an imbalance in bone formation and resorption[3].

Most prevalent clinical symptoms with hypercalcemia relate to neurologic, psychiatric, gastrointestinal, cardiovascular and renal abnormalities[2–4]. Neurologic and psychiatric symptoms include fatigue, lethargy, musculoskeletal pain, depression and even coma. Reduced motility of the gastrointestinal tract can cause constipation and reduced appetite. Cardiovascular symptoms include cardiac arrhythmias and hypertension. Moreover, renal failure is frequently present in hypercalcemia. Symptoms of hypercalcemia are frequently seen in cancer patients. For example, In multiple myeloma patients, serum calcium levels were an independent predictor of quality of life, fatigue and physical functioning[5].

There are three proposed mechanisms by which malignancies can affect the balance between Ca-incorporation in bone and its resorption[2]. The first is associated with increased degradation of bone by osteoclasts which become activated by factors secreted by metastases or primary tumours in or close to the bone. A second mechanism involves increased levels of inflammatory mediators like interleukin 6 (IL-6) and prostaglandin E2 (PGE-2) and of PTH-related protein (PTHrP), which directly cause increased breakdown of bone. A third possibility is based on the connection to coexisting primary hyperparathyroidism. Of these three proposed mechanisms, the one involving PTHrP secreted by the tumour is considered the most prominent and responsible for 80% of all malignancy-related hypercalcemia patients[4].

PTHrP is a protein between 139- and 173-amino-acids in size. Its N-terminal shows homology with PTH. PTHrP is produced in low concentrations by practically all tissues. PTHrP produced by the tumour can bind and activate the PTH receptor leading to increased bone demineralization and increased renal reabsorption of calcium[6]. Both these processes

contribute to the increase in plasma calcium levels. Bone resorption can lead to TGFβ release, which in turn stimulates PTHrP secretion by tumour cells, thus initiating a vicious cycle[6,7]. The elevation of PTHrP in C26 adenocarcinoma cells has been reported to depend on an increase in cyclooxygenase II (COX-2) activity, which in parallel also results in an elevated PGE-2 production[8]. Apart from its effects on bone calcium turnover, PTHrP also directly stimulates muscle wasting and adipose tissue browning[9]. Possibly related to this, serum PTHrP levels were found to be predictive of weight loss in cancer patients independently of hypercalcemia, inflammation and tumour burden[10]. Together, these findings suggest an overlap between features of cancer cachexia and malignancy-related hypercalcemia, 2 clinically relevant paraneoplastic syndromes. In order to investigate whether this overlap would also apply to possible intervention strategies for cachexia, the present study was initiated. We took off to investigate the effects of a diet enriched in leucine, protein and fish oil on PTHrP-related changes of plasma Ca-levels in a tumour-induced cachexia model. In the same animals, we previously showed significant improvement of cachexia-related outcomes in those mice that had received such specific nutritional combination (SNC)[11]. Starting from the hypothesis that supplementation of fish oil and leucine might also reduce plasma Ca^{2+} levels in tumour bearing animals, we further investigated the involvement of PTHrP and COX-2 in the regulation of Ca^{2+} levels by DHA and EPA, respectively. To this end, we performed a series of *in vitro* experiments with C26 cells.

Materials and Methods

In vivo experiments

Animals and Experimental diets

For the present study, we started our research by analysing archived materials from a previous *in vivo* study, which made it possible to limit new animal research. That study investigated the effects of a specific nutritional combination of oligosaccharides, high protein, leucine and fish oil on muscle and daily activity[11]. Experimental procedures have been described in detail in the previous paper. Briefly, male CD2F1 mice aged 6-7 weeks were divided into weight-matched groups: (1) control mice receiving control diet high in protein (C), (2) tumour-bearing mice receiving the same control diet (TB), and (3) tumour-bearing mice receiving experimental diets. In experiment A, the effect of additional leucine (Leu) and fish-oil (FO) on top of the high protein diet was tested. In experiment B the specific nutritional combination (SNC) of oligosaccharides, high protein, leucine and fish oil was used. All diets used in the different experiments were iso-caloric, by exchanging additional

protein or fat with carbohydrates. Experimental procedures were approved by the Animal Ethics Committee (DEC consult, Bilthoven, The Netherlands) and complied with the principles of good laboratory animal care.

Experimental protocol

Murine C-26 adenocarcinoma cells were cultured and inoculated as reported previously[11,12]. Briefly, under general anaesthesia (isoflurane/N_2O/O_2), tumour cells (5 x 10^5 cells in 0.2 mL) were inoculated subcutaneously into the right inguinal flank of the mice. Control (C) animals received a sham injection with 0.2 mL HBSS. Animals were weighed and anaesthetized (isoflurane/N_2O/O_2) at day 20 after tumour inoculation. Skeletal muscle and internal organs were dissected and weighed. Carcass mass was calculated by subtracting tumour mass from body mass.

Plasma PGE-2 and Tumour PTHrP (Experiment A)

In animals from experiment A, plasma PGE-2 was measured using a commercial anti-PGE-2 rabbit polyclonal antibody-based direct enzyme immunoassay (Oxford Biomedical Research, Oxford, MI, USA) according to the manufacturer's protocol. PTHrP levels in the tumour of animals in experiment A were measured using a quantitative PTHrP enzyme-linked immunosorbent (ELISA) assay kit (Uscn Life Science Inc., Wuhan, Hubei, China) according to the manufacturer's protocol. PTHrP levels were expressed as amount per milligram of protein as determined using a Pierce™ BCA protein kit (Thermo Fisher Scientific, Rockford, Illinois, USA). Unfortunately, the amount of stored plasma material was insufficient to determine plasma PTHrP levels.

Plasma Calcium (Experiment A and B)

To investigate if the elevation of calcium levels was linked to body and organ masses and PGE-2 levels, total plasma Ca^{2+}-levels (free calcium + calcium bound to albumin) were determined calorimetrically at the Clinical Chemistry Laboratory hospital Reinier de Graaf (Delft, the Netherlands).

In vitro experiments

To determine possible underlying mechanisms, we set up a series of *in vitro* experiments. First, we tested the main components present in the diets used in the mouse studies on a low number of tumour cells (Experiment C). As a control, viability and toxicity assays were performed to rule out potentially toxic effects of components in the concentrations tested. Subsequently, we continued with the most potent compounds on a larger number of cells (Experiment D) to test their potency in situations more resembling the *in vivo* situation (i.e. the tumour consists of a very large number of cells). Lastly, we examined a possible mechanism of action of the most potent compound (Experiment E) by assessing the possible

involvement of COX-2 by using a specific COX-2 inhibitor. For the last experiments (D and E), only toxicity assays were performed.

Culture of murine C26 cells

All *in vitro* experiments were performed using murine C26 tumour cells (American Type Culture Collection; ATCC, Teddington, UK). Cells were cultured in DMEM with 10% heat-inactivated foetal bovine serum at 37°C in a 5% CO_2 humidified air atmosphere. For supplementation experiments C, D and E, cells were seeded in a 24-wells plate. For experiments C, 25000 cells were seeded leading to a confluence of 10-20 % after 24h with ample cell-cell contact, for experiment D/E 250000 cells were seeded leading to a confluence of 80-90 % after 24h with a high degree of cell-cell contact.

PTHrP and PGE-2 production upon supplementation of C26 cells with DHA, EPA, Leucine and CXB

After 24h of incubation, culture medium from each well was removed and C26 cells were supplemented with test compound or vehicle control. Supplementation for 24h was performed with different concentrations of either docosahexaenoic acid (DHA, 22:6n-3; Sigma-Aldrich, Sigma-Aldrich Chemie GmbH, Schnelldorf, Germany), eicosapentaenoic acid (EPA, 20:5n-3; Sigma-Aldrich Chemie GmbH), leucine (Sigma-Aldrich Chemie GmbH) or celecoxib (CXB, Sigma-Aldrich Chemie GmbH). Ethanol was used as solvent for ω-3 PUFAs (DHA and EPA), DMSO was used as solvent for CXB and leucine was dissolved in PBS. In all cases, final ethanol/DMSO concentration never exceeded 0.1% v/v. All experiments were performed at least three times, and each condition was done in duplicate or triplicate. After 24h of supplementation, supernatant was removed for analysis of PTHrP and PGE-2. PTHrP production in C26 cell supernatant was measured using a commercially available ELISA (Uscn Life Science Inc., Wuhan, Hubei, China) according to the manufacturer's protocol. PGE-2 production was measured using a commercially available monoclonal ELISA kit (Cayman chemical, Ann Arbor, Michigan, USA).

Viability and Cytotoxicity

For experiments C, cell viability was measured with the Cell Proliferation (XTT) Kit II (Roche, Basel, Switzerland) according to manufacturer's protocol. Cells seeded in a 24-wells plate were incubated for 30 to 90 minutes with the XTT reagent mix. After incubation, 100uL supernatant was transferred to a 96-wells plate and absorbance was measured at 450nm using an ELISA plate reader. As a negative control, cells were treated with Triton X100 which resulted in total cell lysis.

Cytotoxicity was measured for each experiment with the Cytotoxicity Detection (LDH) Kit (Roche, Basel, Switzerland) according to the manufacturer's protocol. This kit measures the relative LDH content present in the supernatant, which reflects cytotoxicity.

Supernatant of the cells seeded in a 24-wells plate was transferred to a 96-wells plate and used to measure LDH content. Absorbance was measured at 492nm using an ELISA plate reader. As a positive control, cells were incubated with Triton X100 which results in total cell lysis. Viability and cytotoxicity results are reported in supplemental figures 1 and 2.

Statistics

All data are expressed as means ± SEM. Statistical analyses were performed using Graphpad Prism 5 (Graphpad Software Inc., La Jolla, California, USA). In experiment A, different batches of animals were used. Therefore, for all parameters it was defined that combining the data was allowed, meaning no interaction between groups and experiments was present. For all the *in vivo* experiments, comparisons were made using an analysis of variance (ANOVA) with a Dunnett's multiple comparison test with the tumour bearing group without nutritional supplementation as reference. Differences were considered significant at a p-value < 0.05. Correlations were calculated and Pearson correlation coefficients with a p-value < 0.05 were considered significant. For the *in vitro* experiments, comparisons were made using an ANOVA with a Dunnett's multiple comparison test with the vehicle control as reference. Differences were considered significant at a p-value < 0.05.

Results

Effect of leucine and fish oil in vivo (Experiments A and B)

Calcium levels and their correlation with carcass and organ masses

We determined whether cachexia-associated outcomes might be related to plasma Ca^{2+} levels. As previously published, carcass mass was decreased (figure 3.1 A and C) in TB mice compared to the carcass mass of control mice which was improved to a certain extent by supplementation of fish-oil and leucine or the SNC[11]. Our additional analysis showed a two-fold increase in plasma Ca^{2+} levels in the tumour bearing animals (figure 3.1). The combination of leucine and fish-oil was able to significantly reduce the tumour-induced hypercalcemia, whereas the individual components could not reduce hypercalcemia (Experiment A, figure 3.1 B). Similar reductions in plasma Ca^{2+} levels were found in animals supplemented with the complete SNC containing high protein, leucine, fish oil and oligosaccharides (Experiment B, figure 3.1 D). Moreover, plasma Ca^{2+} levels were negatively correlated with carcass weight and with multiple organ masses (figure 3.1 E and Table 1).

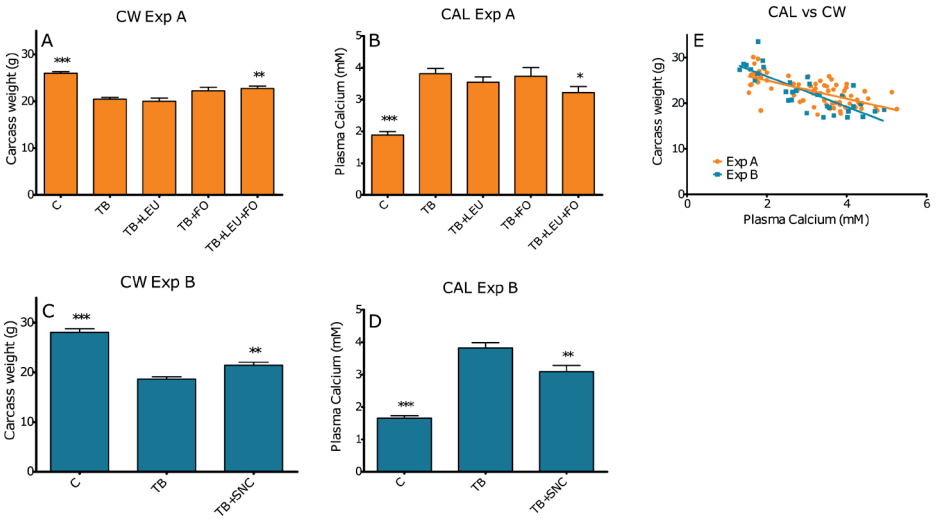

Figure 3.1 *– Effect of leucine (LEU), fish-oil (FO) and a combination of leucine and fish-oil on carcass weight and plasma Ca2+ levels [**A**, **B**]. Effect of a SNC containing added fish-oil and leucine on carcass weight and plasma Ca^{2+} levels [**C**, **D**]. Data represent means ± s.e.m.. Correlation between carcass weight and plasma Ca^{2+} levels (pearson r=-0.6684 [Exp A] and -0.8097 [Exp B], both with p<0.0001) [**E**].*

*,** and *** represent significant differences with TB group (respectively p<0.05, p<0.01 and p<0.001).

Pearson Correlation Coefficients with plasma Ca^{2+} levels	Experiment A	Experiment B
m. tibialis anterior	-0.640**	-0.705**
m. exstensor digitorum longus	-0.498**	-0.628**
m. soleus	-0.579**	-0.603**
m. gastrocnemius	-0.623**	-0.772**
epididimal fat pad	-0.659**	-0.783**
spleen	0.552**	0.695**
kidney	-0.409**	-0.635**
liver	-0.480**	-0.527**
intestine	0.243*	0.141
thymus	-0.701**	-0.561**
heart	-0.338**	-0.743**
lung	0.355**	0.098

Table 3.1 *– Correlation of plasma calcium levels and organ weights. * and ** represent significant Pearson correlation coefficients of Experiment A (combination vs. separate compounds and controls) and B (total product vs. controls) (respectively, p < 0.05 and p < 0.01).*

Plasma PGE-2 and tumour PTHrP

Inflammatory mediators like PGE-2 and PTHrP have been reported to play a potential role in the onset of hypercalcemia. Plasma PGE-2 levels were significantly increased in TB compared to control mice (figure 3.2 B). This increase was reduced upon supplementation of fish-oil either with or without added leucine. Plasma Ca^{2+} and PGE-2 levels correlated significantly (Pearson r= 0.6062 with $p < 0.0001$) (figure 3.2 F). Tumour PTHrP levels were significantly lower in TB animals that had received diets enriched with fish-oil and leucine compared to TB animals without supplementation (figure 3.2 C). Tumour PTHrP levels did not correlate with plasma Ca^{2+} levels. However, it should be noted that there were no PTHrP levels determined in control animals since they have no tumour.

Effect of leucine and fish-oil in vitro (Experiments C, D and E)

Supplementation of C26 cells with nutritional components used in vivo (experiments C and D)

To determine possible mechanisms behind the effects of the nutritional supplementation with leucine and fish-oil in C26 mice, a sequence of *in vitro* experiments was performed. In experiments C, small numbers of C26 cells were incubated with omega-3 fatty acids EPA or DHA or leucine added to the medium and PTHrP production was measured. Experiments showed that DHA and EPA at a concentration of 50 µM (DHA), 100 µM (DHA) and 100 µM (EPA) significantly reduced C26 PTHrP production by 36%, 39% and 35%, respectively (figure 3.3 A and B). Leucine had no effect on PTHrP production *in vitro* (figure 3.3 C). None of the components had any effect on viability or toxicity in the concentrations tested (supplemental figure 3.1). Given that DHA and EPA were found to be the most potent in reducing PTHrP, these were incorporated into the next experiments. To test the consistency of the findings and to mimic the effects of the potent components DHA an EPA on the tumour, we tested the effects on cells with a higher confluence in experiments D. The effect of EPA was no longer present. The effect of DHA, however, was reproducible in these confluent cells with reductions of 32% and 34% at 50 µM DHA and 100 µM DHA, respectively (figure 3.3 D and E).

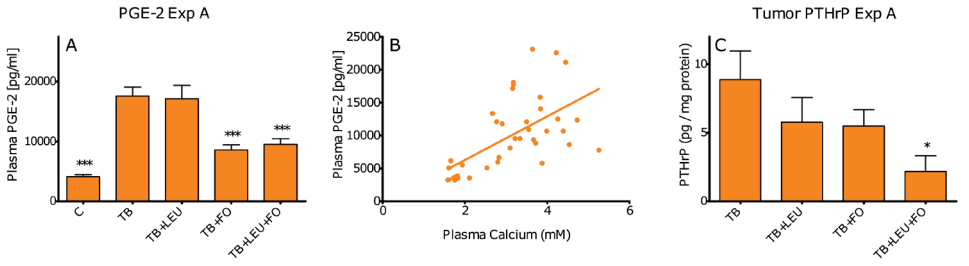

Figure 3.1 *– Effect of leucine (LEU), fish-oil (FO) and a combination of leucine and fish-oil on Plasma PGE-2 [**A**], correlation between Plasma PGE-2 and plasma Ca2+ levels (pearson r= 0.6062 with p<0.0001) [**B**] and Tumour PTHrP [**C**]. Data represent means ± s.e.m..*

*,** and *** represent significant differences with TB group (respectively p<0.05, p<0.01 and p<0.001).

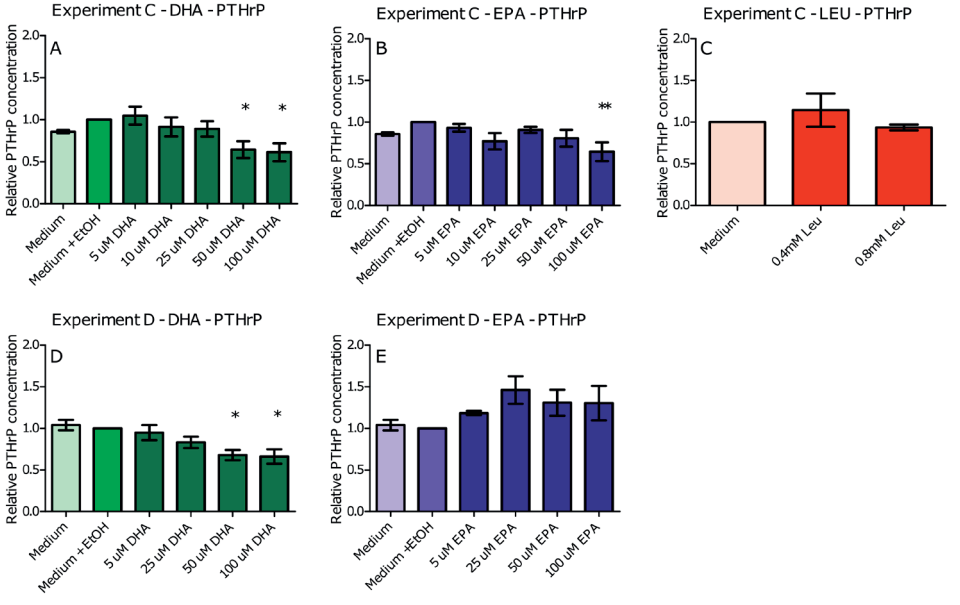

Figure 3.2 *– Effect of supplementation of C26 cells with DHA (A/D), EPA (B/E), and leucine (Leu) (C) on PTHrP levels on low [**A-C**] and high [**D** and **E**] number of cells. Data represent means ± s.e.m..*

, and *** represent significant differences with vehicle control (respectively p<0.05, p<0.01 and p<0.001).*

Possible involvement of COX-2 in the effect of fish-oil (experiments E)

DHA is known to reduce COX-2 activity,[13] and PTHrP production is known to be stimulated upon stimulation of COX-2[8]. Therefore, to further elucidate the possible mode of action of DHA, we determined whether COX-2 was involved in the PTHrP reducing effects of DHA in experiments E. This was done by measuring PGE-2 production upon incubation of C26 cells with DHA. As a positive control the specific COX-2 inhibitor celecoxib (CXB) was used. Results showed that DHA was not able to reduce PGE-2 production in C26 cells where CXB reduced PGE-2 levels with 73% at a dose of 0.01 µM (figure 3.4 A and B). Moreover, PTHrP production of C26 cells was not reduced when COX-2 activity was inhibited by incubation with CXB (figure 3.4 C). This indicates that the effect of DHA was possibly not mediated via the enzyme COX-2. In experiments D and E, none of the conditions resulted in an increased toxicity, as measured by LDH (supplemental figure 3.2).

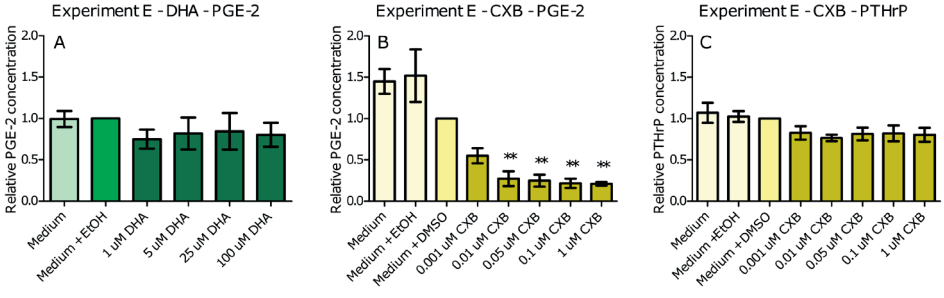

Figure 3.3 *– Effect of supplementation of C26 cells with DHA [**A**] and CXB [**B**] on PGE-2 levels. Effects of supplementation of CXB [**C**] on PTHrP levels. Data represent means ± s.e.m..*
, and *** represent significant differences with vehicle control (respectively p<0.05, p<0.01 and p<0.001).*

Discussion

In line with our hypothesis and the available literature[14,15], tumour-bearing cachectic mice showed hypercalcemia. Our data also demonstrate that plasma Ca^{2+} levels correlated negatively with carcass mass and several organ masses. In addition, Ca^{2+} levels positively correlated with plasma PGE-2 levels. Moreover, the nutritional combination reduced elevated plasma PGE2 levels and PTHrP levels in tumour tissue.

Only a few studies on the relation between fish-oil, or its main components EPA and DHA, and tumour-associated hypercalcemia have been reported in the literature. In a study of 1984, mice bearing the prostaglandin producing HSDM1 fibrosarcoma, received menhaden fish oil high in EPA (EPA:DHA ratio of 2.4:1). This intervention caused a reduction of plasma Ca^{2+} levels in tumour bearing mice[16]. Since hypercalcemia is related to bone mineral density and a reduction of bone mineral density is a well-known feature of the C26 model, we also investigated the literature on reported associations between fish-oil treatment and bone mineral density. However, a systematic review on ω3 fatty acids and osteoporosis concluded that clear conclusions are difficult to make due to the small number of studies and modest sample sizes[17]. In breast cancer survivors, high-doses of EPA and DHA were reported to reduce bone resorption[18]. Moreover, fish-oil was found to prevent breast cancer cell metastasis to bone and osteolytic lesions in a human mouse xenograft model[19].

In our study, decreased Ca^{2+} levels were only observed when leucine and fish oil were combined. Interestingly, this suggests that leucine might have an additional favourable effect, but only in the presence of fish oil. Leucine has been reported to influence insulin sensitivity of tissues and to increase insulin release[20]. In addition, insulin seems to have an anti-phosphaturic effect[21]. It was reported that *in vivo* administration of PTH induced a decline in tubular reabsorption of phosphate, which was reversed by superimposition of an euglycemic hyperinsulinemia within the physiologic range[21]. The effect of leucine on hypercalcemia might, therefore, be explained by increased insulin release, leading to increased renal absorption of phosphate.

In our study, dietary fish-oil alone or combined with leucine reduced plasma PGE-2 levels. Omega-3 PUFAs have been evaluated in various clinical studies for their immunomodulatory capacity[22]. Already after a week of intervention with a medical food high in protein, leucine, fish-oil and specific oligosaccharides, plasma PGE-2 levels decreased in cancer patients receiving radiotherapy[23]. The SNC tested in our study has also been shown to exert immunomodulatory effects by reducing IL-6, TNF-α, IL-4 and PGE-2 plasma levels in the C26 model[24]. Another study reported a decrease in PGE-2 levels in a small intestinal tumour of $Apc^{Min/+}$ mice upon feeding with a high fat diet rich in fish-oil[25]. Eicosapentaenoic acid has been reported to decrease the pro-inflammatory steady state by

reducing the levels of TNF-α, IL-1β, IL-6 and IL-8 in serum or plasma[26]. Moreover, EPA induces a shift in the pattern of prostaglandins produced by COX-2, from PGE-2 production with arachidonic acid (AA) as substrate, to relatively more PGE-3 produced with EPA as substrate[27,28]. These results are all in line with our findings. However, there is also some conflicting evidence showing that both DHA and EPA can stimulate PGE-2 production in both ScGT1 neuronal cells, raw 264.7 murine macrophages and human primary monocyte-derived macrophages[29,30].

Previous studies report that hypercalcemia in the C26 model is mediated by IL-6 and PTHrP[31]. We realize the limitations of this study as we were unable to measure either PTHrP or IL-6 in plasma. From literature, we know that the same SNC is able to reduce IL-6 plasma levels in the C26 model[24]. Moreover, our results showed that the nutritional combination of fish-oil and leucine reduced PTHrP levels in the tumour. Elevation of PTHrP in malignancy is thought to be mediated by an increase in COX-2 activity[8]. Therefore, the strong positive correlations of Ca^{2+} levels with PGE-2, a major COX-2-mediated inflammatory mediator, might suggest that PTHrP is also involved in the induction of hypercalcemia. To test this hypothesis, we performed a sequence of in-vitro experiments.

Our results showed that among the nutrients tested *in vivo*, EPA and DHA seemed most potent when a low number of cells was used (Experiments C). Interestingly, leucine did not have any effect *in vitro,* whereas *in vivo* a combination of fish-oil and leucine was needed to reduce Ca^{2+} and tumour PTHrP. This might be explained by acknowledging a synergistic effect of leucine when combined with EPA/DHA compared to being administered alone on the reduction of Ca2+ and tumour PTHrP. To test the potency in situations more similar to the *in vivo* situation, where C26 cells grow in a solid tumour in the flank of the mice, we incubated larger number of cells with DHA or EPA (Experiments D). It should be mentioned that *in vivo*, the tumour consists of not only C26 cells but also stromal and inflammatory cells, which were not included in our *in vitro* studies. At this higher confluency, where more cell-cell contact was present, only DHA proved able to reduce PTHrP production. Previous research shows that ω3 PUFAs may exert anti-cancer activities on several different cancer types[32]. Moreover, ω3 PUFAs have been found to be pro-apoptotic and anti-proliferative in human colorectal cancer cell lines[33]. However, in our study, the effects on PTHrP production were independent of cytotoxicity or viability. PTHrP production in C26 cells has previously been related to COX-2 activity[8], and DHA is known to be able to inhibit COX-2 activity[13]. Therefore, our next step was to determine possible mediators of PTHrP by testing involvement of COX-2 (Experiments E). To this end, we incubated the large number of cells with a specific COX-2 inhibitor CXB and measured the effect of DHA on PGE-2 production and the effect of CXB on PTHrP and PGE-2 production. Surprisingly, DHA was not able to reduce PGE-2 production, whereas CXB was. Moreover, PTHrP production did

not change upon supplementation with CXB. This was an unexpected result, since a different COX-2 inhibitor (NS-398) was able to reduce PTHrP production in C26 cells[8]. Possible explanation for the difference between our finding and literature is that in the NS-398 experiments, PTHrP production was only present in a spheroid culture and not in monolayer cultures; in our experiments, PTHrP production was already visible in a monolayer culture. From our *in-vitro* experiments, we can conclude that DHA is possibly the most potent component in reducing the PTHrP levels. The reduction in PTHrP production was most likely not mediated by COX-2, leaving the mechanism of action of DHA still an open question.

Bone health and calcium homeostasis are important factors affected by malignancy. In this study, we showed that tumour-induced hypercalcemia is highly correlated with several cachexia related outcomes. We also showed that a nutritional intervention high in leucine and fish-oil can reduce the detrimental effects of the tumour on calcium homeostasis in a tumour bearing C26 mouse model. This is clinically relevant, since calcium homeostasis can have a large impact on the daily life of patients. In a study of 686 multiple myeloma patients, serum calcium levels were associated with quality of life (QOL) scores, appetite loss, nausea/vomiting, physical functioning ($p < 0.001$), cognitive functioning ($p = 0.001$) and the scores for fatigue and pain ($p < 0.001$)[5]. Moreover, we elucidated possible mechanisms behind the beneficial effects of fish-oil supplementation on hypercalcemia. The ω3 PUFA DHA, one of the potent components found *in vivo,* reduced PTHrP production of C26 cells *in vitro*. A reduction in PTHrP is important independent of its effects on calcium homeostasis and bone health, since PTHrP is also related to an increase adipose tissue browning and muscle wasting[9,34]. Further research in the mechanism involved in the beneficial effects of ω3 PUFA is needed to further optimize nutritional support for cancer patients.

Acknowledgements

We would like to thank Judith Hulsman, Jvalini Dwarkasing and Merel van Rooijen for performing part of the in vitro experiments and Diane Kegler for the animal activities and the support of the Animal Care Facility (CKP) of the University of Wageningen.

References

1. Stewart, A. F. Hypercalcemia Associated with Cancer. *http://dx.doi.org.ez.statsbiblioteket.dk:2048/10.1056/NEJMcp042806* **352,** 373–379 (2009).
2. Guise, T. A. & Mundy, G. R. Cancer and Bone. *Endocr. Rev.* **19,** 18–54 (2013).
3. Goldner, W. Cancer-Related Hypercalcemia. *J. Oncol. Pract.* **12,** 426–432 (2016).
4. Mirrakhimov, A. E. Hypercalcemia of malignancy: An update on pathogenesis and management. *N. Am. J. Med. Sci.* **7,** 483–493 (2015).
5. Wisløff, F., Kvam, A. K., Hjorth, M. & Lenhoff, S. Serum calcium is an independent predictor of quality of life in multiple myeloma. *Eur. J. Haematol.* **78,** 29–34 (2007).
6. Mundy, G. R. & Edwards, J. R. PTH-related peptide (PTHrP) in hypercalcemia. *J. Am. Soc. Nephrol.* **19,** 672–5 (2008).
7. Yin, J. J. *et al.* TGF-β signaling blockade inhibits PTHrP secretion by breast cancer cells and bone metastases development. *J. Clin. Invest.* **103,** 197–206 (1999).
8. Saito, H. *et al.* Involvement of cyclooxygenase-2 in the tumor site-dependent production of parathyroid hormone-related protein in colon 26 carcinoma. *Cancer Sci.* **98,** 1563–1569 (2007).
9. Kir, S. *et al.* PTH/PTHrP receptor mediates cachexia in models of kidney failure and cancer. *Cell Metab.* **23,** 315–323 (2016).
10. Hong, N. *et al.* Serum PTHrP predicts weight loss in cancer patients independent of hypercalcemia, inflammation, and tumor burden. *J. Clin. Endocrinol. Metab.* **101,** 1207–1214 (2016).
11. van Norren, K. *et al.* Dietary supplementation with a specific combination of high protein, leucine, and fish oil improves muscle function and daily activity in tumour-bearing cachectic mice. *Br. J. Cancer* **100,** 713–22 (2009).
12. Peters, S. J. *et al.* Dose-dependent effects of leucine supplementation on preservation of muscle mass in cancer cachectic mice. *Oncol. Rep.* **26,** 247–254 (2011).
13. Ringbom, T. *et al.* COX-2 inhibitory effects of naturally occurring and modified fatty acids. *J. Nat. Prod.* **64,** 745–749 (2001).
14. Colloton, M. *et al.* Cinacalcet attenuates hypercalcemia observed in mice bearing either Rice H-500 Leydig cell or C26-DCT colon tumors. *Eur. J. Pharmacol.* **712,** 8–15 (2013).
15. Bonetto, A. *et al.* Differential Bone Loss in Mouse Models of Colon Cancer Cachexia. *Front. Physiol.* **7,** 679 (2017).
16. Tashijan, A. H., Voelkel, E. F., Robinson, D. R. & Levine, L. Dietary menhaden oil lowers plasma prostaglandins and calcium in mice bearing the prostaglandin-producing HSDM1 fibrosarcoma. *J. Clin. Invest.* **74,** 2042–2048 (1984).
17. Orchard, T., Pan, X. & Cheek, F. A systematic review of omega-3 fatty acids and osteoporosis. *Br J Nutr* **107,** S253–S260 (2012).
18. Hutchins-Wiese, H. L. *et al.* High-Dose eicosapentaenoic acid and docosahexaenoic acid supplementation reduces bone resorption in postmenopausal breast cancer survivors on aromatase inhibitors: A pilot study. *Nutr. Cancer* **66,** 68–76 (2014).
19. Mandal, C. C., Ghosh-Choudhury, T., Yoneda, T., Choudhury, G. G. & Ghosh-Choudhury, N. Fish oil prevents breast cancer cell metastasis to bone. *Biochem.*

Biophys. Res. Commun. **402,** 602–607 (2010).
20. Soria, B. & Martin, F. Cytosolic calcium oscillations and insulin release in pancreatic islets of Langerhans. *Diabetes Metab.* **24,** 37–40 (1998).
21. Guntupalli, J., Allon, M. & Bourke, E. Effects of physiologic hyperinsulinemia on renal phosphate handling in the rat: a role for calcium. *Miner. Electrolyte Metab.* **15,** 338–345 (1989).
22. Sijben, J. W. C. & Calder, P. C. Differential immunomodulation with long-chain n-3 PUFA in health and chronic disease. *Proc. Nutr. Soc.* **66,** 237–259 (2007).
23. Faber, J. *et al.* Rapid EPA and DHA incorporation and reduced PGE2levels after one week intervention with a medical food in cancer patients receiving radiotherapy, a randomized trial. *Clin. Nutr.* **32,** 338–345 (2013).
24. Faber, J. *et al.* Beneficial immune modulatory effects of a specific nutritional combination in a murine model for cancer cachexia. *Br. J. Cancer* **99,** 2029–36 (2008).
25. Bose, M. *et al.* Inhibition of tumorigenesis in ApcMin/+ mice by a combination of (-)-epigallocatechin-3-gallate and fish oil. *J. Agric. Food Chem.* **55,** 7695–7700 (2007).
26. Calder, P. C. n Ⲭ 3 Polyunsaturated fatty acids , inflammation , and inflammatory. **83,** (2006).
27. Ross, J. A. & Fearon, K. C. H. Eicosanoid-dependent cancer cachexia and wasting. *Curr. Opin. Clin. Nutr. Metab. Care* **5,** 241–248 (2002).
28. Trebble, T., Wootton, S., Miles, E. & Mullee, M. Prostaglandin E2 production and T cell function after fishoil supplementation. *Am J ClinNutr* **78,** 376–382 (2003).
29. Liu, Y. *et al.* The fish oil ingredient, docosahexaenoic acid, activates cytosolic phospholipase A2 via GPR120 receptor to produce prostaglandin E2 and plays an anti-inflammatory role in macrophages. *Immunology* **143,** 81–95 (2014).
30. Bate, C., Tayebi, M., Diomede, L., Salmona, M. & Williams, A. Docosahexaenoic and eicosapentaenoic acids increase prion formation in neuronal cells. *BMC Biol.* **6,** (2008).
31. Strassmann, G., Jacob, C. O., Fong, M. & Bertolini, D. R. Mechanisms of paraneoplastic syndromes of colon-26: Involvement of interleukin 6 in hypercalcemia. *Cytokine* **5,** 463–468 (1993).
32. Prevete, N. *et al.* New perspectives in cancer: Modulation of lipid metabolism and inflammation resolution. *Pharmacol. Res.* **128,** 80–87 (2017).
33. Brandão, D. & Ribeiro, L. Dietary fatty acids modulation of human colon cancer cells: mechanisms and future perspectives. *Int. J. Food Sci. Nutr.* **0,** 1–14 (2017).
34. Kir, S. *et al.* Tumour-derived PTH-related protein triggers adipose tissue browning and cancer cachexia. *Nature* **1,** 100–104 (2014).

Supplemental figures

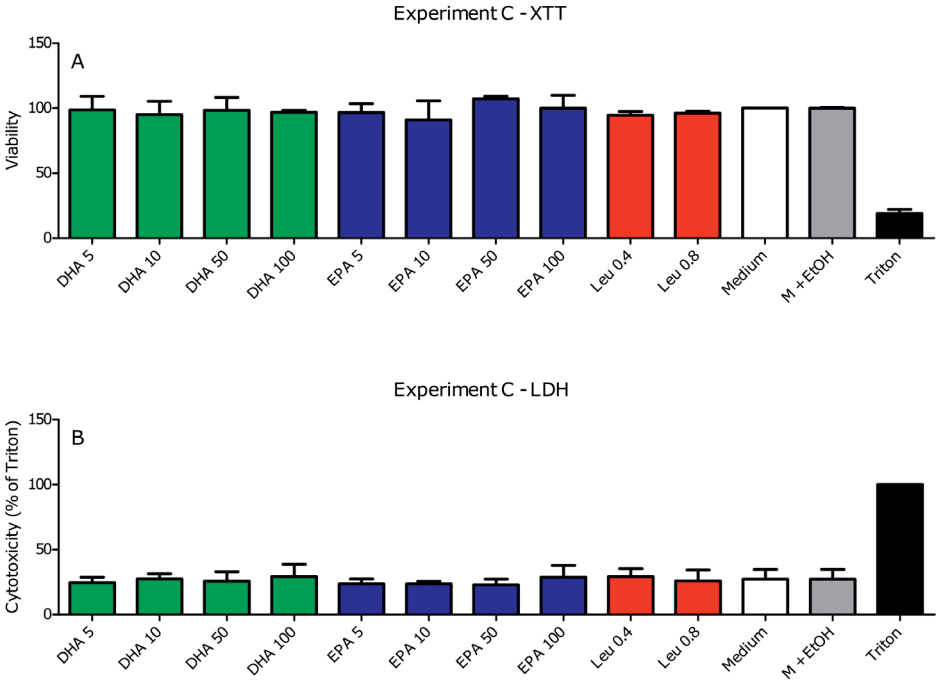

Supplemental Figure 1 *– Measurement of viability in experiments C using XTT [**A**] shows that none of the experimental conditions affected viability. Measurement of cytotoxicity in experiments C using LDH [**B**] indicated that none of the experimental conditions was toxic to the cells.*

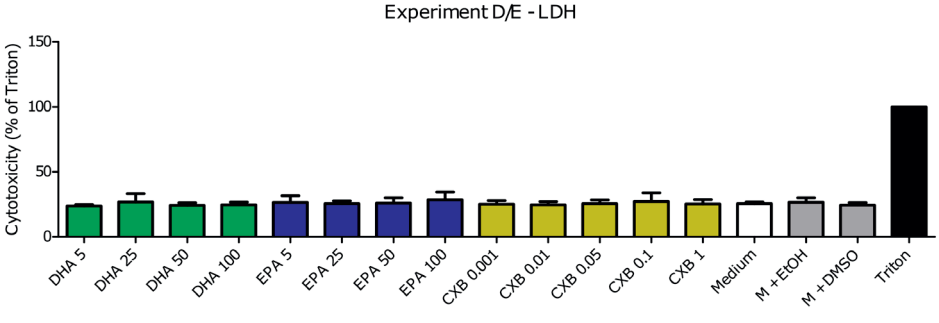

Supplemental Figure 2 *– Measurement of cytotoxicity in experiments D and E using LDH indicated that none of the experimental conditions was toxic to the cells.*

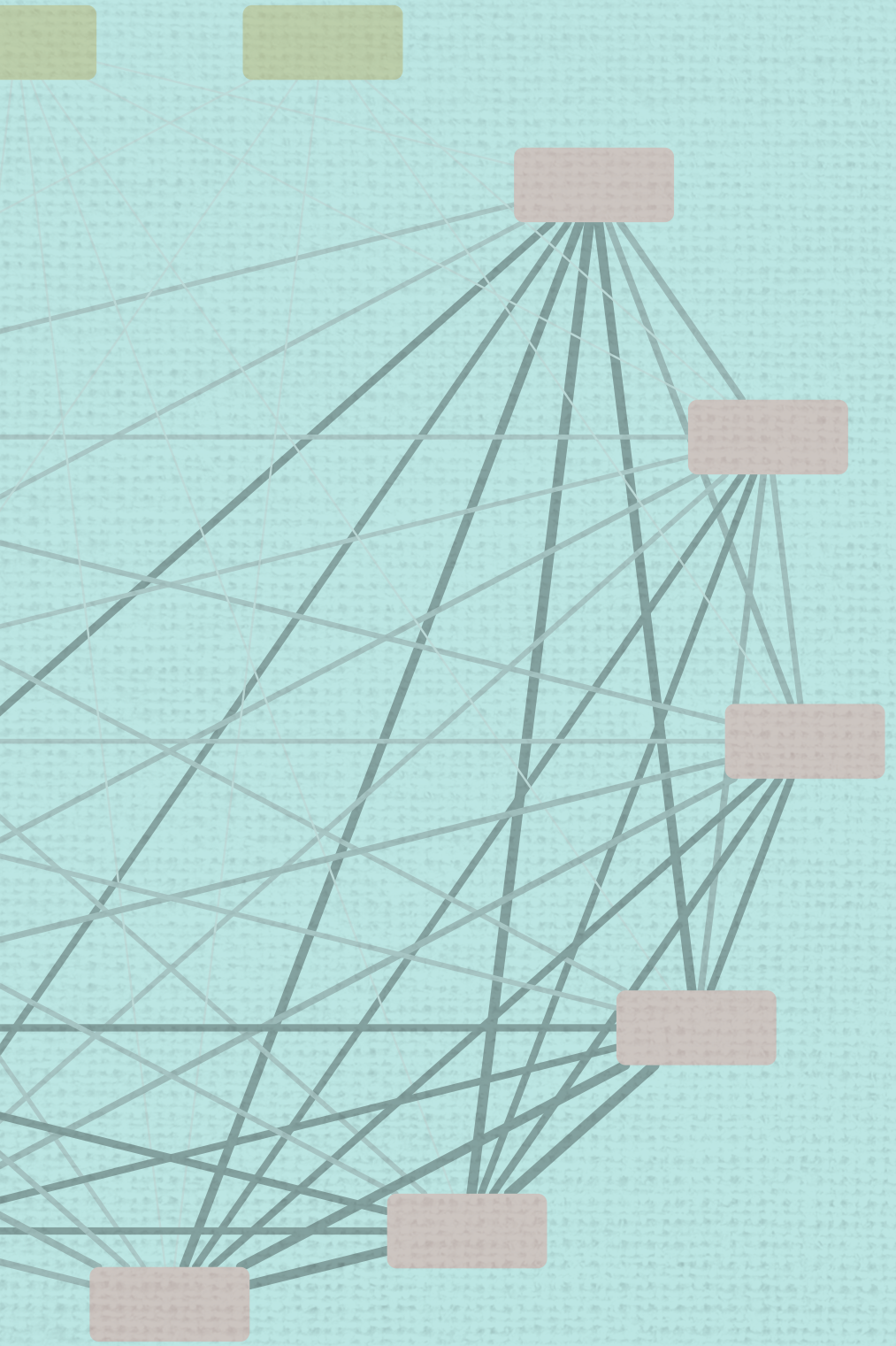

Chapter 4

Whole-body-vibration training positively affects muscle transcriptome in C26 tumour bearing cachectic mice

Rogier L.C. Plas
Miriam van Dijk
Jvalini T. Dwarkasing
Frans van Gemerden
Hans J.M. Swarts
Evert M. van Schothorst
Renger F. Witkamp
Klaske van Norren

In preparation

Abstract

Background The prevailing view is that a combination of nutritional, pharmacological and exercise therapy is most optimal to reduce the development and progression of cancer cachexia. However, in many cancer patients, physical activity is hampered by frailty and fatigue. The present study aimed to investigate whole-body-vibration-training(WBV) as potential alternative to attenuate loss of weight, muscle mass and function in tumour bearing mice.

Methods Twenty-four male CD2F1-mice(21.5±0.2g) were stratified into four groups (control=[C], control+WBV=[C+V], tumour-bearing=[T] and tumour-bearing+WBV=[T+V]), and injected(day 1) with C26 cells or vehicle. From day 1, whole-body-vibration was performed for 19 days(15min,45Hz,1.0g acceleration). General outcome measures included body mass and composition, and daily activity. In addition, blood analysis and assessments of muscle histology and function and whole genome gene expression in *m. soleus*(SOL) and *m. extensor digitorum longus*(EDL) were performed. Two-way ANOVA with factors tumour, training and interaction was used for statistical analysis.

Results Body weight, lean and fat mass and EDL mass were all lower in tumour bearing mice compared to controls. No effects of vibration training were found on systemic cachexia related outcomes. However, WBV increased EDL mass in the control group. SOL mass did not differ, whereas SOL function was affected by both tumour and WBV. Interestingly, WBV reduced the tumour-related effects on muscle gene expression in EDL, SOL and heart.

Conclusion These data suggest that WBV had minor effects on cachexia related outcomes in the present experimental set-up, while muscle transcriptome was positively affected. This merits follow-up studies applying longer treatment periods or incorporating WBV in a multiple-target intervention.

Abbreviations

AUC	area under the curve	**HBSS**	Hanks' balanced salt solution
BMD	bone mineral density	**MHC**	myosin heavy chain
CSA	cross sectional area	**PGE-2**	prostaglandin E2
CT	contraction time	**PTHrP**	parathyroid hormone related protein
DEXA	dual energy X-ray absorptiometry	**RT**	relaxation time
dF/dt	rate of change of force	**SOL**	*m. soleus*
EDL	*m. extensor digitorum longus*	**WBV**	whole body vibration training
$\mathbf{F_{max}}$	maximal force		

Introduction

Cachexia is often seen in patients with chronic kidney disease, heart failure, COPD and cancer and is associated with reduced treatment efficacy and quality of life. A characteristic difference between starvation and cachexia is the progressive loss of muscle mass[1–3]. Cachexia is often accompanied by anorexia, which however appears to be only partly responsible for the loss of body mass[4,5]. There is increasing consensus between experts that cachexia should be treated with a multimodal approach addressing dietary intake, systemic inflammation and physical activity[6,7].

A systematic review of the effects of physical exercise on muscle mass and strength in cancer patients provided evidence that resistance training, aerobic training or a combination of these are able to improve muscle strength during treatment[8]. However, coexisting fatigue and frailty are often limiting factors in these patients[9]. Therefore, there is a need for training methods that are easily accessible for frail patients. Vibration training might meet this demand since it provides an easily accessible and low intensity type of exercise. In older individuals, positive effects of whole-body-vibration training (WBV) on $VO_{2,max}$ and muscle strength have been observed[10]. Moreover, vibration training increased exercise capacity in patients treated for respiratory cancer[11]. However, literature data are scarce and studies are difficult to compare due to differences in set-up. A meta-analysis reported a beneficial effect on leg muscle strength in elderly[12], whereas a systematic review concluded that there would be only weak proof of efficacy of WBV in elderly[13]. Due to the overall inconsistent results of WBV, it remains unclear whether WBV could be a beneficial intervention to improve muscle mass and function in elderly. Moreover, to our knowledge WBV has never been thoroughly investigated during disease-driven net catabolic conditions. Therefore, in this study, we investigated the effects of WBV using a colon-derived-tumour-induced C26 cachexia mouse model.

Effects of WBV in rodents found so far seem promising but have also provided contradicting results. In healthy mice, a study has shown that low-intensity WBV can partially improve muscle contractility, in particular strength and relaxation rates[14]. Another study demonstrated effectiveness of WBV in suppressing the muscle atrophy pathway both *in vivo* and *in vitro*[15]. Apart from effects on muscle, WBV is also able to improve bone health in mice[16]. One study investigated the effect of vibration training in a mouse model for Duchenne muscular dystrophy but found no effect on bone or muscle improvement[17]. However, there appear to be no studies in literature investigating a condition of cancer-induced atrophy, so addressing the question whether WBV might be able to attenuate muscle wasting during disease still remains unknown.

To this end, we here investigated the effects of WBV in a murine cachexia model, studying cachexia outcomes at different levels, including the muscle transcriptome, markers for bone and muscle function, whole body composition and muscle performance.

Materials and Methods

Tumour model

Twenty-four male CD2F1 mice weighing ~20g (BALB/c x DBA/2, Charles River, The Netherlands) were individually housed in macrolon type 3 cages with sawdust and tissues as cage enrichment, in a climate-controlled room (21 °C ± 1 °C) with a 12:12 hour dark-light cycle. Mice had *ad libitum* access to chow and water. Upon arrival, mice were stratified on body weight and divided into groups of 6 animals (Control [C], Control + WBV [C+V], Tumour bearing [T] and Tumour bearing + WBV [T+V]). Subsequently, mice were allowed to acclimatize for 1 week prior to the start of the experiment. Murine C26 adenocarcinoma cells, kindly obtained from Nutricia Research, The Netherlands, were cultured and suspended as described previously[18]. Tumour cells ($1x10^6$ cells in 0.2 ml of Hanks' balanced salt solution (HBSS)) were inoculated subcutaneously into the right inguinal flank of the mice under general anaesthesia (isoflurane/N_2O/O_2). HBSS was used as sham injection (0.2 ml). All experimental procedures were approved by the Animal Ethical Committee (DEC, Wageningen, The Netherlands) and complied with the principles of good laboratory animal care and the ethical standards laid down in the 1964 Declaration of Helsinki and its later amendments.

Experimental Design

On day 0 (D0), an injection with tumour cells or HBSS was given and blood was collected using a tail-vein cut. After two days of acclimatization (on D-5), body mass, activity and grip strength was measured daily. On D0, D7, D14 and D19, body composition was measured using an EchoMRI Whole Body Composition Analyzer (EchoMRI, Houston, TX, USA). Starting on D1 mice were subjected to a whole body vibration training (WBV) protocol, similar to previous rodent studies, with 15 min of vibration training for 7 days/week, with a frequency of 45 Hz and 1.0 g acceleration. The vibration platform used was an adjusted commercially available VG® Professional (VibroGym, Badhoevedorp, The Netherlands) power plate. Four Plexiglas cages were mounted onto the power plate to enable WBV in 4 mice simultaneously. The power plate was calibrated using accelerometers on all four corners to ensure the frequency and acceleration specifics. On D19, at least 24h after the last training session, blood was collected by cardiac puncture and animals were killed. Subsequently, organs and hind limb muscles were weighted and snap-frozen in liquid nitrogen. Carcass

mass was determined as body mass excluding tumour. *M. soleus* (SOL) and *m. extensor digitorum longus* (EDL) were divided in two parts; one for histology and one for RNA isolation. Front legs were cut off and frozen for bone mineral density (BMD) measurement.

To assure compliance of mice with the WBV, a small pilot was executed prior to the experiment. Three additional control mice were used and apart from the vibration training no other treatment was applied. Mice did not show any signs of aberrant behaviour when exposed to the vibration training. Video recordings of mice subjected to WBV showing the behavioural response of the mice to the training are provided in supplemental data.

Grip strength

Daily forelimb grip strength was measured as previously described[19], using a calibrated grip strength apparatus from Panlab (Cornella, Spain), following the protocol delivered with the equipment. Each day, a set of five maximum effort repetitions was performed. From these five measurements, the average of the middle three measurements was determined. To eliminate measurement variation, grip strength was expressed per mouse as mean grip strength on D15-18 as a percentage of the mean on D-3 to D0.

Daily activity

Physical activity was monitored throughout the acclimatisation and study period starting at D-7, using activity sensors (dual technology detector DUO 240, Visonic; adapted by R Visser, NIN, Amsterdam, The Netherlands) according to an adapted protocol previously described[20]. Sensors translated individual changes in the infrared pattern caused by movements of the animals into arbitrary activity counts. Sensors were mounted above the home cages and connected through input ports and interface to a computer equipped with MED-PC IV software for data collection (MED associates, St Albans, VT, USA). Activity was expressed in counts per half hour. The activities of each dark cycle was summed, to dampen the hour to hour variability. To eliminate measurement variation, daily activity was expressed per mouse as mean daily activity on D16-19 as a percentage of the mean on D-3 to D0.

BMD – DEXA

Frozen front legs were used for determination of BMD measured at a later time point by dual energy X-ray absorptiometry (DEXA) scan, using a PIXImus imager (GE Lunar, Madison, WI, USA).

Blood plasma cytokines and PTHrP

The following cytokines were measured using a mouse cytokine Milliplex bead immunoassay (MCYTOMAG-70K-09, Merck chemicals [Millipore], Amsterdam, The Netherlands): IFNγ, IL1-β, IL4, IL6, IL10, IL15, MCP1, TNFα and VEGF. PTHrP was measured using a quantitative PTHrP enzyme-linked immunosorbent (ELISA) assay kit (SEA819Mu, Cloud-Clone Corp., Uscn Life Science Inc., Wuhan, Hubei, PRC).

Ex vivo muscle function

At the end of the experiment (D19), *ex-vivo* muscle function of right SOL and EDL was measured according to an adapted protocol previously described[21]. Muscles were allowed to stabilize in the organ bath for 30 minutes. Subsequently, optimal stimulation strength was determined. Force frequency characteristics (10-167 Hz, 250 ms (EDL) and 500 ms (SOL)) were determined after refreshing the organ buffer and 5 minutes of rest. Next, an exercise protocol was performed of 100 contractions (83 Hz, 250 ms every 1000 ms for EDL and 83 Hz, 500 ms every 2000 ms for SOL). At the used frequencies, complete tetanic contraction of the muscle was reached. Force signals of the force frequency curve and the exercise protocol were analysed for maximal force (F_{max}), contraction and relaxation time (CT and RT respectively) and rate of change of force (dF/dt). Area under the curve (AUC) for F_{max} was determined for both force frequency and exercise protocols. CT, RT and dF/dt were analysed between 83-167 Hz.

Immunofluorescent histology

Staining MHC type I in m. soleus

Immunofluorescent staining was performed as previously described[22]. SOL sections (10 µm) were cut using a cryostat at –20°C, air dried and stored at −20°C until use. Based on MHC isoform, fibre-type abundancy was determined and classified as MHC type I and II using monoclonal antibody against mouse MHC type I (BAD-5, 1 µg/mL, as developed by Schiaffino; the Developmental Studies Hybridoma Bank, The University of Iowa, IA, USA) and immunofluorescent secondary anti-mouse immunoglobulin G2b antibody (IgG2b Alexa F488, 2 µg/mL; Fisher Scientific, Landsmeer, The Netherlands). Normal goat serum was diluted 1:10 (dNGS) in phosphate buffered saline (PBS). Sections were first air-dried for 15 minutes and then blocked with dNGS for 60 minutes at 37°C. Primary antibody dilution was prepared in dNGS, added to the sections and incubated for 60 minutes at 37°C. Sections were gently washed three times with PBS. Secondary antibody dilution was prepared in dNGS and added to the slides to incubate for 60 minutes at 37°C in the dark. After incubation, sections were gently washed again three times with PBS. Wheat germ agglutinin dilution (WGA, 20 µg/mL) was prepared in PBS. WGA was added to the sections and

incubated for 20 min at 37°C in the dark. Sections were gently washed three times PBS before enclosure with a drop of Vectashield-hard set (with DAPI; Fisher Scientific).

Fibre Area Analysis

Gray-scale images of the sections were taken under a Leica DMIL LED microscope with a 10x objective (Leica Microsystems, Amsterdam, The Netherlands). Images were taken at 10x magnification with the settings presented in Appendix III. The microscope was equipped with Red (Excitation: BP 546/11 nm; Emission BP 605/75 nm), Green (Excitation: BP 470/40 nm; Emission BP 525/50 nm), Blue (Excitation: BP 360/40 nm; Emission LP425 nm) filters, a Leica DFC450C camera (resolution of 52294 DPI), and LAS X 2.0 software (Leica). Images were made combined using ImageJ 1.15f for Windows (National Institutes of Health, Bethesda). Total area of a muscle section was analysed using Image J. Muscle fibre properties were analysed using SMASH muscle image analysis application for MATLAB r2015b (Mathworks, Natick)[23]. Abundance of type II muscle fibres was measured as MHC type I negative fibres as percentage of total fibre count. Muscle fibre cross-sectional area (CSA) was determined by measuring minimal Feret's diameter of fibres, a reliable measure for CSA[24]. The ratio of type II/type I fibre CSA and the relative abundance of type II MHC (total type II CSA as % of total muscle CSA) were also determined.

Statistics

All data are expressed as means ± SEM. Statistical analyses were performed using Graphpad Prism 5 (Graphpad Software Inc., La Jolla, California, USA). Differences in daily body mass, body composition and *ex vivo* measures (F_{max}, CT, RT and dF/dt) were tested using a repeated measures two-way ANOVA with group and time as factors. Differences at a specific point were all tested using a two-way ANOVA with tumour and training as factors. All *post hoc* testing was done with a Bonferroni multiple comparison correction. Differences were considered significant at $p<0.05$. Correlation of PTHrP and BMD was assessed using a Pearson correlation.

Gene expression

Microarray analysis

RNA from EDL, SOL and heart was isolated (RNeasy Micro kit, Qiagen, Venlo, the Netherlands). Subsequently, RNA was quantified (Nanodrop ND1000, Nanodrop technologies Wilmington, DE, USA) and integrity was checked by an Agilent 2100 Bioanalyser with RNA 6000 microchips (Agilent Technologies, South Queensferry, UK). Total RNA was labelled with the GeneChip® WT plus Reagent Kit and hybridized to GeneChip® Mouse Gene 1.1 ST Array (Affymetrix, Inc. Santa Clara, Ca, USA). Sample labelling, hybridization to chips and image scanning were performed according to the manufacturers' instructions.

Microarray Data analysis

Microarray quality control was performed in MADMAX, a pipeline for statistical analysis of microarray data[25]. Data were normalized using the robust multi-array analysis (RMA) algorithm[26] as implemented in the Bioconductor package *AffyPLM*. Probe sets were identified with genome information according to Dai *et al.*[27] based on annotations provided by the Entrez Gene database, which resulted in the profiling of 22,135 unique genes (custom CDF v22). Differential expression of probe sets (genes) was determined using linear models (package *limma*) and an intensity-based moderated t-statistic[28,29]. T and T+V groups were compared to C group for EDL, SOL and Heart samples. P-values were adjusted for multiple testing by Benjamini-Hochberg false discovery rate (FDR) procedure[30]. Probe sets with an adjusted *p*-value of $p < 0.01$ were considered to be regulated. Venn diagrams and scatter plots were made using the R libraries gglot2[31] and VennDiagram[32]. To find genes most regulated by either tumour or training, a sparse Partial Least Squares Discriminant (sPLS-DA) analysis was performed using the mixOmics package[33]. Changes in individual genes were related to changes in pathways by gene set enrichment analysis (GSEA)[34] and the subset of metabolic and signalling pathways retrieved from the expert-curated Kyoto Encyclopedia of Genes and Genomes (KEGG) database[35]. Only gene sets consisting of more than 10 and fewer than 500 genes were taken into account, which resulted in the inclusion of 226 gene sets. For each comparison, genes were ranked on their t-value that was calculated by the empirical Bayes method. Statistical significance of GSEA results was determined using 10,000 permutations. GSEA and visualization was performed using the Bioconductor package *clusterProfiler*[36]. Microarray data has been submitted to the Gene Expression Omnibus database under accession number GSE121972.

Results

Development of systemic cachexia outcomes was not affected by WBV

Body mass differed significantly between groups from day 14 onwards (figure 4.1 A). Mice in the T+V group had a significantly lower body mass compared to C (D14-19) and C+V (D16-19). Mice in the T group had a significantly lower body mass compared to C (D15-19) and C+V (D17-19). EchoMRI measurements indicated a decrease in fat mass measured on D14 and D19 coinciding with body weight loss without loss of lean mass yet, and also a decrease of lean mass on D19 in both tumour bearing groups (figure 4.1 C and 4.1 D). For carcass mass there was a significant tumour effect with the tumour groups being lighter compared to the control groups (figure 4.1 B). In all organs, muscles and fat compartments, except for the SOL there was a tumour effect (table 4.1). Only on the EDL mass there was a training effect with C+V being larger than C in *post hoc* comparison. In the liver there was an interaction effect with no *post hoc* differences.

Grip strength and daily activity not affected by WBV

Mean grip strength and daily activity at the end of the experiment were lower in the tumour bearing groups compared to the control groups (figure 4.2 A+B). The trained control group showed a trend of a lower mean daily activity, although not significant (figure 4.2 A).

ORGAN	C	C+V	T	T+V	STATISTICS	POST HOC
EDL	7.8 ± 0.8	9.0 ± 0.5	6.4 ± 1.1	6.9 ± 0.6	**** Tumour * Training	C+V > C
SOL	6.8 ± 0.3	7.2 ± 1.4	6.0 ± 0.4	6.9 ± 0.8		
M. TIBIALIS ANTERIOR	40.6 ± 2.5	41.0 ± 1.4	30.3 ± 4.6	31.3 ± 5.8	**** Tumour	
M. GASTROCNEMIUS	117.9 ± 7.5	125.6 ± 11.5	80.9 ± 8.9	85.2 ± 11.3	**** Tumour	
HEART	139.8 ± 10.7	147.6 ± 9.7	116.5 ± 16.8	133.4 ± 16.5	** Tumour	
EPIDIDIMAL FAT PAD	476.8 ± 52.0	379.8 ± 66.9	41.0 ± 67.0	111.4 ± 171.0	**** Tumour	
SUBCUTANEOUS FAT PAD	41.5 ± 8.7	40.0 ± 14.7	5.2 ± 6.5	12.0 ± 11.5	**** Tumour	
BROWN FAT PAD	283.7 ± 125.4	195.1 ± 32.4	25.9 ± 37.2	65.1 ± 81.1	**** Tumour	
SPLEEN	62.6 ± 8.1	61.9 ± 7.2	113.4 ± 35.6	141.4 ± 15.3	**** Tumour	
THYMUS	35.68 ± 12.96	34.02 ± 3.91	17.87 ± 8.62	16.38 ± 9.61	*** Tumour	
LIVER	1118 ± 129	1039 ± 130	841 ± 107	989 ± 74	** Tumour * Interaction	
INTESTINE	1140 ± 103	1167 ± 82	1324 ± 128	1316 ± 119	** Tumour	
TUMOUR	n.a.	n.a.	883 ± 264	1007 ± 253		

*Table 4.1 – Organ masses at section. All values are given as milligram (mean ±SEM). Two way ANOVA with factors Tumour, Training and Tumour-Training interaction and Bonferroni Post-Hoc analysis. Significant effects are represented with * p<0.05, ** p<0.01, *** p<0.005, and **** p<0.001.*

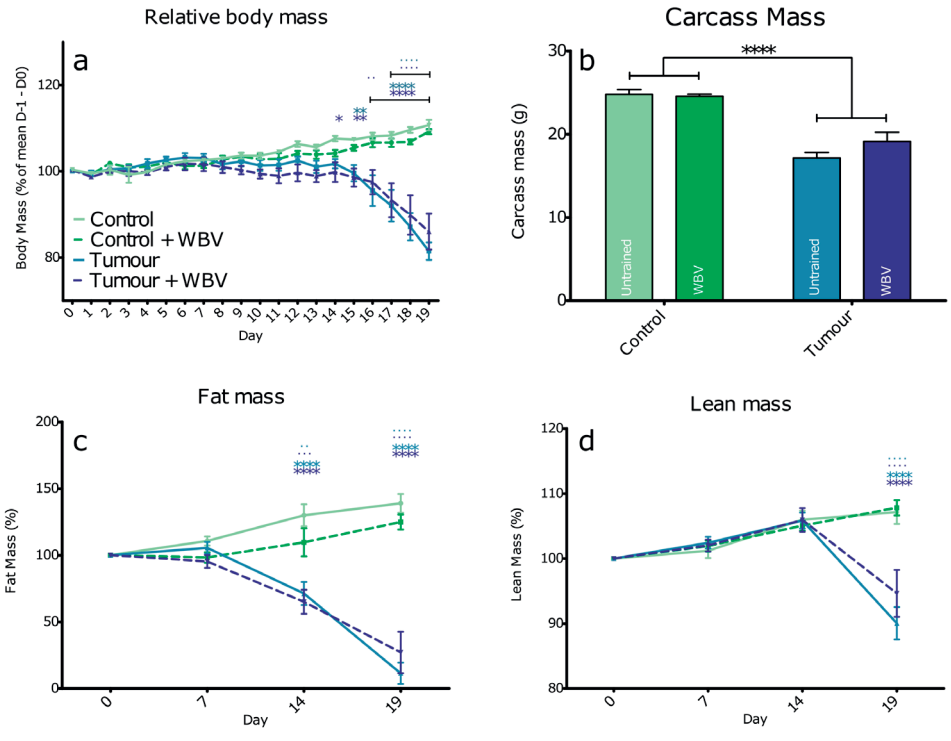

Figure 4.1 *– Relative body mass over time [A], carcass mass at section [B] and body composition [C and D]. Data represent mean ± SEM. In Fig A,C,D *'s indicate significantly different from C and •'s indicate significantly different from C+V. */ •, **/ ••, ***/ ••• and ****/ •••• indicate p<0.05, 0.01, 0.005 and 0.001 respectively. Color of the *'s and •'s indicate group that differs (C light blue or C+V dark blue).*

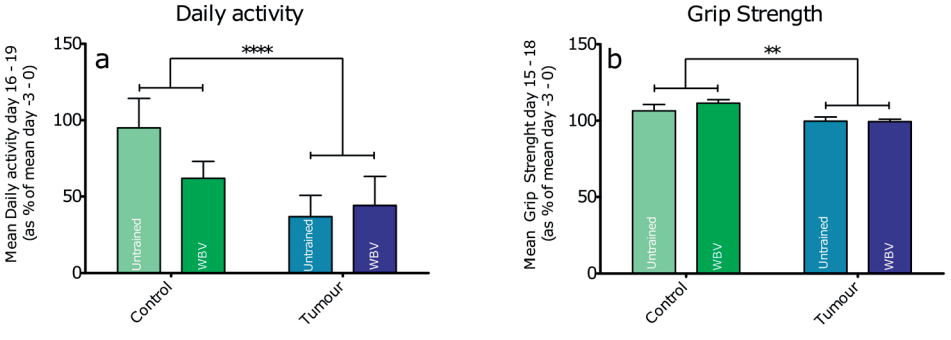

Figure 4.2 *– Mean daily activity [A] and grip strength [B] at the end of the experiment. Data represent mean ± sem. ** and **** indicate 0.01 and 0.001 respectively.*

No training effect on bone mineral density, PTHrP and cytokine levels

Front leg BMD was significantly lower in tumour bearing mice compared to control mice (figure 4.3 A). Plasma PTHrP was significantly higher in tumour bearing groups compared to control groups (figure 4.3 B). BMD and PTHrP correlated significantly with Pearson r of -0.5812 (p = 0.0144) (figure 4.3 C). Plasma INFγ and IL-6 showed an increase due to tumour injection while the other tested cytokines showed no response. Also, no WBV effect was found in any of the cytokines (supplemental figure 4.1).

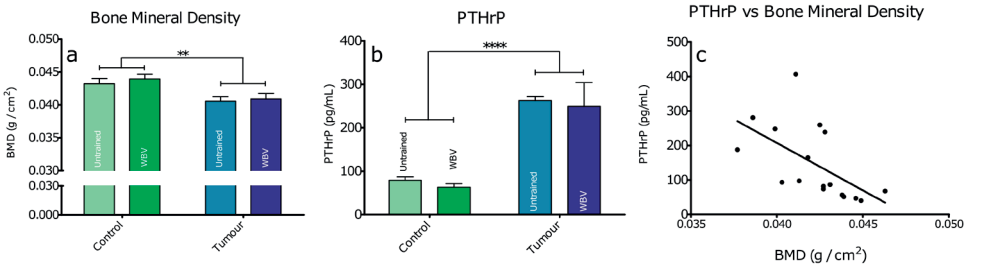

Figure 4.3 *– Front leg BMD [A] and plasma PTHrP [B] at section. Correlation between front leg BMD and plasma PTHrP [C]. Data represent mean ± sem. ** and **** indicate 0.01 and 0.001 respectively.*

WBV increases contraction and relaxation speed in SOL but not in EDL

EDL only showed minor differences in *ex vivo* muscle function. Contraction and relaxation time were slightly longer due to the tumour (figure 4.4 D), however, this was only significantly different between C+V and T at 100 and 143 Hz (CT) and between C and T groups at 83 Hz (RT). In the SOL, clearer differences were present showing a slight WBV effect. Tumour bearing mice without training had a significantly lower F_{max} compared to trained control mice at >83 Hz where the trained tumour bearing mice only differed from C and C+V at higher frequencies (>143 Hz and 167 Hz respectively)(figure 4.5 A). Next to that, force AUC for both the force-frequency as the exercise protocol differed significantly between the tumour bearing groups and the control groups. Clearest training effect was in the contraction and relaxation time and the rate of force development of the SOL. At all frequencies >83 Hz, C+V contracted faster than the T group where T+V and C did not differ from any other groups (figure 4.5 D). Also in the RT, only the T group showed significantly higher RT values compared to both C and C+V where T+V did not differ from the control groups (figure 4.5 E). Rate of force development also differed only between T and C+V with mice in the T group having a lower dF/dt than mice in the C+V group (figure 4.5 F).

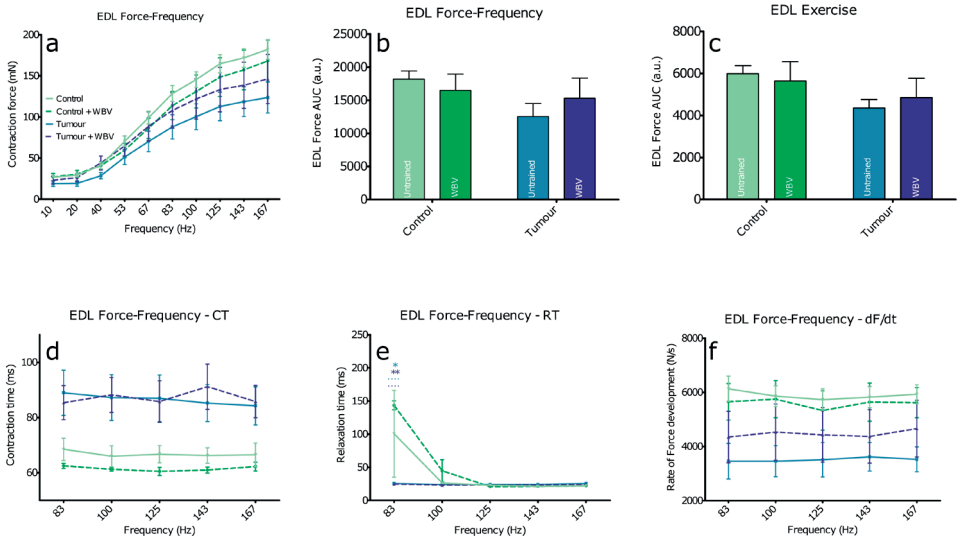

Figure 4.4 *– EDL ex-vivo muscle characteristics. Maximal tetanic force, at different stimulation frequencies [A] and area under the curve of the force-frequency (FF) relationship [B] and the exercise protocol [C]. Contraction time [D], relaxation time [E] and rate of force development [F]. Data represent mean ± SEM. In Fig D and E *'s indicate significantly different from C and •'s indicate significantly different from C+V. */ •, **/ ••, and ****/ •••• indicate p<0.05, 0.01, and 0.001 respectively. Color of the *'s and •'s indicate group that differs (C light blue or C+V dark blue).*

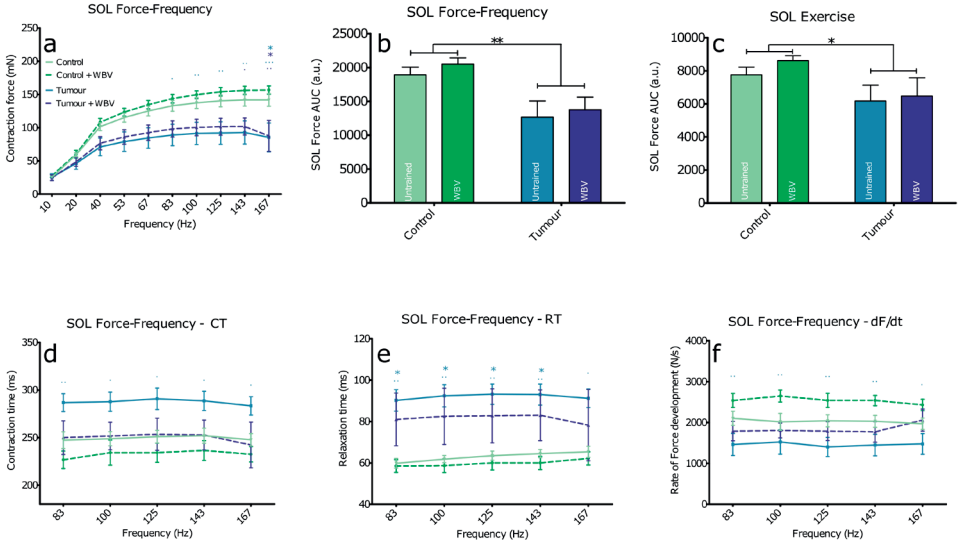

Figure 4.5 *– SOL ex-vivo muscle characteristics. Maximal tetanic force, at different stimulation frequencies [A] and area under the curve of the force-frequency relationship [B] and the exercise protocol [C]. Contraction time [D], relaxation time [E] and rate of force development [F]. Data represent mean ± sem. In Fig A, D, E and F *'s indicate significantly different from C and •'s indicate significantly different from C+V. */ •, **/ ••and ***/ ••• indicate p<0.05, 0.01 and 0.005 respectively. Color of the *'s and •'s indicate group that differs (C light blue or C+V dark blue).*

Tumour affects type II fibres more than type I in SOL, no training effect.

To further investigate the difference in *ex vivo* outcomes in the SOL, we performed an immunofluorescent staining to measure fibre properties of type I dominant and type II dominant fibres. No clear differences between groups were found in total fibre cross sectional area (CSA), type I fibre CSA or type II fibre CSA (figure 4.6 A-C). We did find a tumour effect in fibre CSA ratio (type II/type I CSA) and type II relative abundance with the tumour groups being lower than the control groups indicating a heavier wasting in type II fibres (figure 4.6 D and F).

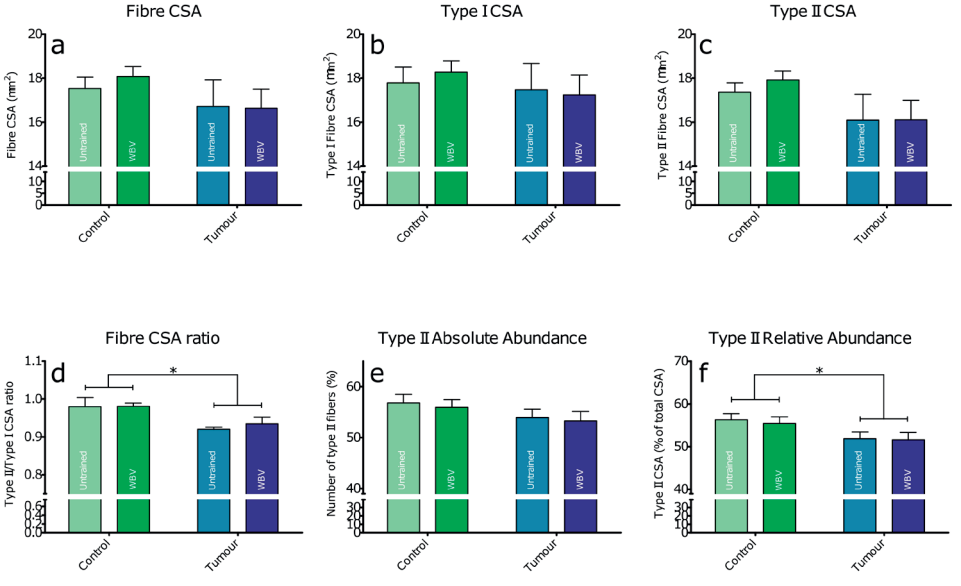

Figure 4.6 *– SOL muscle fibre characteristics. Fibre cross sectional area of all fibres [A], type I dominant fibres [B] and type II dominant fibres [C]. Relative measures for fibre CSA ratio [D], type II dominant fibre abundance (in % of total fibres) [E] and type II dominant relative abundance (sum of total type II CSA as % of sum all fibre CSA) [F]. Data represent mean ± sem. * indicates p<0.05.*

Vibration attenuates tumour-induced effects on gene expression in muscle tissue

In both EDL, SOL and heart samples, WBV reduces the impact of the tumour on the muscle transcriptome. Vibration showed to reduce the number of genes being affected by tumour growth dramatically (figure 7A,C,E) and the log-ratio of all genes (figure 7B,D,F). Number of changed genes was lower in the T+V group in all muscle tissues (43% [EDL], 44% [SOL] and 40% [heart]). The direction of the change was very similar with clear correlations between the log-ratio of all genes in T and T+V groups (Pearson r of 0.94 [EDL], 0.89 [SOL] and 0.84 [Heart]). Moreover, the magnitude of change in gene expression was similar in all tissues where the slope of a linear regression fit was between 0.72 and 0.77 in all tissues. Subsequently, we tested if we could separate groups based on gene expression using a sPLS-DA with two components and a maximum of 50 genes per component (figure 8). Here we noticed that the tumour effect was very distinct explaining 21 – 26% of variance (figure 8A-C) with some common genes in the first component (figure 8D), indicating the tumour effect. The second component separated groups based on training. For all tissues, tumour bearing groups were separated in trained and untrained where for the control groups only in EDL the groups were separated slightly. This indicates that there was a small training effect in the tumour bearing groups, whereas there was little to no training effect in the control groups. The clearest training effect was visible in the cardiac tissue with 9% explained variance. No commonalities were found in the genes driving this training effect in the three different muscle tissues (figure 8E). GSEA shows that the proteasome and RNA pathways are the most abundantly upregulated pathways for skeletal muscle with no significant regulation in heart muscle (figure Sup2). Thermogenesis and oxidative phosphorylation are the most abundant pathways being down-regulated in all muscle tissues. The WBV prevented the upregulation of the proteasome pathway in the SOL but not in the EDL.

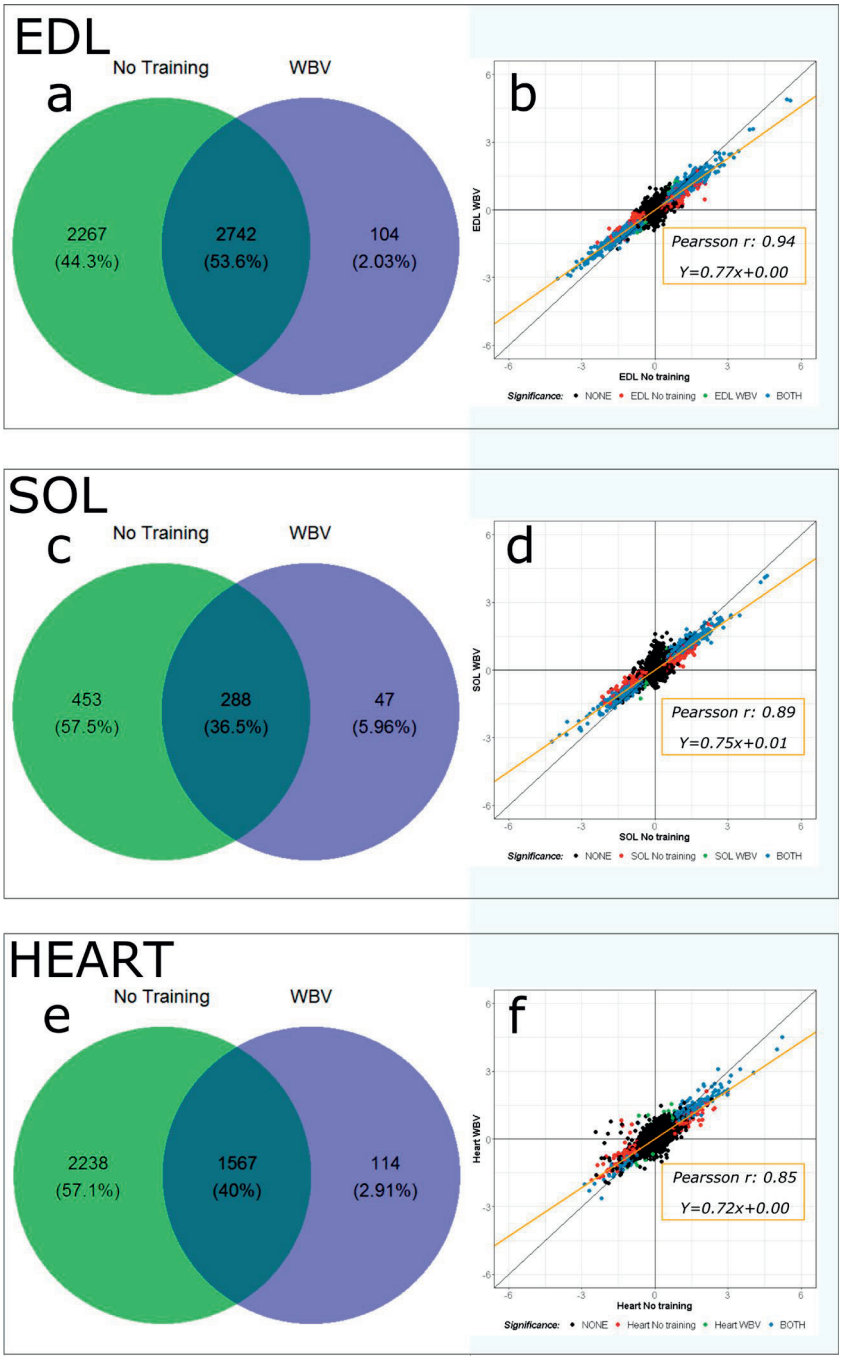

Figure 4.7 *– Microarray results showing the comparison of C with T and T+V group for three different tissues: EDL [A, B], SOL [C, D], and heart [E, F]. Venn diagrams [A,C,E] display number of genes with q<0.01 in T (green) and WBV (blue) mice. Scatter plots [B,D,F] show a correlation and linear regression of log-ratio of all genes from T+V (y-axis) and T (x-axis) compared to C mice with colors indicating significance.*

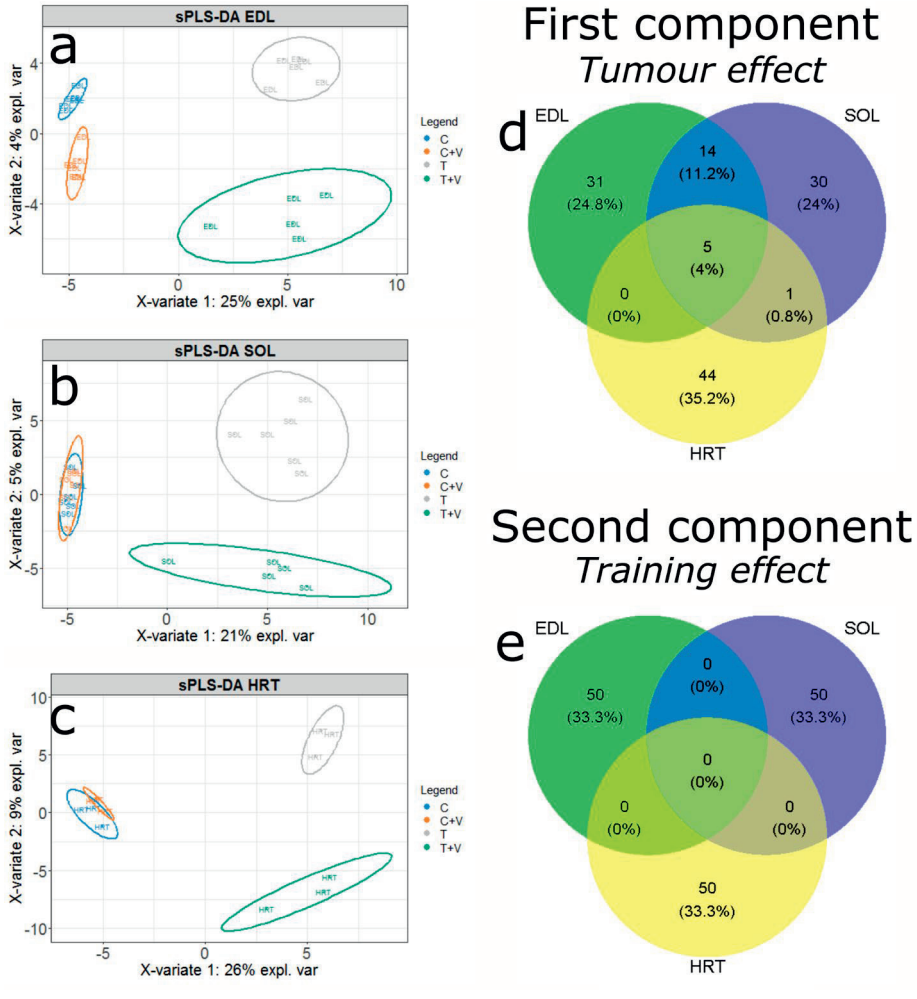

Figure 4.8 *– Microarray results showing a partial least squares discriminant analysis of all four groups with two components and 50 genes per component. sPLS-DA is performed per tissue, EDL [A], SOL [B] and heart [HRT][C]. Venn diagrams display genes per tissue in component 1 [D] and 2 [E].*

Discussion

The current study primarily aimed to determine possible protective effects on loss of muscle mass and function of WBV on cancer induced cachexia in the tumour-induced C26 cachexia mouse model. Our most interesting finding was that WBV reduced the effects of the tumour on muscle gene expression in both EDL, SOL and heart. We also found that WBV increased EDL muscle mass in the control group and improved muscle function in the SOL of tumour bearing mice. Surprisingly, there was a trend for WBV to reduce daily activity in control animals. Although not significant, WBV appeared to affect BMD and PTHrP, which were correlated. Both whole body lean and fat mass were lower in tumour bearing groups compared to control groups on day 19, which was preceded by lower fat mass and body weight at day 14; however, training did not affect either fat or lean mass. Looking at the plasma levels of several cytokines, only IL-6 and IFNγ were higher in tumour bearing groups compared to control groups. WBV affected *ex vivo* muscle function in MHC type I dominant SOL. In isolated SOL, contractility was improved with CT and RT being lower and dF/dt being higher in C+V compared to T group, where the T+V group did not differ from the control groups. Overall gene expression profiles showed a decreased tumour effect in both EDL, SOL and heart upon training. However, we were not able to pinpoint specific genes or pathways involved in a training effect. All results combined suggest that WBV might have a positive and partly protective effect on cachexia-induced alterations of muscle physiology in a C26 mouse model.

When we compare our results with other studies using the C26 model, we see that effects of tumour inoculation are largely similar. We found a clear reduction in body, muscle and fat mass of a similar order of magnitude as reported in comparable studies[18,37,38]. Moreover, reductions in daily activity[18], grip strength[39] and BMD[40] are similar to other studies. On cytokine levels we saw a clear IL-6 induction and a small reduction of IFNγ where others also found effects on TNF-α and IL-4[38]. When looking at muscle specific effects we see similar effects of the tumour compared to other studies with decreases in maximal force and increases in contraction and relaxation times[18,41]. Although we do not see an effect in the EDL, this is likely to be a power issue since figures clearly show a trend in the tumour effect decreasing maximal force and increasing contraction and relaxation times. For fibre type-specific effects, our results are also in line with other studies concerning the heavier tumour burden on type II fibres compared to type I fibres[41]. Taken together, our tumour model largely supports previous findings.

We only see mild effects of the WBV with little to no effect on systemic outcomes with our major finding being the effect on gene expression. Literature on effects of WBV in rodents shows some contradicting results. In our *ex vivo* set-up we saw an improvement in

contractility and a trend of improved strength. This is in line with literature where WBV in healthy mice was shown to partially improve muscle contractility, specifically strength and relaxation rates[14]. However, we could not explain our results based on changes in muscle MHC content or muscle fibre size. A 6-week WBV training in healthy mice did show to increase total cross-sectional area of the soleus muscle as well as its type I and II muscle fibres[16]. A study into the long-term effects of WBV on the gastrocnemius muscle in rats found a decrease in type I content in favour of type II[42]. On the other hand, two other studies found no significant effect of WBV on myosin heavy chain (MHC) isoforms in the soleus muscle of mice [14,43]. Possibly, we do not see an effect on muscle morphology due to the short period of training in our study. Similar to our results WBV was not able to improve musculoskeletal function in a specific muscle disease like Duchenne muscular dystrophy[17]. However, it should be noted that the underlying mechanisms in Duchenne muscular dystrophy are different from those in cancer induced wasting. A recent study comparing aerobic training (treadmill exercise) with resistance training (ladder climbing) in C26 mice indicated possible beneficial effects of aerobic training and not resistance training[39]. However, aerobic training was only able to mildly preserve muscle size, sensory motor function and relative *m. gastrocnemius* mass but was unable to prevent weight loss[39]. Another study in $Apc^{Min/+}$ mice showed that moderate treadmill exercise is able to attenuate body and muscle mass loss in IL-6-dependent cachexia[44]. Moreover, oxidative capacity was improved which is an important factor in cachexia since mitochondria play a key role in cachexia[45]. This can also be seen in our GSEA results with oxidative phosphorylation coming up as one of the top enriched pathways. Taken together, our results and those from previous studies seem to indicate that different forms of training have mostly small but distinct effects. In Lewis lung carcinoma bearing mice, endurance training combined with supplementation of the poly unsaturated fatty acid eicosapentaenoic acid proved to partially rescue muscle strength and mass[46]. Moreover, a specific nutritional combination high in fish oil and leucine was able to reduce cachectic symptoms and improve functional performance[18]. Therefore, it could be beneficial to study whether combining whole body vibration training with endurance training and targeted nutrition might prove useful.

As to the best of our knowledge, this is the first study looking at the possible beneficial effects of WBV in cachexia. Since we examined the possible effects on different outcomes, both *in vivo* and *ex vivo*, we were able to pinpoint the level at which vibration training might have an effect. Since we only see mild training effects, mostly on gene expression, the C26 model might have been too acute to study long term effects of a low impact training as WBV. It might be beneficial to study a multi-targeted treatment including exercise and nutrition.

To conclude, our data suggest that WBV had no effect on systemic factors in the present set-up, but caused a small effect on muscle specific cachexia related outcomes in tumour bearing mice. No effects were found on body mass, body composition, inflammation or bone. Although small, muscle specific findings are very consistent and no adverse effects were found. Specifically, the gene-expression data are promising since all log-ratios are changing in the same direction. This merits follow-up studies applying for example longer treatment periods or as part of a multiple-target intervention.

References

1. De Blaauw, I., Deutz, N. E. P. & Von Meyenfeldt, M. F. Metabolic changes of cancer cachexia — second of two parts. *Clin. Nutr.* **16,** 223–228 (1997).
2. De Blaauw, I., Deutz, N. E. P. & Von Meyenfeldt, M. F. Metabolic changes in cancer cachexia — first of two parts. *Clin. Nutr.* **16,** 169–176 (1997).
3. Nitenberg, G. & Raynard, B. Nutritional support of the cancer patient: issues and dilemmas. *Crit Rev Oncol Hematol* **34,** 137–68. (2000).
4. Tisdale, M. J. Mechanisms of Cancer Cachexia. *Physiol. Rev.* **89,** 381–410 (2009).
5. Laviano, A., Meguid, M. M., Inui, A., Muscaritoli, M. & Rossi-Fanelli, F. Therapy insight: Cancer anorexia-cachexia syndrome--when all you can eat is yourself. *Nat. Clin. Pract. Oncol.* **2,** 158–65 (2005).
6. Fearon, K., Arends, J. & Baracos, V. Understanding the mechanisms and treatment options in cancer cachexia. *Nat. Rev. Clin. Oncol.* **10,** 90–9 (2013).
7. Witkamp, R. F. & van Norren, K. Let thy food be thy medicine….when possible. *Eur. J. Pharmacol.* **836,** 102–114 (2018).
8. Stene, G. B. *et al.* Effect of physical exercise on muscle mass and strength in cancer patients during treatment-A systematic review. *Crit. Rev. Oncol. Hematol.* **88,** 573–593 (2013).
9. Kilgour, R. D. *et al.* Cancer-related fatigue: the impact of skeletal muscle mass and strength in patients with advanced cancer. *J. Cachexia. Sarcopenia Muscle* **1,** 177–185 (2010).
10. Bogaerts, A. C. G. *et al.* Effects of whole body vibration training on cardiorespiratory fitness and muscle strength in older individuals (a 1-year randomised controlled trial). *Age Ageing* **38,** 448–454 (2009).
11. Salhi, B. *et al.* Rehabilitation in patients with radically treated respiratory cancer: A randomised controlled trial comparing two training modalities. *Lung Cancer* **89,** 167–174 (2015).
12. Lau, R. W. *et al.* The effects of whole body vibration therapy on bone mineral density and leg muscle strength in older adults: a systematic review and meta-analysis. *Clin. Rehabil.* **25,** 975–988 (2011).
13. Mikhael, M., Orr, R. & Fiatarone Singh, M. A. The effect of whole body vibration exposure on muscle or bone morphology and function in older adults: A systematic review of the literature. *Maturitas* **66,** 150–157 (2010).
14. McKeehen, J. N. *et al.* Adaptations of mouse skeletal muscle to low-intensity vibration training. *Med. Sci. Sports Exerc.* **45,** 1051–9 (2013).
15. Ceccarelli, G. *et al.* Low-amplitude high frequency vibration down-regulates myostatin and atrogin-1 expression, two components of the atrophy pathway in muscle cells. *J. Tissue Eng. Regen. Med.* **8,** 396–406 (2014).
16. Xie, L., Rubin, C. & Judex, S. Enhancement of the adolescent murine musculoskeletal system using low-level mechanical vibrations. *J. Appl. Physiol.* **104,** 1056–1062 (2008).
17. Novotny, S. A. *et al.* Low intensity, high frequency vibration training to improve musculoskeletal function in a mouse model of Duchenne muscular dystrophy. *PLoS One* **9,** e104339 (2014).
18. van Norren, K. *et al.* Dietary supplementation with a specific combination of high

protein, leucine, and fish oil improves muscle function and daily activity in tumour-bearing cachectic mice. *Br. J. Cancer* **100,** 713–22 (2009).
19. van Norren, K. *et al.* Behavioural changes are a major contributing factor in the reduction of sarcopenia in caloric-restricted ageing mice. *J. Cachexia. Sarcopenia Muscle* **6,** 253–268 (2015).
20. van Dijk, M. *et al.* Improved muscle function and quality after diet intervention with leucine-enriched whey and antioxidants in antioxidant deficient aged mice. *Oncotarget* **7,** 17338–17355 (2016).
21. Gorselink, M. *et al.* Mass-dependent decline of skeletal muscle function in cancer cachexia. *Muscle Nerve* **33,** 691–3 (2006).
22. Plas, R. L. C. *et al.* Muscle contractile properties as an explanation of the higher mean power output in marmosets than humans during jumping. *J. Exp. Biol.* **218,** 2166–2173 (2015).
23. Smith, L. R. & Barton, E. R. SMASH – semi-automatic muscle analysis using segmentation of histology: a MATLAB application. *Skelet. Muscle* **4,** 21 (2014).
24. Briguet, A., Courdier-Fruh, I., Foster, M., Meier, T. & Magyar, J. P. Histological parameters for the quantitative assessment of muscular dystrophy in the mdx-mouse. *Neuromuscul. Disord.* **14,** 675–682 (2004).
25. Lin, K. *et al.* MADMAX - Management and analysis database for multiple ~omics experiments. *J. Integr. Bioinform.* **8,** 160 (2011).
26. Irizarry, R. A. *et al.* Exploration , Normalization , and Summaries of High Density Oligonucleotide Array Probe Level Data. 249–264 (2018).
27. Dai, M. *et al.* Evolving gene/transcript definitions significantly alter the interpretation of GeneChip data. *Nucleic Acids Res.* **33,** e175 (2005).
28. Ritchie, M. E. *et al.* Limma powers differential expression analyses for RNA-sequencing and microarray studies. *Nucleic Acids Res.* **43,** e47 (2015).
29. Sartor, M. A. *et al.* Intensity-based hierarchical Bayes method improves testing for differentially expressed genes in microarray experiments. *BMC Bioinformatics* **7,** 1–17 (2006).
30. Benjamini, Y. & Hochberg, Y. Controlling the False Discovery Rate: A Practical and Powerful Approach to Multiple Testing. *Source J. R. Stat. Soc. Ser. B J. R. Stat. Soc. Ser. B J. R. Stat. Soc. B* **57,** 289–300 (1995).
31. Wilkinson, L. ggplot2: Elegant Graphics for Data Analysis by WICKHAM, H. *Biometrics* **67,** 678–679 (2011).
32. Chen, H. & Boutros, P. C. VennDiagram: a package for the generation of highly-customizable Venn and Euler diagrams in R. *BMC Bioinformatics* **12,** 35 (2011).
33. Lê Cao, K.-A., Boitard, S. & Besse, P. Sparse PLS discriminant analysis: biologically relevant feature selection and graphical displays for multiclass problems. *BMC Bioinformatics* **12,** 253 (2011).
34. Subramanian, A. *et al.* Gene set enrichment analysis: A knowledge-based approach for interpreting genome-wide expression profiles. *Proc. Natl. Acad. Sci.* **102,** 15545–15550 (2005).
35. Kanehisa, M., Sato, Y., Kawashima, M., Furumichi, M. & Tanabe, M. KEGG as a reference resource for gene and protein annotation. *Nucleic Acids Res.* **44,** D457–D462 (2016).
36. Yu, G., Wang, L.-G., Han, Y. & He, Q.-Y. clusterProfiler: an R Package for Comparing

Biological Themes Among Gene Clusters. *Omi. A J. Integr. Biol.* **16,** 284–287 (2012).
37. Dwarkasing, J. T. *et al.* Hypothalamic food intake regulation in a cancer-cachectic mouse model. *J. Cachexia. Sarcopenia Muscle* **5,** 159–169 (2014).
38. Faber, J. *et al.* Beneficial immune modulatory effects of a specific nutritional combination in a murine model for cancer cachexia. *Br. J. Cancer* **99,** 2029–36 (2008).
39. Khamoui, A. V. *et al.* Aerobic and resistance training dependent skeletal muscle plasticity in the colon-26 murine model of cancer cachexia. *Metabolism* **65,** 685–698 (2016).
40. Bonetto, A. *et al.* Differential Bone Loss in Mouse Models of Colon Cancer Cachexia. *Front. Physiol.* **7,** 679 (2017).
41. Roberts, B. M., Frye, G. S., Ahn, B., Ferreira, L. F. & Judge, A. R. Cancer cachexia decreases specific force and accelerates fatigue in limb muscle. *Biochem. Biophys. Res. Commun.* **435,** 488–92 (2013).
42. Łochyński, D., Kaczmarek, D., Rędowicz, M. J., Celichowski, J. & Krutki, P. Long-term effects of whole-body vibration on motor unit contractile function and myosin heavy chain composition in the rat medial gastrocnemius. **13,** 430–441 (2013).
43. Murfee, W. L. *et al.* High-frequency, low-magnitude vibrations suppress the number of blood vessels per muscle fiber in mouse soleus muscle. *J. Appl. Physiol.* **98,** 2376–2380 (2005).
44. Puppa, M. J. *et al.* The effect of exercise on IL-6-induced cachexia in the Apc (Min/+) mouse. *J. Cachexia. Sarcopenia Muscle* **3,** 117–37 (2012).
45. van der Ende, M. *et al.* Mitochondrial dynamics in cancer-induced cachexia. *Biochim. Biophys. Acta - Rev. Cancer* **1870,** 137–150 (2018).
46. Penna, F. *et al.* Combined approach to counteract experimental cancer cachexia: Eicosapentaenoic acid and training exercise. *J. Cachexia. Sarcopenia Muscle* **2,** 95–104 (2011).

Supplemental figures

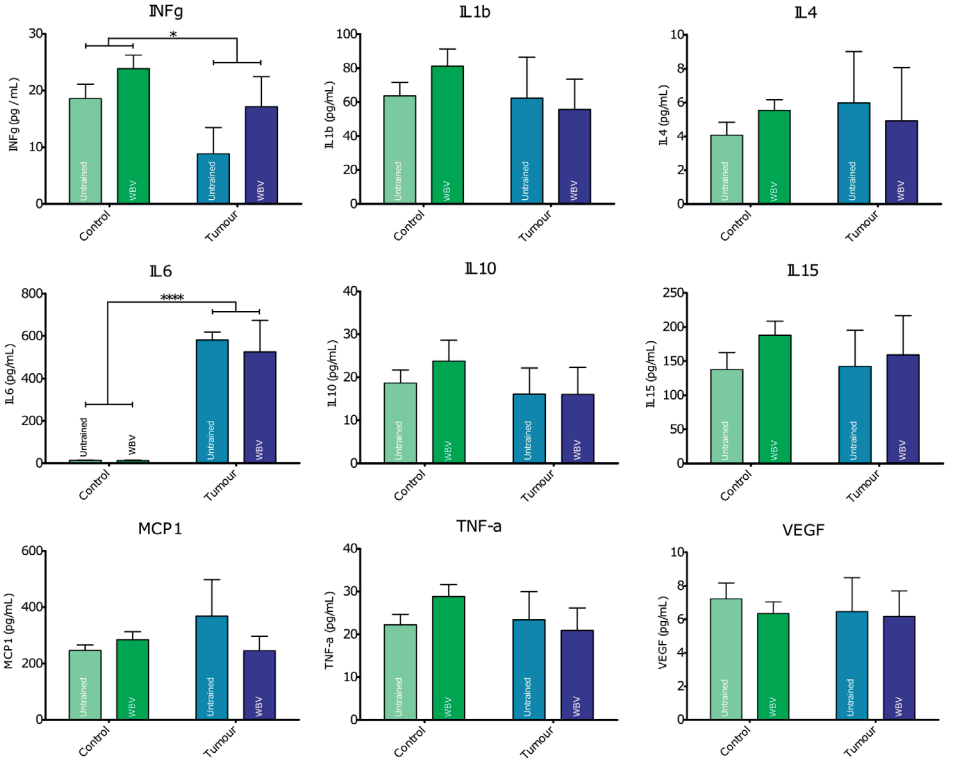

Supplemental figure 4.1 *– Plasma cytokine levels. Data represent mean ± sem. In Fig D and E *'s indicate significantly different from C and +'s indicate significantly different from C+V. * and **** indicate p<0.05 and 0.001 respectively.*

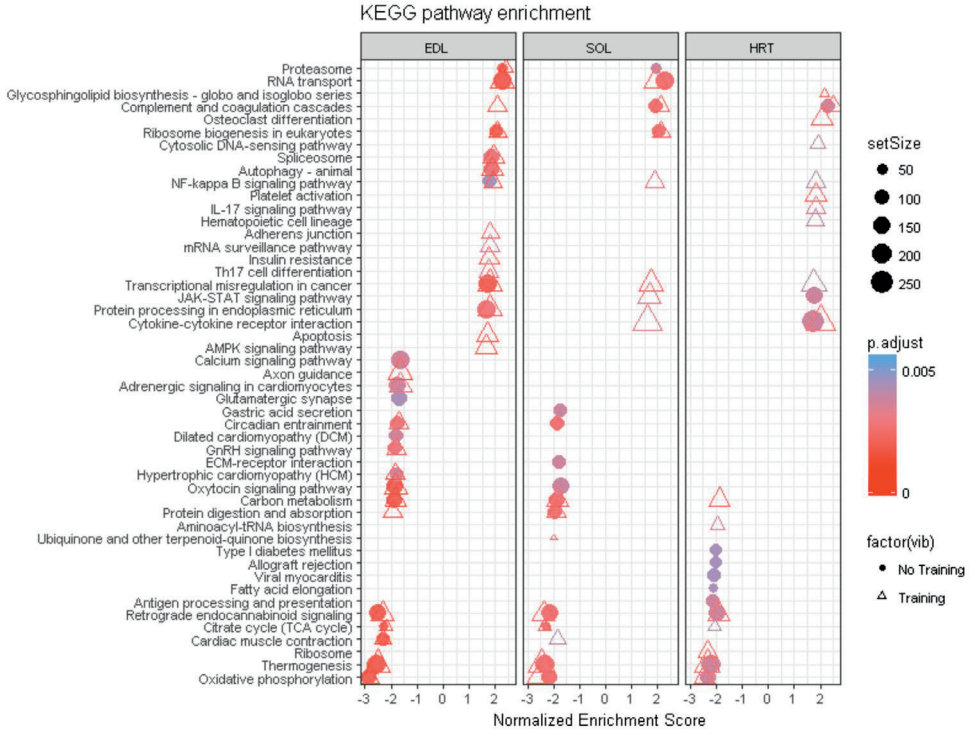

Supplemental figure 4. 2 *– Microarray results showing enrichment of KEGG pathways of tumour groups (with and without WBV) compared to control group without WBV.*

Still from supplemental movie 4.3 *– Short clip showing the reaction of the mice to the start of the vibration training.*

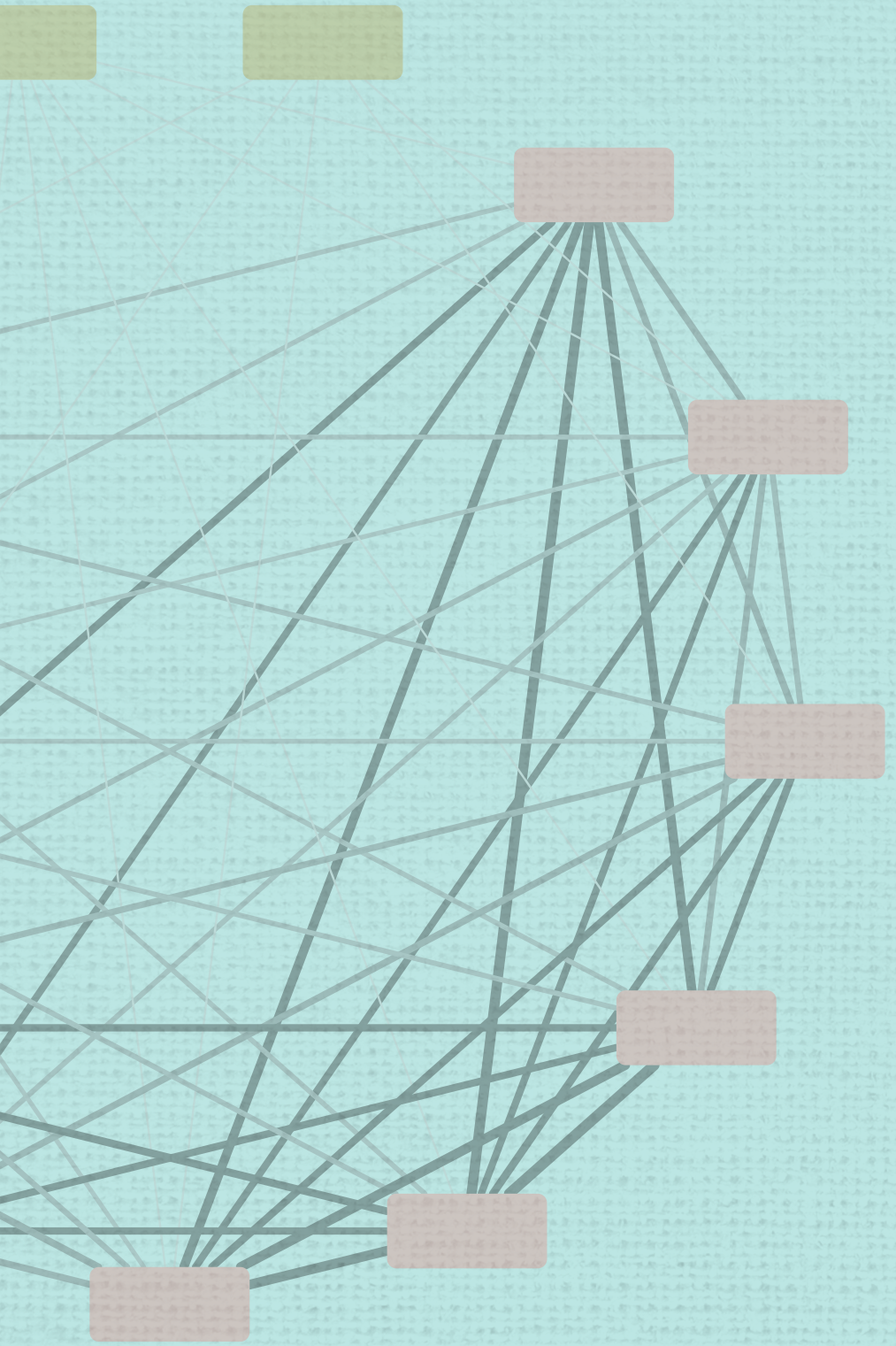

Chapter 5

Relevance of cancer cachexia animal models – comparison of muscle whole genome gene expression in human and animal cachexia

Rogier L.C. Plas
Guido Hooiveld
Renger F. Witkamp
Klaske van Norren

Submitted

Abstract

Background Cancer cachexia is a complex and multi-factorial syndrome. As currently available therapeutic options are limited, more in-depth knowledge on cachexia pathophysiology and the underlying molecular mechanisms remains warranted. Studies with animal models provide useful insights but they only mimic the human situation to a certain degree. Furthermore, there is heterogeneity in the design of published animal studies and outcomes. To further address this issue, we performed a comparative study analysing muscle whole genome gene expression of different cachexia studies in mice and human.

Methods We selected data sets from the NCBI Gene Expression Omnibus database containing muscle gene expression data measured by micro-array or RNA-sequencing, at least comprising a cachectic/tumour bearing group (n>3) and a non-cachectic/control group (n>3). This provided 12 datasets; 9 from mouse models and 3 human datasets. All datasets were quality checked, normalised and annotated. Datasets were merged and compared at different levels. General similarity and differences in gene expression were determined using ordered list analysis and principal component analysis (PCA). Moreover, similarities and differences at pathway level were studied by applying gene set enrichment analysis (GSEA) of KEGG pathways.

Results Animal models displayed similarities to each other and to human datasets at different levels and with different processes. At the gene level, a similarity analysis indicated little similarity between the animal models and the human datasets, while animal models showed high similarity. Only one of the C26 mice models (GSE121972) showed significant similarity to more than one human dataset. Moreover, one human dataset comparing cachectic and non-cachectic cancer patients showed no similarity to any of the other datasets. PCA results indicated that a xenograft model showed most different expression from the other datasets and the Lewis lung carcinoma model to be least different from the human datasets. GSEA results showed four pathways clearly standing out across experiments with downregulation of oxidative phosphorylation and thermogenesis pathway, and upregulation of the proteasome and RNA transport pathway. However, these pathways were not consistently changed in the human datasets.

Conclusions Our comparative analysis showed that there is currently no basis to define a preferred animal model for human cachexia. More human datasets containing proper controls are needed. Repetition of the current analysis upon publication of additional human datasets is warranted.

Introduction

Cachexia is a multifactorial syndrome characterised by disease-induced progressive loss of muscle and/or fat mass. It is often present in patients with chronic kidney disease, heart failure, COPD or cancer. In many patients cachexia contributes to reduced treatment efficacy and quality of life. Experts generally agree that cachexia should be treated with a multimodal approach addressing dietary intake, systemic inflammation and physical activity[1,2]. These different treatment components are often studied using different mouse models. The current study aimed to evaluate the relevance of different animal models mimicking human cancer cachexia by comparing muscle gene expression in different mouse models with that in human cancer cachexia. To this end, we used a big data approach by analysing publicly available datasets present in the GEO database containing whole genome gene expression measured by either microarray or sequencing.

Different types of tumours can cause cachexia both directly, by secreting cachexia-inducing factors, and indirectly, by triggering a systemic inflammatory process. To simulate human cancer cachexia and investigate treatment options, different types of animal models exist[3–10]. The traditional and most common models, i.e. C26 or Lewis Lung Carcinoma (LLC), use direct injection of *in vitro* cultured tumour cells[3,4,6–8,10]. These are usually injected in the flank or muscle of the mouse where they grow into a solid tumour. More recent are models with genetic modifications causing spontaneous tumours[5], models using adenoviruses to induce tumour development[9], and xenograft models where tumour cells are harvested from human tumours and implanted in mice[8]. The difference between the models not only lies in the type of tumour induction. Different models have different time-spans ranging from 14 days to 8.5 weeks after tumour induction. In addition to the different types of models, experimental conditions may also vary between experiments using the same model. Despite these differences, all these models aim to mimic human cancer cachexia. To assess animal model relevance, meta-analyses and systematic reviews have been performed on differences and commonalities of molecular processes between mice and men[11,12]. However, no studies directly compared data of molecular processes driving the cachexia in animals or humans, which makes the relevance of the animal models used a subject for debate. Therefore, our aim was to elucidate possible differences and commonalities in molecular processes in muscle tissues from different cachexia samples.

Whole genome gene expression of muscle tissue has been measured in several cachexia studies using micro array analysis or RNA sequencing. Upon publication of these whole genome gene expression studies, raw data is often made available via the NCBI Gene Expression Omnibus database. By comparing the different datasets using a big data approach, differences and similarities between models and experimental conditions can be

examined. Moreover, possible knowledge can be gathered on underlying processes causing muscle wasting and on possible differences between animal models for cancer cachexia and human cancer cachexia.

Materials and Methods

Tumour model Dataset inclusion

We selected data series present in the NCBI Gene Expression Omnibus database using the keywords *cachexia* or *(cancer AND skeletal muscle).* From these, we selected those series containing muscle gene expression data of a cachectic/tumour bearing group (n>3) and a non-cachectic/control group (n>3). This provided 12 data series; 9 from mouse models and 3 human datasets (figure 5.1 and table 5.1).

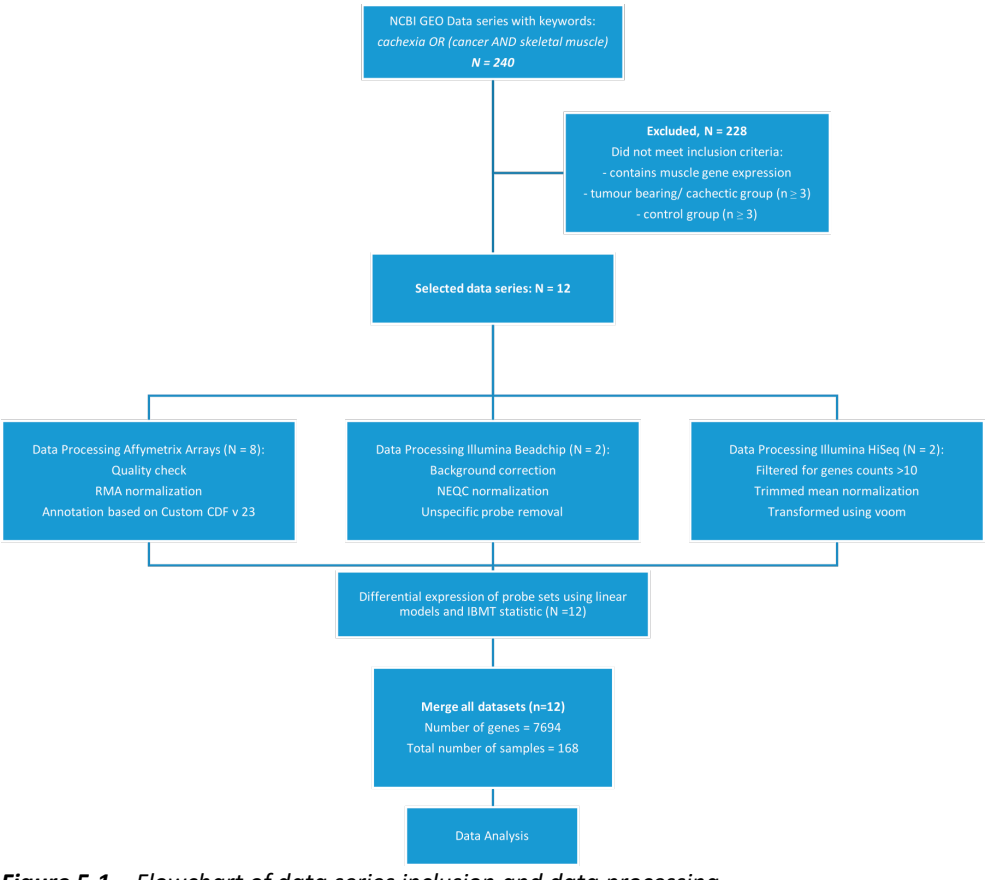

Figure 5.1 *– Flowchart of data series inclusion and data processing.*

GEOCODE ABREVIATION	STUDY	MODEL	CONTROL	TUMOUR	DURATION	MUSCLE	PLATFORM
GSE24112 C26 Quad	Bonetto A et al., *PloS ONE*, 2015	Mouse - C26	4	4	24 d	Quadriceps	Illumina MouseWG-6 v2.0
GSE48363 C26 Gas+Plan	Cornwell EW et al., *PloS ONE*, 2014	Mouse - C26	3	3	25 d	Gastrocnemius and Plantaris mix	Affymetrix Mouse Gene 1.0 ST
GSE56555 C26 Tib	Judge SM et al., *BMC Cancer*, 2014	Mouse - C26	4	3	~26 d	Tibialis Anterior	Affymetrix Mouse Gene 1.0 ST
GSE63032 C26 Gastr	Shum AM et al., *Physiol. Genomics*, 2015	Mouse - C26	3	3	14 - 19 d	Gastrocnemius	Affymetrix Mouse Gene 1.0 ST
GSE121972 C26 EDL / SOL	Plas RLC, *journal 2018*	Mouse - C26	6	6	19 d	Soleus & Extensor Digitorum Longus	Affymetrix Mouse Gene 1.1 ST
GSE114820 LLC Gastr	Blackwell T et al., *Physiol Genomics*, 2018	Mouse - LLC	8	8	4 wk	Gastrocnemius	Illumina HiSeq 2500 (Mus musculus)
GSE107470 NSCLC Gastr	Goncalves M et al., PNAS, 2018	Mouse - non small cell lung cancer (adenovirus induced)	5	5	8.5 wk	Gastrocnemius	Illumina HiSeq 4000 (Mus musculus)
GSE51931 PAN BicFem	Gilabert M et al., *J Cell Physiol*, 2014	Mouse - Pancreatic cancer (spontaneous)	3	3	8 - 12 wk	Biceps Femoris	Affymetrix Mouse Gene 1.0 ST
GSE80081 XEN Quad	Fukawa T et al., *Nat Med*, 2016	Mouse - Human Xenograft (RXF393 vs SKRC39)	3	3	22 d	Quadriceps	Illumina MouseWG-6 v2.0
GSE85017 HUM_NC RectAbd	Narasimhan A et al., *JCSM*, 2017	Human - Pancreatic and Colorectal cancer (cachectic vs non cachectic)	19 *	21	40 - 83 y	Rectus Abdominis	Affymetrix Human Transcriptome Array 2.0
GSE34111 HUM Quad	Gallagher I et al., *Clin Cancer Res*, 2012	Human - upper gastrointestinal cancer (cancer vs control)	6	12	~65 y	Quadriceps	Affymetrix GeneChip Human Genome U133 Plus 2.0
GSE18832 HUM RectAbd	Stephens NA et al., *Genome Med.*, 2010	Human - upper gastrointestinal cancer (cancer vs control)	3	18	51 y (control) 65.5 y (cancer)	Rectus Abdominis	Affymetrix GeneChip Human Genome U133 Plus 2.0

Table 5.1 *– Overview of basic characteristics of included datasets. *Control group in GSE85017 consisted of non-cachectic cancer patients*

Data processing

All datasets were quality checked, normalised and annotated with the latest annotations available using R statistical computing software (https://www.r-project.org/). The flowchart in figure 5.1 summarizes data selection and processing work flow. Three different measurement modalities were distinguished; (1) Affymetrix arrays, (2) Illumina bead-chip arrays and (3) Illumina HiSeq RNA-sequencing results. (1) Data obtained with Affymetrix arrays were quality checked and normalized using the robust multi-array analysis (RMA) algorithm[13] as implemented in the Bioconductor package *AffyPLM*. Probe sets were identified with genome information according to Dai *et al.*[14] based on annotations provided by the Entrez Gene database (custom CDF v23). (2) Data collected with Illumina beadchip arrays were background corrected and normalized using quantile normalization (neqc)[15]. Subsequently, unspecific probes were removed[16] (3) Illumina HiSeq RNA-sequencing results were filtered for genes having an expression level greater than 10 counts. Next to that, the library size and the experimental design was taken into account and corrected for, using the Bioconductor package *edgeR*[17,18]. Subsequently, library size differences were adjusted using the trimmed mean of M-values normalization method[19], implemented in the Bioconductor package *edgeR*[18]. Counts were then log-transformed and the observed mean-variance trend was converted into precision weights by the voom function[20] in the Bioconductor package *limma*[21].

After normalization, all different data types were analysed similarly. Differential expression of probe sets (genes) was determined using linear models (package *limma*) and an intensity-based moderated t-statistic[21,22]. For each data set, samples from tumour bearing animals/patients were compared to a healthy control group, with one exception: in GSE85017 a comparison between cachectic and non-cachectic cancer patients was made, because this dataset did not contain a non-cancer control group. Genes with a *p*-value of $p < 0.01$ were considered to be significantly differing between groups. Individual sample values were scaled based on full groups to enable comparison of samples obtained in separate experiments. Mouse and human expression data was merged based on the gene homology database obtained from the Mouse Genome Informatics website, The Jackson Laboratory, Bar Harbor, Maine, accessible via the World Wide Web (URL: http://www.informatics.jax.org) [download September, 2017]. For all subsequent analyses, only genes measured in all experiments were taken into account, which resulted in a final dataset of 7694 genes and 168 samples.

Data analysis

All data analysis was performed in R. Data visualisation was done using *ggplot2* and *corrplot* [23,24]. For similarity analysis we used the Bioconductor R library *OrderedList* [25]. Here, we used ranked listed based on the t-test statistic to compare all experiments in a pairwise fashion. Similarity scores with $p<0.05$ were normalized and visualized in an association matrix using *corrplot* and in a network plot using *Cytoscape* [26]. To assess differences between experiments, a sparse principal component analysis (sPCA) was performed available in the *mixOmics* package [27,28]. Using this sPCA, we reduced the dimensions and identified the top genes responsible for variation between the different datasets. Based on the number of different experimental types we selected the number of components to be (n-1) and we specified to keep the 100 genes most responsible for the variation within each component. Changes in individual genes were related to changes in pathways by gene set enrichment analysis (GSEA)[29] using the subset of metabolic and signalling pathways retrieved from the expert-curated Kyoto Encyclopedia of Genes and Genomes (KEGG) database[30]. For each comparison, genes were ranked on their t-value that was calculated by the empirical Bayes method. Statistical significance of GSEA results was determined using 10,000 permutations. GSEA and visualization was performed using the Bioconductor package *clusterProfiler* [31]. To assess variation between separate samples of all datasets, an sPCA with 6 components of each 25 genes was performed on gene expression, normalized per experiment, of individual samples of all experiments (n=168).

Results

Included datasets

We identified data sets from five different animal models that met our criteria for inclusion: two inoculation models; C26 (n=5) and Lewis Lung Carcinoma (LLC), one adenovirus-induced model (non-small cell lung cancer [NSCLC]), one spontaneous model (pancreatic cancer) and one xenograft model. General model characteristics differ in several aspects. The C26 model and the human xenograft model are rather acute models with a duration between 14 – 25 days between inoculation and sacrifice. The LLC model has a slightly longer experimental duration of 4 weeks, and the NSCLC and pancreatic cancer have a duration of >8 weeks. Moreover, different muscle types were used for analysis in the animal models.
Next to this, we included 3 human datasets, one of which containing whole genome gene expression data of *m. rectus abdominis* samples of cachectic or non-cachectic pancreatic and colorectal cancer patients, one containing quadriceps samples of upper gastrointestinal cancer (UGI) patients and healthy controls, and one containing *m. rectus abdominis* samples

of UGI patients and weight stable (WS) patients undergoing surgery for benign, non-inflammatory conditions.

Number of significantly changed gene transcription activities

Analysis of the number of significantly changed gene transcription activities in each experiment showed that there were large differences in the magnitude of tumour effects on the muscle (figure 5.2). The C26 model was found to be overall the most invasive model affecting expression of up to 56% (GSE56555) of all genes. However, this model also showed considerable between-study variation, as in the apparently least invasive study (GSE63032) transcription of only 16% of all genes was changed. The other mouse models showed on average a lower number of changed gene transcription activities. The adenovirus-induced non-small cell lung cancer (NSCLC, GSE107470) affected 31%, the Lewis Lung Carcinoma (LLC, GSE114820) affected 29%, the human xenograft model (GSE80081) affected 16%, and the spontaneous pancreatic cancer (GSE81931) affected transcription of 12% of all genes. Compared to these mouse models, human datasets showed only very mild effects with 6%, 2% and 1% of all genes being affected in transcription (respectively GSE34111, GSE85017 and GSE18832).

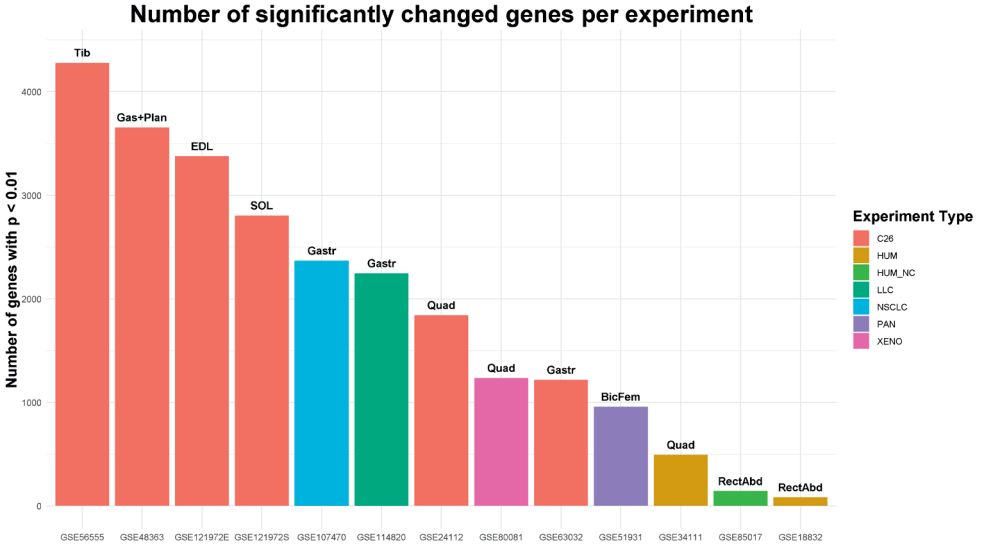

Figure 5.2 – Number of significantly changed genes (p<0.01) per experiment based on the complete dataset containing gene expression of 7694 genes present in all datasets.

Similarity analysis

Subsequently, we created a similarity network and matrix (figure 5.3 and 5.4) based on our pair-wise similarity analysis. Results showed that the highest similarity is among the C26 models and that only very minor similarities are found between the mouse models and the human models. Surprisingly, the similarity of two skeletal muscle samples from the same experiment (the *m. soleus* and *m. extensor digitorum longus* of [GSE121972]) was lower than the similarity between the transcriptome of four other experiments including the xenograft and spontaneous pancreatic cancer model. Moreover, there was little to no similarity between the human experiments. The human dataset comparing non-cachectic with cachectic cancer patients showed no significant similarity to other datasets at all.

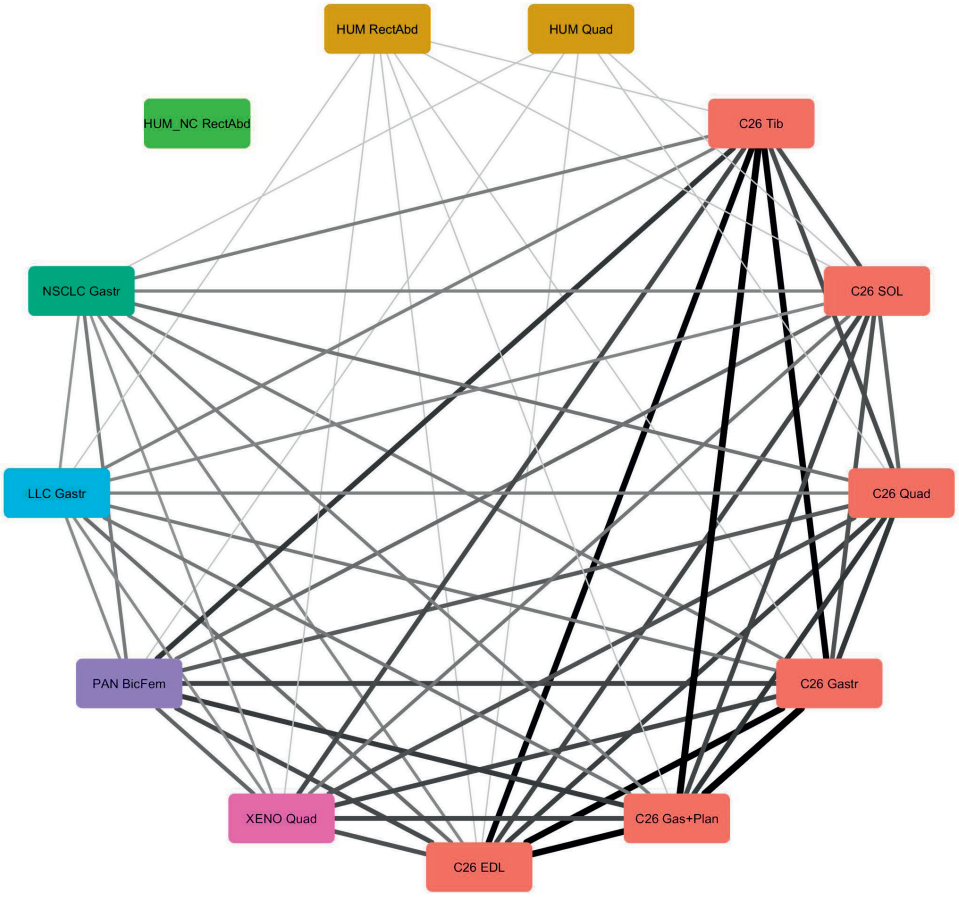

Figure 5.3 *– Network plot of similarity scores. Line width represent strength of similarity. Only similarities with p<0.05 are shown.*

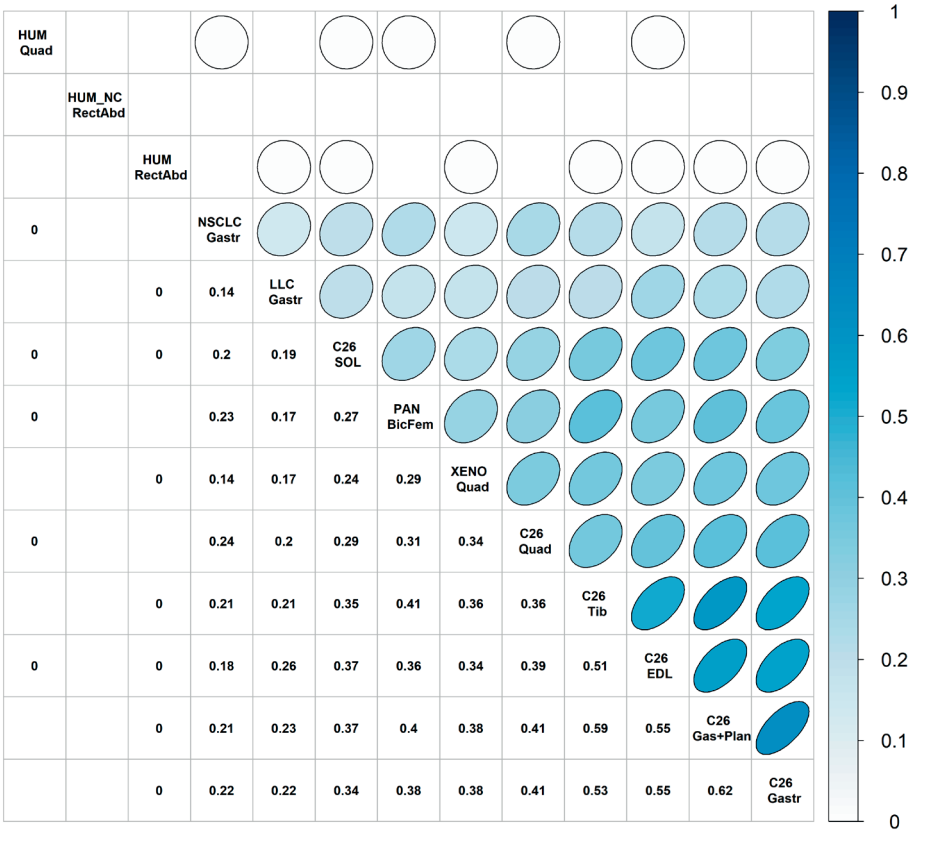

Figure 5.4 – Similarity matrix showing normalized similarity with p<0.05. All similarity scores were normalized to the maximal possible similarity score. Numbers, colours and shapes all indicate normalized similarity scores.

Sparse Principal Component Analysis Expression Differences

To assess differences between datasets, we performed a sparse Principal Component Analysis with 6 components of 100 genes, together explaining a total variance of 86 %. The first and second principal component clearly explained the largest separation with the human and C26 models clearly clustering together (figure 5.5 A). Component 3, 4 and 5 separated respectively the NSCLC, LLC and PAN models from the other models and component 6 explains variance within the C26 models (figure 5.5 A). However, the explained variance in component 3:6 is less than half that of component 1 and 2 (figure 5.5 B and C). In a heat map depicting expression of all genes present in the 6 components of the sPCA, the hierarchical clustering shows that the xenograft model is clearly separated from the other experiments and that the model closest to the human experiments is the LLC model (figure 5.5 D).

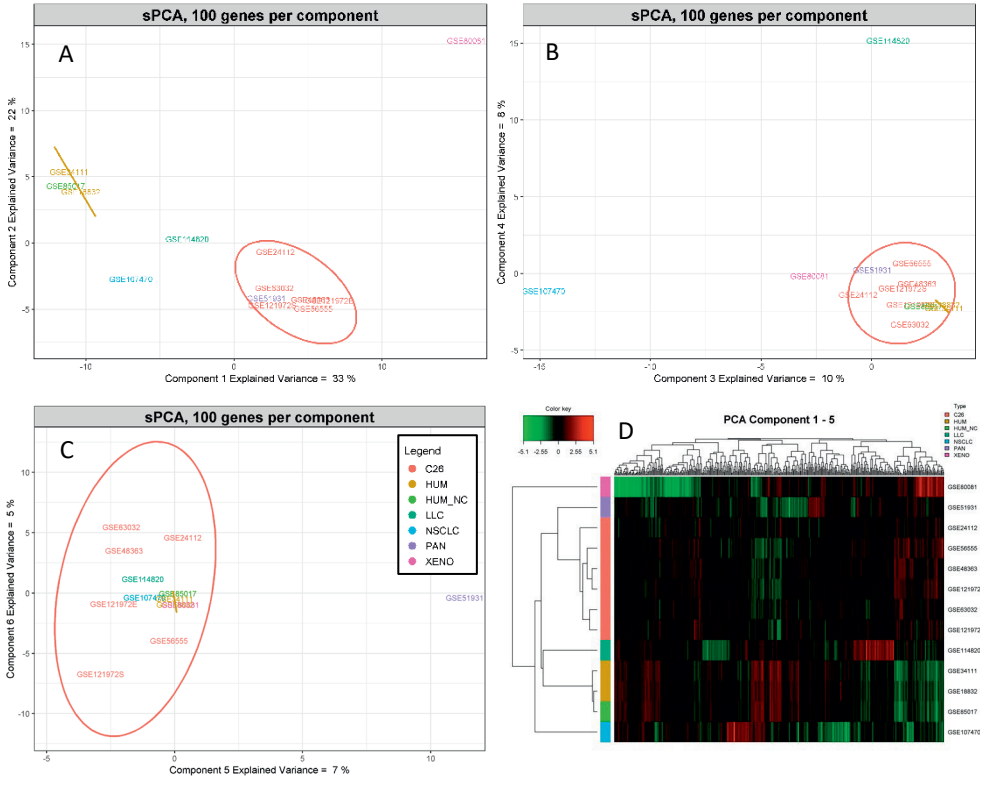

Figure 5.5 *– Sparse principal component analysis with 6 components and 100 genes per component. A-C show individual components 1-6 with ellipses indicating 95% confidence interval. D shows normalized expression values of genes present in the first 5 components with hierarchical clustering for both genes and datasets.*

Gene Set Enrichment Analysis

When looking at the KEGG pathway enrichment, four pathways seemed to be important in all experiments; the proteasome and RNA transport pathway were both strongly upregulated in most experiments, while the oxidative phosphorylation and thermogenesis pathway were strongly downregulated in most experiments (figure 5.6). Interestingly, the effects on these pathways were quite uniform along all animal models, but differed to some extent between the human experiments with the Proteasome and RNA transport pathway being downregulated in the human *m. quadriceps* (GSE34111). When looking at the change in expression of the genes in these separate pathways (figure 5.7), it became clear that different models had differential effects on these four important pathways. In the most upregulated proteasome pathway and the downregulated oxidative phosphorylation and thermogenesis pathway, the human experiments clustered together, while separating from the mouse models. Regarding the RNA transport pathway, some overlap was found between the human experiments and the LLC, and NSCLC animal models. The xenograft model showed a distinct response in all but the proteasome pathway since it splits off first in the hierarchical clustering. When looking at correlation of normalized expression values for all experiments (figure 5.8), the human *m. quadriceps* shows a clearly distinct response correlating negatively with the other human datasets and only correlating positively with the LLC model. Moreover, clear correlations between the C26 models were visible.

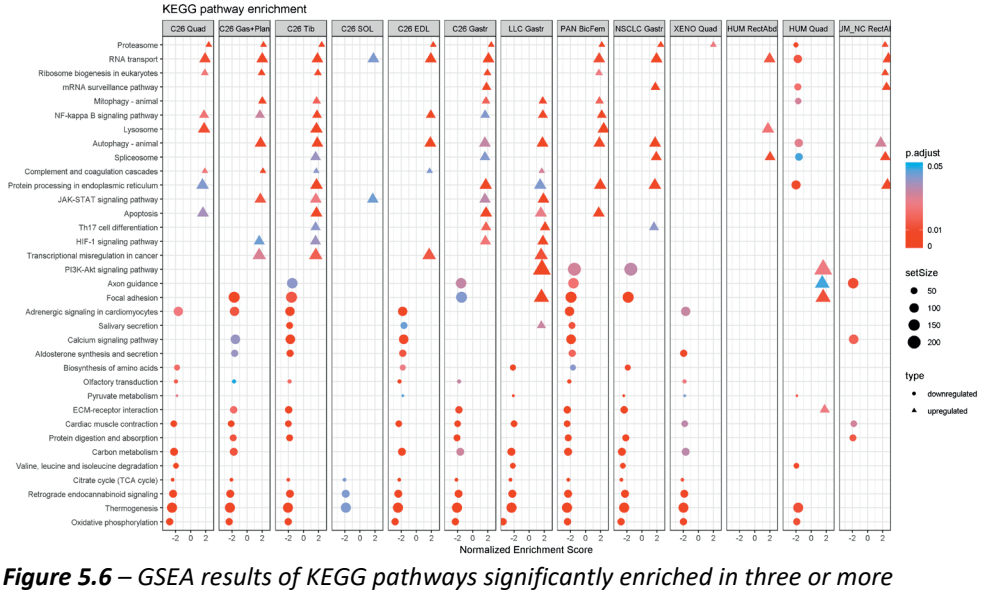

Figure 5.6 *– GSEA results of KEGG pathways significantly enriched in three or more datasets (see supplemental figure 5.1 for full list). Disease specific pathways are removed from the list.*

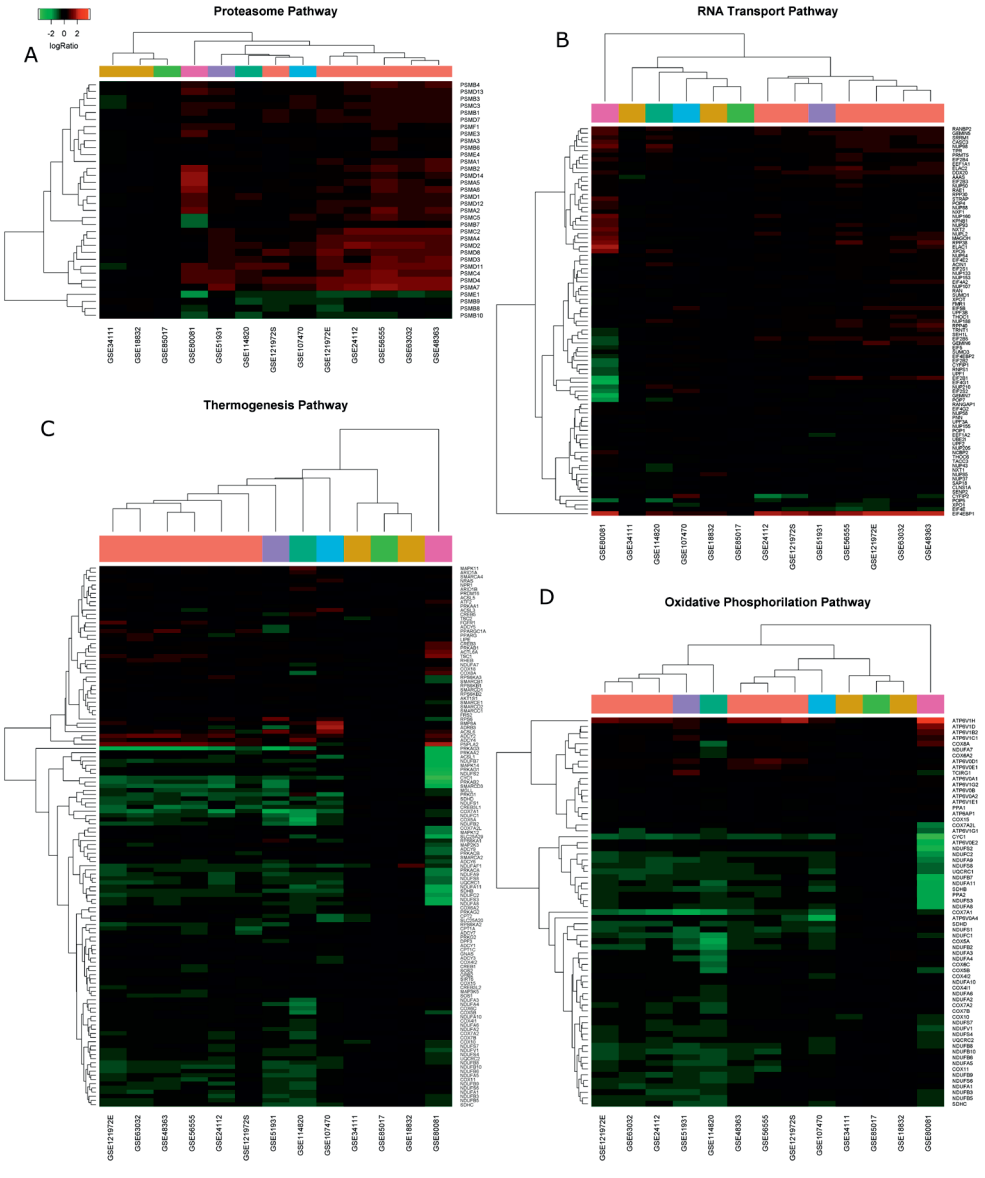

Figure 5.7 *– Log ratios of genes in the two most upregulated (Proteasome [A] and RNA Transport [B]) and downregulated (Thermogenesis [C] and Oxidative Phosphorylation [D]) pathways. Hierarchical clustering is used for both experiments and genes.*

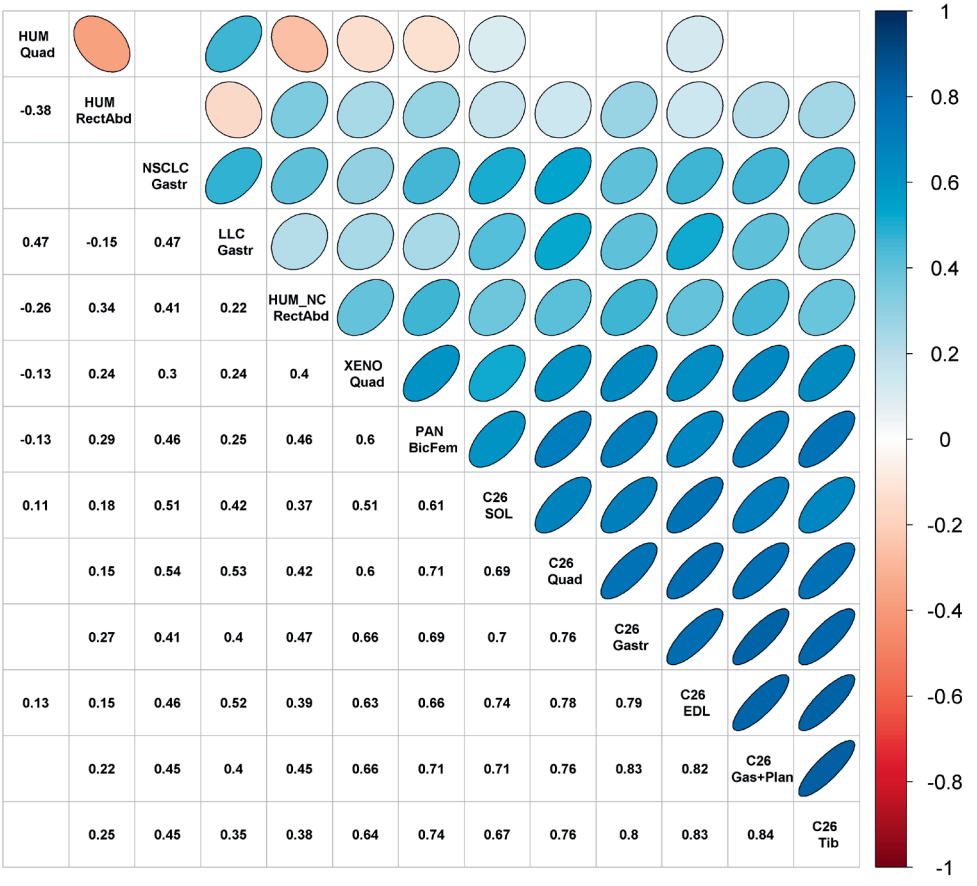

Figure 5.8 – Correlation matrix of normalized enrichment scores of all KEGG pathways. Only significant correlations are shown ($p<0.05$). Experiments are ordered based on hierarchical clustering. Numbers, colours and shapes all indicate correlation coefficients.

sPCA of separate samples

We assessed differences between samples and inter-experimental variation using a sPCA with 6 components of each 25 genes explaining a total variance of 48%. In the hierarchical clustering of the heatmap created with genes present in each of the components, some clear clusters become visible indicating distinct expression in some experiments (supplemental figure 5.2). The NSCLC (GSE114820) and LLC (GSE107470) model cluster together [left side of the heatmap] and there is a cluster of the xenograft (GSE80081) model together with one of the C26 models (GSE24112) [just right of the center of the heatmap].

However, the analytical platform may also be a dominating determinant as the data sets from the NSCLC and LLC models both contained Illumina-based RNA-seq data, while the xenograft and C26 quadriceps were generated with Illumina bead chips. Within the group of data sets generated with Affymetrix arrays, a clear separation between tumour-bearing animals [right of the xenograft/C26 cluster] and control animals [left of the xenograft/C26 cluster] of the other C26 models and the pancreatic cancer model was observed. Moreover, we see that most human controls are clustered together with the control animals. At the same time, no specific clustering of data from cancer patients with those from tumour bearing animals was observed. For the dataset with cachectic/non cachectic cases also no clear separation between cachectic- and non-cachectic cases was seen. Overall, human samples showed considerably more variation compared to those from the animal models and no clear separation became visible between datasets from control and cancer patients used in our analysis.

Discussion

Different models are in use to evaluate possible therapeutic strategies in cachexia, like those based on nutritional, exercise and pharmacological intervention. The present study aimed to determine the relevance of mouse models used to mimic human cachexia, by comparing their effects on muscle gene expression, both between models and with data from human cancer cachexia studies. Publicly available datasets like those present in the GEO database are increasingly offering opportunities for such meta-analyses without the need to perform additional (animal) studies. Overall, our analysis revealed some similarities between animal models and, to lesser extent, to human datasets, in particular with respect to biological process level.

On gene level, analysis indicated only little similarity between the data from animal models and those from human datasets, while more similarities were found between the animal models. Only the *m. extensor digitorum longus* and *m. soleus* data from one of the C26 models (GSE121972) showed significant similarity to more than one human dataset. Moreover, the human dataset without healthy controls showed no similarity to any of the other datasets. However, principal component analysis to examine the specific differences between datasets revealed that the xenograft model showed the most different expression pattern compared to those of the other datasets. Here, the LLC model seems the least different from the human datasets based on clustering in the sPCA heatmap (figure 5.5 D). These results give a good impression of general similarities and differences between data obtained from animal models and those from human cachectic patients. However, for analysis of relevant molecular processes, GSEA results are preferred. With GSEA, four

pathways were found to be clearly standing out. A clear downregulation of oxidative phosphorylation was observed in all animal models, which is in line with literature data[32]. However, this downregulation was only seen in the human *m. quadriceps,* while in the other human datasets, oxidative phosphorylation was not significantly enriched. For the thermogenesis pathway, a clear downregulation was seen in all animal models, whereas also here only the human *m. quadriceps* data showed significant downregulation. The downregulation in muscle thermogenesis is surprising since literature suggests an important role for increased thermogenesis during cachexia, not only in brown adipose tissue[33] but also in muscle[34]. When considering upregulated pathways, the proteasome pathway appeared to be strongly upregulated which is in line with literature[35]. However, the term proteasome is most frequently used in combination with the ubiquitin system[12,36,37]. In our analysis, we do not see the ubiquitin mediate proteolysis to be significantly enriched in any of the datasets. This is in line with previous suggestions that the ubiquitin-proteasome system is not as important in cancer-induced cachexia as previously thought[38]. Another relevant pathway is the strongly upregulated RNA transport pathway which is the only pathway where human datasets cluster together with some animal models (NSCLC and the LLC model). In this pathway, Eukaryotic translation initiation factor 4E binding protein 1 [EIF4EBP1] seems to be an important factor being highly downregulated (figure 5.7 B). Interestingly, this gene is mostly referred to in the context of its influence on the mTOR and AKT pathways in cachexia, whereas we obtained no indication of importance of either the mTOR nor the AKT pathway in our analysis (supplemental figure 5.1)[39]. Finally, some pathways came out of the human datasets without apparently being relevant in the animal models. For example, the RNA degradation was upregulated in both human *m. rectus abdominis* samples, while not significantly found to be enriched in any of the animal models (supplemental figure 5.1).

In line with literature, we see that the measurement platform markedly influenced clustering based on individual gene expression of separate samples[40]. This occurred despite the fact that we used the mixOmics analysis package correcting for differences in platform and experiment[27,28]. However, we do not see platforms clustering together in analyses on differential expression on gene or pathway level making these comparisons still highly relevant. Another limitation of this analysis is that the merge of all data from different platforms causes some data loss.

This is the first study on muscle gene expression in cachexia directly comparing whole genome gene expression data from different experiments. This type of analysis is getting more important due to the large increase in raw data made available and is already used for analysis of tumour gene expression in different types of cancer[41–44]. However, in case of muscle gene expression in cancer, the number of available data sets are still limited,

making a repetition of this analysis upon publication of new data highly relevant. Unfortunately, phenotypic (meta-) data was often not present or insufficient with the datasets, making integration with other data like body weight loss and gene expression not possible for this analysis. Moreover, integration of different omics data like protein expression might be highly relevant to also gain insight into post-transcriptional processes important in cancer cachexia[45].

In conclusion, this study allows to do some suggestions, based on the currently available data, on the relevance of different models mimicking human cancer cachexia. Most importantly, we do not see one model out-performing other models. Each model shows its own differences and similarities to the publicly available human datasets. Thus, the choice for a specific model should be based on several characteristics. Most important is the duration of the experiment which is specifically important when looking at type of intervention; mild interventions might need experiments with longer duration while pharmacologic experiments could do with shorter duration. Moreover, the main targeted outcomes should also be considered since different experiments show similarity to the human situation with respect to different levels and pathways. Taken together, more human datasets containing proper controls are needed before we can draw firm conclusions on mechanisms involved and the usefulness of different models based on a big-data analysis of muscle whole genome gene expression.

References

1. Fearon, K., Arends, J. & Baracos, V. Understanding the mechanisms and treatment options in cancer cachexia. *Nat. Rev. Clin. Oncol.* **10,** 90–9 (2013).
2. Witkamp, R. F. & van Norren, K. Let thy food be thy medicine….when possible. *Eur. J. Pharmacol.* **836,** 102–114 (2018).
3. Bonetto, A. *et al.* STAT3 activation in skeletal muscle links muscle wasting and the acute phase response in cancer cachexia. *PLoS One* **6,** (2011).
4. Cornwell, E. W., Mirbod, A., Wu, C.-L., Kandarian, S. C. & Jackman, R. W. C26 Cancer-Induced Muscle Wasting Is IKKβ-Dependent and NF-kappaB-Independent. *PLoS One* **9,** e87776 (2014).
5. Gilabert, M. *et al.* Pancreatic cancer-induced cachexia is Jak2-dependent in mice. *J. Cell. Physiol.* **229,** 1437–1443 (2014).
6. Judge, S. M. *et al.* Genome-wide identification of FoxO-dependent gene networks in skeletal muscle during C26 cancer cachexia. *BMC Cancer* **14,** 997 (2014).
7. Shum, A. M. Y. A. A. M. Y. *et al.* Cardiac and Skeletal Muscles Show Molecularly Distinct Responses to Cancer Cachexia. *Physiol. Genomics* **47,** physiolgenomics.00128.2014 (2015).
8. Fukawa, T. *et al.* Excessive fatty acid oxidation induces muscle atrophy in cancer cachexia. *Nat. Med.* **22,** 666–671 (2016).
9. Goncalves, M. D. *et al.* Fenofibrate prevents skeletal muscle loss in mice with lung cancer. *Proc. Natl. Acad. Sci.* **115,** E743 LP-E752 (2018).
10. Blackwell, T. A. *et al.* A Transcriptomic Analysis of the Development of Skeletal Muscle Atrophy in Cancer-Cachexia in Tumor-Bearing Mice. *Physiol. Genomics* (2018). doi:10.1152/physiolgenomics.00061.2018
11. Widner, D. B., Files, D. C., Weaver, K. E. & Shiozawa, Y. Preclinical and clinical studies on cancer-associated cachexia. *Front. Biol. (Beijing).* **13,** 11–18 (2018).
12. Mueller, T. C., Bachmann, J., Prokopchuk, O., Friess, H. & Martignoni, M. E. Molecular pathways leading to loss of skeletal muscle mass in cancer cachexia - can findings from animal models be translated to humans? *BMC Cancer* **16,** 75 (2015).
13. Irizarry, R. A. *et al.* Exploration , Normalization , and Summaries of High Density Oligonucleotide Array Probe Level Data. 249–264 (2018).
14. Dai, M. *et al.* Evolving gene/transcript definitions significantly alter the interpretation of GeneChip data. *Nucleic Acids Res.* **33,** e175 (2005).
15. Shi, W., Oshlack, A. & Smyth, G. K. Optimizing the noise versus bias trade-off for Illumina whole genome expression BeadChips. *Nucleic Acids Res.* **38,** (2010).
16. Barbosa-Morais, N. L. *et al.* A re-annotation pipeline for Illumina BeadArrays: Improving the interpretation of gene expression data. *Nucleic Acids Res.* **38,** (2009).
17. Chen, Y., Lun, A. T. L. & Smyth, G. K. From reads to genes to pathways: differential expression analysis of RNA-Seq experiments using Rsubread and the edgeR quasi-likelihood pipeline. *F1000Research* **5,** 1438 (2016).
18. Robinson, M. D., McCarthy, D. J. & Smyth, G. K. edgeR: A Bioconductor package for differential expression analysis of digital gene expression data. *Bioinformatics* **26,** 139–140 (2009).
19. Robinson, M. D. & Oshlack, A. A scaling normalization method for differential expression analysis of RNA-seq data. *Genome Biol.* **11,** R25 (2010).

20. Law, C. W., Chen, Y., Shi, W. & Smyth, G. K. voom: precision weights unlock linear model analysis tools for RNA-seq read counts. *Genome Biol.* **15,** R29 (2014).
21. Ritchie, M. E. *et al.* Limma powers differential expression analyses for RNA-sequencing and microarray studies. *Nucleic Acids Res.* **43,** e47 (2015).
22. Sartor, M. A. *et al.* Intensity-based hierarchical Bayes method improves testing for differentially expressed genes in microarray experiments. *BMC Bioinformatics* **7,** 1–17 (2006).
23. Wilkinson, L. ggplot2: Elegant Graphics for Data Analysis by WICKHAM, H. *Biometrics* **67,** 678–679 (2011).
24. Wei, T. & Simko, V. R package 'corrplot': Visualization of a Correlation Matrix (Version 0.84). (2017).
25. Lottaz, C., Yang, X., Scheid, S. & Spang, R. OrderedList - A bioconductor package for detecting similarity in ordered gene lists. *Bioinformatics* **22,** 2315–2316 (2006).
26. Shannon, P. *et al.* Cytoscape: a software environment for integrated models of biomolecular interaction networks. *Genome Res.* **13,** 2498–504 (2003).
27. Witten, D. M., Tibshirani, R. & Hastie, T. A penalized matrix decomposition, with applications to sparse principal components and canonical correlation analysis. *Biostatistics* **10,** 515–534 (2009).
28. Shen, H. & Huang, J. Z. Sparse principal component analysis via regularized low rank matrix approximation. *J. Multivar. Anal.* **99,** 1015–1034 (2008).
29. Subramanian, A. *et al.* Gene set enrichment analysis: A knowledge-based approach for interpreting genome-wide expression profiles. *Proc. Natl. Acad. Sci.* **102,** 15545–15550 (2005).
30. Kanehisa, M., Sato, Y., Kawashima, M., Furumichi, M. & Tanabe, M. KEGG as a reference resource for gene and protein annotation. *Nucleic Acids Res.* **44,** D457–D462 (2016).
31. Yu, G., Wang, L.-G., Han, Y. & He, Q.-Y. clusterProfiler: an R Package for Comparing Biological Themes Among Gene Clusters. *Omi. A J. Integr. Biol.* **16,** 284–287 (2012).
32. van der Ende, M. *et al.* Mitochondrial dynamics in cancer-induced cachexia. *Biochim. Biophys. Acta - Rev. Cancer* **1870,** 137–150 (2018).
33. Argilés, J. M., Busquets, S., Stemmler, B. & López-Soriano, F. J. Cancer cachexia: understanding the molecular basis. *Nat. Rev. Cancer* **14,** 754–762 (2014).
34. Tisdale, M. J. Mechanisms of Cancer Cachexia. *Physiol. Rev.* **89,** 381–410 (2009).
35. Acharyya, S. & Guttridge, D. C. Cancer cachexia signaling pathways continue to emerge yet much still points to the proteasome. *Clin. Cancer Res.* **13,** 1356–1361 (2007).
36. Khal, J., Wyke, S. M., Russell, S. T., Hine, A. V. & Tisdale, M. J. Expression of the ubiquitin-proteasome pathway and muscle loss in experimental cancer cachexia. *Br. J. Cancer* **93,** 774–780 (2005).
37. Williams, A., Sun, X., Fischer, J. E. & Hasselgren, P.-O. The expression of genes in the ubiquitin-proteasome proteolytic pathway is increased in skeletal muscle from patients with cancer. *Surgery* **126,** 744–750 (1999).
38. Gallagher, I. J. *et al.* Suppression of skeletal muscle turnover in cancer cachexia: evidence from the transcriptome in sequential human muscle biopsies. *Clin. Cancer Res.* **18,** 2817–27 (2012).
39. Constantinou, C. *et al.* Nuclear magnetic resonance in conjunction with functional

genomics suggests mitochondrial dysfunction in a murine model of cancer cachexia. *Int. J. Mol. Med.* **27,** 15–24 (2011).
40. Östlund, G. & Sonnhammer, E. L. L. Avoiding pitfalls in gene (co)expression meta-analysis. *Genomics* **103,** 21–30 (2014).
41. Jiang, R. *et al.* Mixomics analysis of breast cancer: Long non-coding RNA linc01561 acts as ceRNA involved in the progression of breast cancer. *Int. J. Biochem. Cell Biol.* **102,** 1–9 (2018).
42. Rau, A., Flister, M., Rui, H. & Auer, P. L. Exploring drivers of gene expression in the Cancer Genome Atlas. *Bioinformatics* **35,** 62–68 (2018).
43. Warnat, P., Eils, R. & Brors, B. Cross-platform analysis of cancer microarray data improves gene expression based classification of phenotypes. *BMC Bioinformatics* **6,** 1–15 (2005).
44. Waldron, L. & Riester, M. Meta-Analysis in Gene Expression Studies. in *Applied and environmental microbiology* **55,** 161–176 (2016).
45. Rappoport, N. & Shamir, R. Multi-omic and multi-view clustering algorithms: review and cancer benchmark. *Nucleic Acids Res.* **46,** 10546–10562 (2018).

Supplemental figures

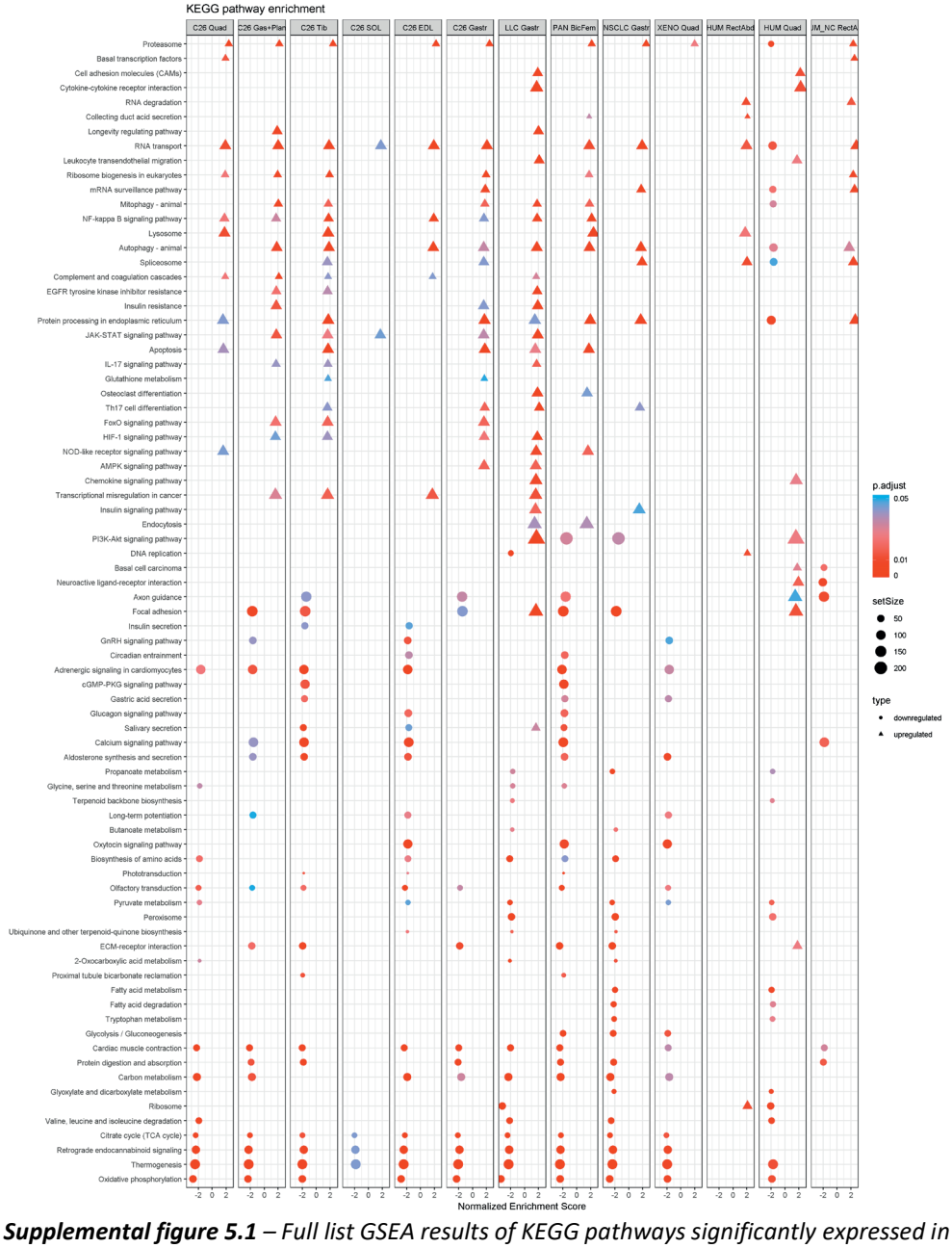

Supplemental figure 5.1 *– Full list GSEA results of KEGG pathways significantly expressed in more than one of the datasets. Some disease specific pathways are removed from the list.*

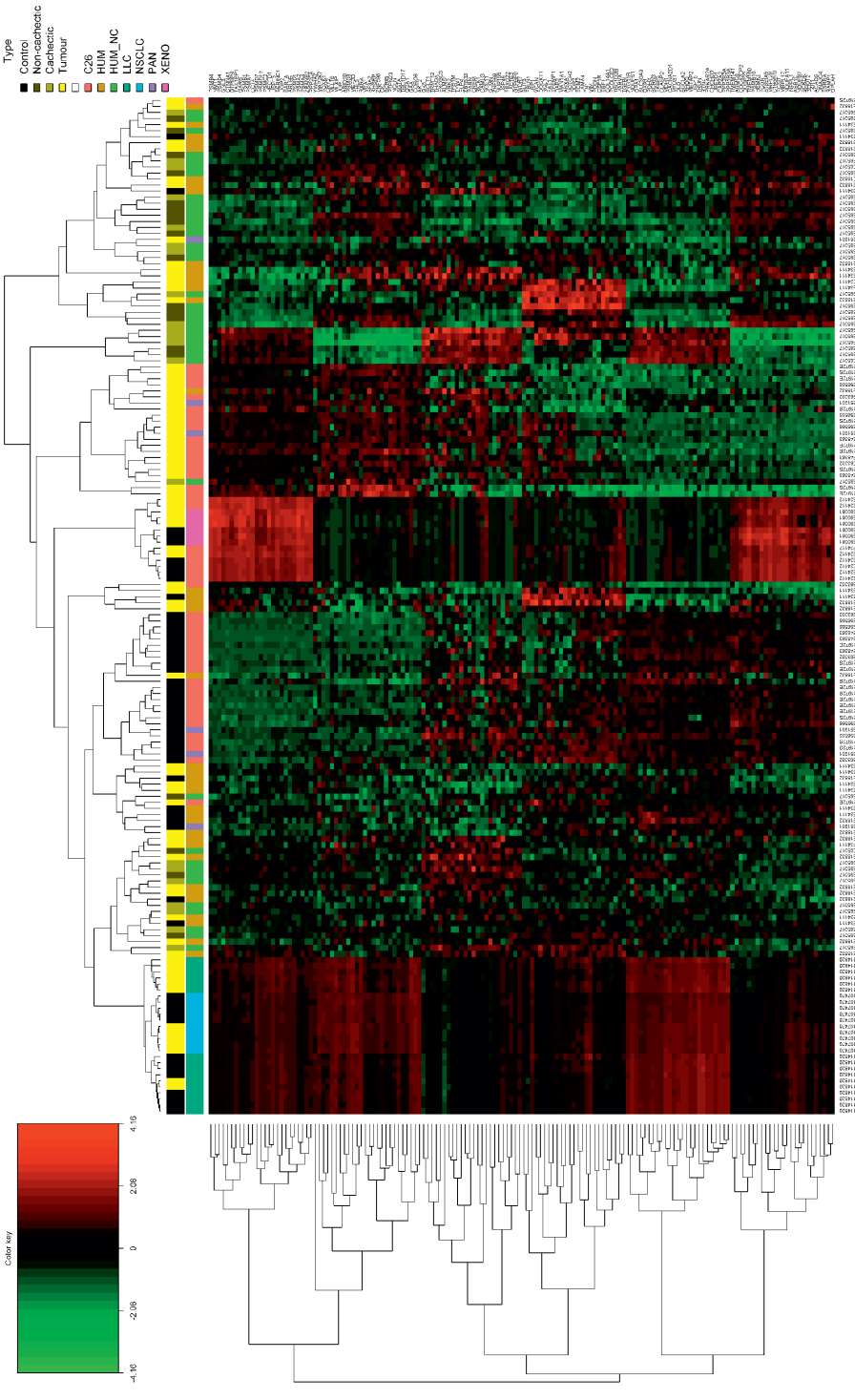

***Supplemental figure** 5.2 – Heatmap of sPCA (6 components with each 25 genes) results of all samples, normalized per experiment.*

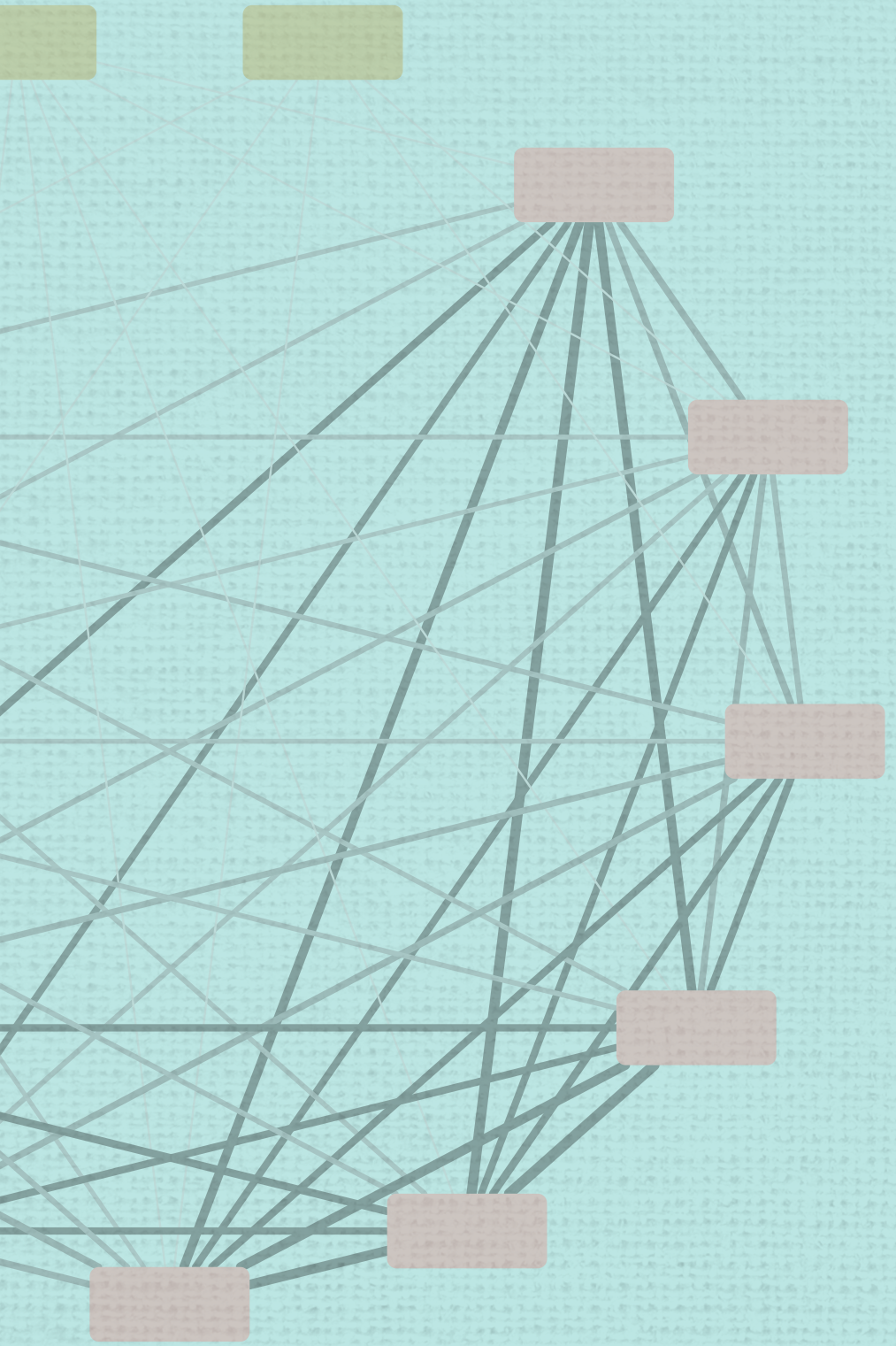

Chapter 6

General Discussion

Main results and strategy

In this thesis, different aspects of the cancer cachexia syndrome have been touched upon. In **chapter 2**, the possible consequences of cancer cachexia are studied in a retrospective cohort of colon cancer patients receiving a chemotherapy regime with capecitabine and oxaliplatin (CAPOX). Main finding was that patients with more intramuscular adipose tissue had more dose-limiting toxicities while there was no association with the absolute or relative amounts of muscle, visceral or subcutaneous adipose tissue. Subsequently, two potential treatment components for a multi modal treatment, nutrition (**chapter 3**) and training (**chapter 4**), were tested in a widely used cancer cachexia mouse model. In **chapter 3**, results show that a nutritional intervention rich in protein, leucine and fish-oil is able to reduce hypercalcemia in a C26 cancer induced cachexia mouse model. Moreover, it was suggested that this reduction is probably due to a reduction of parathyroid hormone related protein (PTHrP) production by the tumor in the presence of docosahexaenoic-acid (DHA). In **chapter 4**, whole body vibration training (WBV) was tested as easily accessible training modality in a C26 mouse model. WBV was able to reduce the tumor effects on the overall muscle transcriptome and showed promising trends on muscle mass and function.

Originally, the thesis was planned to consist of two research lines; one retrospective research line (as described in **chapter 2**) and one translational research line focusing on the differences and similarities between a widely used cancer cachexia mouse model and human colon cancer patients. Original aim was to perform a large data integration and comparison on different levels ranging from muscle strength and body composition to muscle transcriptome. For the translational research line, a mouse study was performed (**chapter 4**) and a human study was designed and started (COMUNEX study, ClinicalTrials.gov [NCT03789136]). Unfortunately, timely inclusion of all patients for this human study was not possible and therefore the study is still ongoing during the writing of this thesis. To approach the translational part, a comparative analysis was performed using publically available muscle transcriptome data of different cachexia studies (**chapter 5**). This comparison was useful, because data from many different labs were compared. At the same time it should be kept in mind that these studies could only be compared on transcriptional level. Data integration at different levels, both horizontal [between experiments] and vertical [within experiments], as designed in the original plan, would probably have brought more complete new insights.

In this final chapter, results of all chapters will be discussed in light of propositions posed based on literature and research results. Moreover, suggestions for future research will be made.

Associations of body composition and cancer cachexia outcomes

Cachexia prevention and treatment should be based on functional analysis of muscle quality, not merely on muscle mass

Clinicians should start measuring body composition and specifically muscle quality of every cancer patient before starting treatment.

There is general consensus that low muscle mass, often independently of fat mass, is related to poor outcomes (e.g. early mortality or low treatment compliance) in cachectic cancer patients. However, in **chapter 2** we describe that we did not observe this relation in a retrospective cohort study among colon cancer patients treated with CAPOX. In our cohort, not muscle mass but intramuscular fat was associated with induced toxicities.

The general consensus of muscle mass being associated with poor outcomes is based on numerous retrospective cohort studies similar to the study described in **chapter 2**. Multiple meta-analyses and systematic reviews of these studies have been performed recently for several cancer types among which colorectal cancer[1,2], ovarian cancer[3], renal cell cancer[4], gastric cancer[5] or different types of solid tumours[6]. Most of these reviews endorse this general consensus associating low muscularity and poor outcomes like postoperative complications[1,5], increased chemotherapy toxicities[4] and survival[4–7]. However, as indicated by most of these reviews, comparing data of these retrospective cohort studies is very difficult. Different standards are used for both predictors as outcomes[8]. Muscularity can for instance be expressed as absolute muscle surface, muscle surface relative to total surface or m. psoas muscle surface. Subsequently, low muscularity is defined by lowest tertile or quartile, or specific sarcopenia cut-offs. Unfortunately, there is not a consensus on the value used for cut-off values and therefore many different versions are used. This is also acknowledged in the many meta-analyses and systematic reviews on prognostic effects of body composition parameters in different cancers[1–6]. As also discussed in **chapter 2**, it is unclear why we did not find an association between muscle mass and chemotherapy-induced toxicities. We suggested that one of the differences could have been the differences between cohorts. This seems in line with a recent study in a similar cohort in the Netherlands where there was no relation between muscle mass and disease-free survival or cancer-specific mortality prospectively[9]. Moreover, in cohort studies of esophagogastric cancer patients and cervical cancer patients there was also no association between muscle mass and progression free or overall survival[10,11]. Maybe, the general consensus about muscle mass does not hold true for all cohorts of cancer patients. However, what distinguishes cohorts where this consensus holds true from those where it does not remains unclear.

Next to muscle mass, there is also consensus about muscle quality as predictor of poor outcomes in cancer cachexia. Similar to muscle mass, muscle quality is determined by analysis of single slice CT scans. Like with muscle mass determination, different measures and cut-offs are used to assess muscle quality. Using a CT scan, the amount of fat in a muscle can be assessed as an indication for muscle quality and this can be performed in two different ways. Most common is by using muscle radiation attenuation, also referred to as myosteatosis, muscle density or muscle attenuation[12]. We will refer to this as muscle attenuation. Muscle attenuation is associated with the amount of lipid droplets inside the muscle tissue[13], but also with muscle strength[14]. In cancer it has been found to be associated with systemic inflammation[15], chemotherapy induced toxicities[10], progression free survival[9,16] and overall survival[9,16,17].The amount of fat infiltration in muscle tissue can also be determined by assessing the amount of intramuscular fat, measured as amount of adipose tissue within the muscle area[18]. We will refer to this as intramuscular adipose tissue (IMAT). The amount of IMAT has previously been associated with general muscle quality measures such as strength and functionality and with mortality[19–21]. In our study presented in **chapter 2**, we did not find an association between muscle attenuation and CAPOX-related toxicities. We did, however, find an association between the amount of IMAT and CAPOX-related toxicities. Unfortunately, very few other studies related IMAT to outcome measures. Thus, muscle quality may also be a good predictor of poor outcomes but more methodological standardization is warranted.

In view of the limitations associated with the currently available studies and standards, there is no clear advice yet for clinicians which body composition parameters should preferably be used to decide on treatment options. Taken together, based on our results, the current consensus and literature available, my opinion is that **cachexia prevention and treatment should be based on functional analysis of muscle quality, not merely on muscle mass**. Improved muscle quality is associated with improved strength and thereby enables patients to enroll in training programs. I think that when patients are able to train, improvement in muscle mass will follow. By improving muscle quality, patients might also improve in treatment compliance. Moreover, improved muscle quality could also improve general fitness and quality of life. To test this hypothesis, I would recommend that **clinicians should start measuring body composition and specifically muscle quality of every cancer patient before starting treatment.** By making these measurements standard care, more prospective cohort studies can be easily set up to confirm this hypothesis. Moreover, with more evidence for the associations between body composition and treatment outcomes, clinicians can make more data driven decisions and provide more personalized care.

Nutrition as part of a multi-modal treatment

The multi-factorial nature of the cachexia syndrome requires a multi-modal treatment including training, nutrition and pharmacological intervention[22]. In **chapter 3**, we tested the effect of a specific nutritional combination high in protein with added leucine and fish oil on calcium homeostasis in a C26 cancer induced cachexia mouse model.

Micronutrient disbalance should always be targeted in clinical and preclinical cachexia trials.

Cancer patients are at high risk of developing deficiencies or potentially also accumulation of micronutrients. Especially in cancer patients suffering from cachexia, many factors can disrupt micronutrient homeostasis. Anorexia, caused directly by the tumor, or indirectly via the hypothalamus, cancer treatment and systemic inflammation can all lead to a decrease in food intake leading to nutrient deficiencies[23]. Moreover, fatigue, lack of exercise, or a decreased nutrient absorption are common in cachexia and also can lead to reduced uptake of nutrients[23]. Apart from reduced intake, the tumor can also cause metabolic disorders disrupting micronutrient homeostasis causing both deficiencies and accumulation[23]. Although patients are clearly at risk of disbalance in micronutrient levels, most clinicians do not screen for possible deficiencies or accumulation. Moreover, there are only very few studies recording micronutrient levels in cancer cachexia. This is surprising since micronutrients are of importance for both energy balance and muscle health[24], two processes often impaired during cancer cachexia. I would argue that especially calcium, vitamin D and magnesium levels should be monitored in cancer patients. Calcium levels are of great importance for physical function and muscle health[25]. Hypercalcemia is frequently found in patients with advanced stage cancer[26]. Therefore, measuring of and possible treating disrupted calcium homeostasis might be relevant for cancer cachectic patients. In our animal study described in **chapter 3**, we found that tumor induced hypercalcemia was present, which was correlated to reductions in carcass and organ masses. Calcium homeostasis is in the normal situation regulated by parathyroid hormone (PTH), Vitamin D and bone cells[26]. Moreover, next to being important in calcium homeostasis, vitamin D is also important for muscle health[27]. However, no evidence exists yet for positive treatment effects of vitamin D in cachexia[27]. In view of this vitamin D level monitoring and possible treatment of deficiencies is a possible interesting research topic. Another micronutrient that is of importance for muscle health is magnesium since it has been found to be associated with muscle mass and power[28] and physical performance[29]. In cancer patients, it has been associated with chemotherapy-induced peripheral neuropathy[30]. Moreover, proton pump inhibitors, a drug frequently used in cancer patients[31], are related to hypomagnesemia[32]. So next to calcium and vitamin D levels, measuring and possibly

treating magnesium levels in cancer cachexia could prove useful. Currently, there are no clear treatment protocols for micronutrient deficiencies or excesses. Guidelines from the European Society for Clinical Nutrition and Metabolism (ESPEN) on nutrition in cancer patients strongly recommend vitamin and mineral supplementation according to the RDA and discourage the use of high-dose micronutrients when no deficiencies are present[33]. However, evidence for this recommendation is low and it is also acknowledged that micronutrient levels should be assessed more often[33]. A recent systematic review on the role of vitamins, minerals, proteins and other supplements for treating cancer cachexia also concluded that there is a lack of evidence about nutritional status and the potential benefits of supplementation[34]. Taken together, monitoring micronutrient levels in the clinic would be of great value. Moreover, based on current knowledge, it is my opinion that **micronutrient disbalance should always be targeted in clinical and preclinical cachexia trials.** Reducing disbalance in micronutrient levels in cachectic patients could improve general and muscle health and thereby improve treatment tolerability and quality of life.

Fish-oil supplementation should be added to standard care in all cachectic cancer patients.

In **chapter 3**, we concluded that a specific nutritional combination high in protein with added leucine and fish-oil was able to reduce cachexia related hypercalcemia in a mouse model. The benefits of fish-oil derived ω-3 polyunsaturated fatty acids (PUFAs) for cancer cachexia are widely studied and include reducing muscle mass and body mass loss, improving appetite, reducing inflammation and improving physical performance[35,36]. Main proposed mechanisms for the effects of these PUFAs are reduction of proteolysis, reduction of tumour growth and size, and reduction of inflammation[37].

The two main fish-oil derived PUFAs are eicosapentaenoic acid (EPA) and docosahexaenoic acid (DHA). Most evidence available is for the benefits of EPA on cancer cachexia outcomes[37]. Main proposed mechanism for the effect of EPA is that it serves as a substrate of cyclooxygenase 2 (COX-2) and thereby reduces the formation of prostaglandin E2 (PGE2), an important inflammatory mediator[38]. In our study, we found that the reduction in hypercalcemia was probably due to a reduction of PTHrP production by the tumor. In approximately 80% of the patients suffering from hypercalcemia, this is mediated by PTHrP secreted by the tumour[26]. This PTHrP reduction in our experiment was most likely induced by DHA and not EPA since only supplementation of DHA was able to reduce PTHrP production of C26 cells *in vitro*. Moreover, we found that this reduction was COX-2 independent since a specific COX-2 inhibitor was unable to reduce PTHrP production of C26 cells and DHA was unable to reduce PGE2 production of C26 cells *in vitro*. Our results indicate that DHA, compared to EPA, could have a more indirect role in the treatment of cancer cachexia. This indirect effect, however, is highly relevant in cancer cachexia since

PTHrP not only causes hypercalcemia but also triggers adipose tissue browning and thereby increases energy expenditure[39,40]. Since cross-talk between adipose, bone and muscle tissue can exacerbate cancer cachexia[41], improving the functioning of these tissues seems useful.

Taken together, Fish-oil seems to have a beneficial effect in cancer cachexia by reducing inflammation and PTHrP production. Moreover, supplementation of EPA and DHA have proven to be safe in relatively high doses of 5 g/day DHA and EPA combined and 1.8 g/day EPA[42]. ESPEN guidelines provide a weak recommendation for supplementation of ω-3 PUFAs in patients with advanced cancer undergoing chemotherapy and at risk of weight loss or malnourishment[33]. However, considering current evidence and our results indicating a potential and important role for fish oil, I would even go one step further and pose that **fish-oil supplementation should be added to standard care in all cachectic cancer patients.** Nevertheless, more evidence backing up these claims, both in clinical studies as well as via mechanistic research, is needed.

Exercise as part of multi-modal treatment

All clinical and preclinical cachexia research into exercise should be combined with nutrition.

As mentioned in the general introduction, experts suggest that treatment of cancer cachexia should be a combination of nutrition, training and pharmacology (see Figure 1.3)[22,43]. However, cachexia symptoms may sometimes hamper practical implementation of the training component. Since cachexia is characterized by loss of muscle mass and muscle weakness and the presence of fatigue, starting a training program can be difficult.

The effects of training in cancer patients able to enroll in training programs are promising for cachectic cancer patients. Training has been able to reduce cancer related inflammation[44]**,** fatigue[45] and improve quality of life[46,47]. Moreover, both aerobic and resistance type exercise are able to improve muscle strength in during treatment in cancer patients[48]. However, very limited research is available on exercise in cancer patients suffering from cachexia. Most evidence on the effect of training on cancer cachexia consists of studies in animal models. In rodents, exercise training programs have been able to reduce inflammation and oxidative stress[49]. Moreover, a recent study on the effect of aerobic and resistance type exercise indicated that both can have beneficial effects on muscle[50]. Aerobic type exercise can preserve muscle function and mass where resistance type exercise was able to induce expression of genes associated with muscle damage and repair[50]. Combined exercise including both aerobic and resistance type exercise was able to improve both muscle mass and strength[51]. However, when translated to human treatment, these training methods might be too strenuous for cancer cachectic patients suffering from muscle weakness. Therefore, in our study, presented in **chapter 4**, we investigated the effect of an

easily accessible training method, whole body vibration training, in a C26 induced cachexia mouse model. We found that the training reduced the tumor induced shift of the muscle transcriptome. Effects on muscle health were minimal, most likely due to the short and aggressive nature of the C26 model. Together, the effects on transcriptome and the minor effects on muscle health in combination with the absence of adverse effects make whole body vibration training a potential treatment for weak and cachectic cancer patients.

Unfortunately, most studies performed so far are based on only one modality, while only few studies have combined exercise and nutrition. In age-related sarcopenia (muscle-loss), this combination has been studied somewhat more frequently and in-depth and results suggest an enhanced benefit of exercise training upon combination with nutrition[52]. Moreover, based on literature, experts strongly recommended to combine resistance type exercise with adequate nutrition for optimal benefits on muscle health in elderly[53]. This is in line with the idea of multimodal care for cancer cachexia. Therefore, I would argue that in future research **all clinical and preclinical cachexia research into exercise should be combined with nutrition.** Especially since some patients suffer from both fatigue and anorexia, nutritional intake should be optimal and should therefore always be assessed in clinical trials. Suggestions for practical implementation of multi-modal care have been made indicating that it can be achieved using simple treatments and without the need for dedicated cachexia specialists[54]. Moreover, a recent phase II trial has shown that multimodal treatment is feasible and safe in advanced stage lung or pancreatic cancer patients[55].

Translating results from animal to human

Molecular biology analysis is crucial to select the most appropriate animal model for cachexia research

Due to the complexity and severity of the condition, cachexia mechanisms and possible treatment is more often studied in animal models than in studies including humans. The use of animal models to predict mechanisms or responses to treatment in humans has been used since the ancient Greeks. Already in the 6th century before Christ, the Greek natural philosopher Alcmaeon of Croton used research in dogs to determine that the brain is the location of intelligence and sensory integration[56]. The current definition of an animal model, as available from the National Cancer Institute Dictionary of Cancer Terms, is: "*An animal with a disease either the same as or like a disease in humans. Animal models are used to study the development and progression of diseases and to test new treatments before they are given to humans.*"[57]. With the current techniques, science is able to determine to what extent animal models mimic the human situation on many different levels. Animal

experiments should always be executed keeping in mind the three R's; replacement, reduction and refinement[58]. When taking these principles into account, establishing the relevance of animal models by comparing them with the human situation is very important. Therefore, in **chapter 5**, we tried to establish differences and similarities at transcriptional level in skeletal muscle tissue between commonly used animal models, using data available in the NCBI gene expression omnibus database. We found some marking differences in muscle whole genome gene expression between different animal models and the, albeit limited, human data. Only a few models showed some similarity to the available human datasets. However, this similarity was very low and not consistent for a specific type of model. Moreover, four specific pathways, oxidative phosphorylation, thermogenesis, proteasome and RNA transport, which were clearly up- or downregulated in animal models, did not consistently show up in human datasets. To the best of our knowledge, this was the first attempt to directly compare different animal models to human data based on raw data stored in public databases. Previously, animal models have been compared in reviews and studies focusing on specific outcomes[59–62]. General conclusion is that on other levels than transcription, animal models also differ. Models differ in how they affect inflammation[60], muscle breakdown[59], the role of adipose tissue[63] and bone loss[64]. Most models induce inflammation just like in human cachexia but do this in different ways; the C26 model that we used in chapter 3 and 4 is known for inducing inflammation by strongly increasing IL6 levels whereas the Lewis Lung Carcinoma (LLC) model is notorious for increasing TNF-α levels[62]. Moreover, different types of tumor secrete different factors inducing different molecular processes. In our studies, we found PTHrP as an important factor of the C26 model being already secreted by C26 cells without inflammatory stimulants *in vitro*. Moreover, PTHrP levels were also increased in plasma and were correlated with decreased bone mineral density. Not only is PTHrP related to bone health but also to adipose tissue browning leading to increased energy expenditure[40]. All these different molecular processes can in turn contribute to different types of cross-talk between affected organs increasing the complexity of interpretation and translation from animal to human[41].

Taken together, animal models can differ in almost all molecular processes driving cachexia. But similar to animal models, human tumors also show different characteristics and induce different pathways causing cachexia. Moreover, cross-talk between different organs might be different under different circumstances, both in animal and human. Therefore, I would pose that **molecular biology analysis is crucial to select the most appropriate animal model for cachexia research**. By doing so, treatments can be tested for efficacy on specific processes or pathways instead of general cachexia. This can improve personalized care in patients as well. Clinicians could establish the direct causes of cachexia in individual patients using gene expression in muscle tissue (harvested during surgery) and

plasma cytokine levels and presence of specific cachexia inducing factors secreted by the tumor. Based on the molecular cachexia profile, adequate treatment can be selected from pre-clinical and clinical studies.

Future Perspectives

The principles of FAIR data sharing enabling collaboration and data integration are fundamental to advance cachexia research

Throughout this discussion, some suggestions have been made on potential options for future research. In this last paragraph some more general reflections and recommendations will be discussed in view of their usefulness and potential to improve cancer cachexia research. In general, most can be gained by increased sharing and integration of research data and the use of the FAIR data principles. FAIR data is a concept to improve the sharing and reuse of scholarly data and it is based on four principles; Findability, Accessibility, Interoperability, and Reusability[65]. Findability means that all research data should be accompanied by appropriate meta-data and stored in an easily searchable database. Accessibility includes that data should be open, free, universally implementable and retrievable via a communications protocol that is widely available. Interoperable (meta)data is stored in a broadly acceptable language and includes proper references. Reusability means all data is accompanied by rich metadata to accurately describe the data. These principles of FAIR data are fully in line with the principles as described in the Code of Conduct for Research Integrity 2018[66], and should therefore be implemented by any scientist.

For the discussion on chapter 2, the main question on the predictability of muscle mass and quality is how firm these two general consensuses are. Unfortunately, it is difficult to test this properly since a direct comparison is impossible due to the different standards used. Possibly, these theories might also be prone to publication bias since most journals favor presenting studies showing strong and clear associations instead of studies indicating no or weak associations. This could encourage researchers to try different cut-offs and measures to find an association. Since most of the data presented in these studies is usually quite straightforward and mostly as simple as one data table, making the raw data available according to the FAIR data principles would enable direct comparative analyses. This would also enable solid confirmation or rejection of the existing consensuses. Another scientific improvement can be achieved when hospitals would collect more quantitative data. In our cohort described in chapter 2, we were limited in measures for chemotherapy-induced toxicities. General practice in most hospitals is to record toxicities in a qualitative instead of quantitative manner. Usage of generally accepted quantitative adverse event recording, like

the Common Terminology Criteria for Adverse Events (CTCAE[67]), would greatly improve the quality of retrospective studies using hospital collected patient data. Also, for body composition measures, general hospitals could play a more prominent role in advancing science. Recently developed automated segmentation and analysis of single slice CT scans also allows assessment of body composition measures in the clinic[68]. As low skeletal muscle attenuation is associated with multiple co-morbidities[69], early detection could also be of great value in the clinic. Moreover, in light of the discussion on micro-nutrients based on our findings in chapter 3, clinicians could play a more prominent role. If clinicians would start measuring nutritional status as a general routine, especially micro-nutrient levels, this would give insights into possible deficiencies in patients, its determinants and consequences. Obviously, collecting more quantitative data would be instrumental to advance the case of personalized multi-modal treatment. For chapter 5, where we compared different gene expression datasets, inclusion of more (meta)data would have greatly improved our ability to determine the validity of different animal models. Based on literature, it is clear that many more datasets exist containing whole genome muscle gene expression from tumor bearing and healthy animals or humans. Unfortunately, many datasets are not submitted to the GEO database or lack proper metadata for inclusion in our analysis. Taken together, I think that **the principles of FAIR data sharing enabling collaboration and data integration are fundamental to advance cachexia research**. With the use of emerging artificial intelligence and machine learning models, data integration, both within experiments as between experiments, as originally planned for this thesis will be a great step forward for cancer cachexia research. The key is not designing a new perfect study but bringing the data already generated for cancer cachexia research together.

References

1. Sun, G. *et al.* Can sarcopenia be a predictor of prognosis for patients with non-metastatic colorectal cancer? A systematic review and meta-analysis. *Int. J. Colorectal Dis.* **33,** 1419–1427 (2018).
2. Malietzis, G. *et al.* The role of body composition evaluation by computerized tomography in determining colorectal cancer treatment outcomes: A systematic review. *Eur. J. Surg. Oncol.* **41,** 186–196 (2015).
3. Purcell, S. A., Elliott, S. A., Kroenke, C. H., Sawyer, M. B. & Prado, C. M. Impact of Body Weight and Body Composition on Ovarian Cancer Prognosis. *Curr. Oncol. Rep.* **18,** 1–11 (2016).
4. Vrieling, A. *et al.* Body Composition in Relation to Clinical Outcomes in Renal Cell Cancer: A Systematic Review and Meta-analysis. *Eur. Urol. Focus* **4,** 420–434 (2018).
5. Kamarajah, S. K., Bundred, J. & Tan, B. H. L. Body composition assessment and sarcopenia in patients with gastric cancer: a systematic review and meta-analysis. *Gastric Cancer* **22,** 10–22 (2018).
6. Shachar, S. S., Williams, G. R., Muss, H. B. & Nishijima, T. F. Prognostic value of sarcopenia in adults with solid tumours: A meta-analysis and systematic review. *Eur. J. Cancer* **57,** 58–67 (2016).
7. Brown, J. C., Cespedes Feliciano, E. M. & Caan, B. J. The evolution of body composition in oncology-epidemiology, clinical trials, and the future of patient care: facts and numbers. *J. Cachexia. Sarcopenia Muscle* (2019). doi:10.1002/jcsm.12379
8. Daly, L. E., Prado, C. M. & Ryan, A. M. A window beneath the skin: How computed tomography assessment of body composition can assist in the identification of hidden wasting conditions in oncology that profoundly impact outcomes. *Proc. Nutr. Soc.* **77,** 135–151 (2018).
9. van Baar, H. *et al.* Low radiographic muscle density is associated with lower overall and disease-free survival in early-stage colorectal cancer patients. *J. Cancer Res. Clin. Oncol.* **144,** 2139–2147 (2018).
10. Dijksterhuis, W. P. M. *et al.* Association between body composition, survival, and toxicity in advanced esophagogastric cancer patients receiving palliative chemotherapy. *J. Cachexia. Sarcopenia Muscle* (2019). doi:10.1002/jcsm.12371
11. Matsuoka, H. *et al.* Sarcopenia Is Not a Prognostic Factor of Outcome in Patients With Cervical Cancer Undergoing Concurrent Chemoradiotherapy or Radiotherapy. *Anticancer Res.* **39,** 933–939 (2019).
12. Aubrey, J. *et al.* Measurement of skeletal muscle radiation attenuation and basis of its biological variation. *Acta Physiol.* **210,** 489–497 (2014).
13. Goodpaster, B. H., Kelley, D. E., Thaete, F. L., He, J. & Ross, R. Skeletal muscle attenuation determined by computed tomography is associated with skeletal muscle lipid content. *J. Appl. Physiol.* **89,** 104–110 (2000).
14. Goodpaster, B. H. *et al.* Attenuation of skeletal muscle and strength in the elderly: The Health ABC Study. *J. Appl. Physiol.* **90,** 2157–2165 (2001).
15. Malietzis, G. *et al.* Low Muscularity and Myosteatosis Is Related to the Host Systemic Inflammatory Response in Patients Undergoing Surgery for Colorectal Cancer. *Ann. Surg.* **263,** 320–325 (2015).
16. Antoun, S. *et al.* Skeletal muscle density predicts prognosis in patients with

metastatic renal cell carcinoma treated with targeted therapies. *Cancer* **119,** 3377–3384 (2013).

17. Fujiwara, N. *et al.* Sarcopenia, intramuscular fat deposition, and visceral adiposity independently predict the outcomes of hepatocellular carcinoma. *J. Hepatol.* **63,** 131–140 (2015).
18. Mourtzakis, M. *et al.* A practical and precise approach to quantification of body composition in cancer patients using computed tomography images acquired during routine care. *Appl. Physiol. Nutr. Metab.* **33,** 997–1006 (2008).
19. Perkisas, S., De Cock, A.-M., Verhoeven, V. & Vandewoude, M. Intramuscular Adipose Tissue and the Functional Components of Sarcopenia in Hospitalized Geriatric Patients. *Geriatrics* **2,** 11 (2017).
20. Bang, E., Tanabe, K., Yokoyama, N., Chijiki, S. & Kuno, S. Relationship between thigh intermuscular adipose tissue accumulation and number of metabolic syndrome risk factors in middle-aged and older Japanese adults. *Exp. Gerontol.* **79,** 26–30 (2016).
21. Pritchard, J. M. *et al.* The Relationship between Intramuscular Adipose Tissue, Functional Mobility, and Strength in Postmenopausal Women with and without Type 2 Diabetes. *J. Aging Res.* **2015,** (2015).
22. Argilés, J. M., López-Soriano, F. J., Stemmler, B. & Busquets, S. Novel targeted therapies for cancer cachexia. *Biochem. J.* **474,** 2663–2678 (2017).
23. Gröber, U., Holzhauer, P., Kisters, K., Holick, M. F. & Adamietz, I. A. Micronutrients in oncological intervention. *Nutrients* **8,** 1–30 (2016).
24. Maughan, R. J. Role of micronutrients in sport and physical activity. *Br. Med. Bull.* **55,** 683–690 (1999).
25. van Dronkelaar, C. *et al.* Minerals and Sarcopenia; The Role of Calcium, Iron, Magnesium, Phosphorus, Potassium, Selenium, Sodium, and Zinc on Muscle Mass, Muscle Strength, and Physical Performance in Older Adults: A Systematic Review. *J. Am. Med. Dir. Assoc.* **19,** 6–11.e3 (2018).
26. Mirrakhimov, A. E. Hypercalcemia of malignancy: An update on pathogenesis and management. *N. Am. J. Med. Sci.* **7,** 483–493 (2015).
27. Garcia, M., Seelaender, M., Sotiropoulos, A., Coletti, D. & Lancha, A. H. Vitamin D, muscle recovery, sarcopenia, cachexia and muscle atrophy. *Nutrition* (2018). doi:10.1016/j.nut.2018.09.031
28. Welch, A. A. *et al.* Dietary Magnesium Is Positively Associated with Skeletal Muscle Power and Indices of Muscle Mass and May Attenuate the Association between Circulating C-Reactive Protein and Muscle Mass in Women. *J. Bone Miner. Res.* **31,** 317–325 (2016).
29. Veronese, N. *et al.* Veronese N, Berton L, Carraro S, Bolzetta F, De Rui M, Perissinotto E, et al. Effect of oral magnesium supplementation on physical performance in healthy elderly women involved in a weekly exercise program: a randomized controlled trial. Am J Clin Nutr. 2. 974–981 (2014). doi:10.3945/ajcn.113.080168.Magnesium
30. Wesselink, E. *et al.* Dietary intake of magnesium or calcium and chemotherapy-induced peripheral neuropathy in colorectal cancer patients. *Nutrients* **10,** 1–13 (2018).
31. Numico, G., Fusco, V., Franco, P. & Roila, F. Proton Pump Inhibitors in cancer patients: How useful they are? A review of the most common indications for their

use. *Crit. Rev. Oncol. Hematol.* **111,** 144–151 (2017).
32. van Orten-Luiten, A. C. B., Janse, A., Verspoor, E., Brouwer-Brolsma, E. M. & Witkamp, R. F. Drug use is associated with lower plasma magnesium levels in geriatric outpatients; possible clinical relevance. *Clin. Nutr.* (2018). doi:10.1016/j.clnu.2018.11.018
33. Arends, J. *et al.* ESPEN guidelines on nutrition in cancer patients. *Clin. Nutr.* **36,** 11–48 (2017).
34. Mochamat *et al.* A systematic review on the role of vitamins, minerals, proteins, and other supplements for the treatment of cachexia in cancer: a European Palliative Care Research Centre cachexia project. *J. Cachexia. Sarcopenia Muscle* **8,** 25–39 (2017).
35. Baracos, V. E., Mazurak, V. C. & Bhullar, A. S. Cancer cachexia is defined by an ongoing loss of skeletal muscle mass. *Ann. Palliat. Med.* **8,** 3–12 (2019).
36. Seelaender, M. *Cachexia*. *Fish and Fish Oil in Health and Disease Prevention* (Elsevier Inc., 2016). doi:10.1016/B978-0-12-802844-5/00026-9
37. Gorjao, R. *et al.* New Insights on the Regulation of Cancer Cachexia By N-3 Polyunsaturated Fatty Acids. *Pharmacol. Ther.* (2018). doi:10.1016/j.pharmthera.2018.12.001
38. Calder, P. C. Omega-3 fatty acids and inflammatory processes. *Nutrients* **2,** 355–374 (2010).
39. Kir, S. *et al.* PTH/PTHrP receptor mediates cachexia in models of kidney failure and cancer. *Cell Metab.* **23,** 315–323 (2016).
40. Thomas, S. S. & Mitch, W. E. Parathyroid hormone stimulates adipose tissue browning. *Curr. Opin. Clin. Nutr. Metab. Care* 1 (2017). doi:10.1097/MCO.0000000000000357
41. Argilés, J. M., Stemmler, B., López-Soriano, F. J. & Busquets, S. Inter-tissue communication in cancer cachexia. *Nat. Rev. Endocrinol.* **15,** 9–20 (2019).
42. EFSA Panel on Dietetic Products, N. and A. (NDA). Scientific Opinion on the Tolerable Upper Intake Level of eicosapentaenoic acid (EPA), docosahexaenoic acid (DHA) and docosapentaenoic acid. *EFSA J.* **10,** 2815 (2012).
43. Baracos, V. E., Martin, L., Korc, M., Guttridge, D. C. & Fearon, K. C. H. Cancer-associated cachexia. *Nat. Rev. Dis. Prim.* **4,** 17105 (2018).
44. Gould, D. W., Lahart, I., Carmichael, A. R., Koutedakis, Y. & Metsios, G. S. Cancer cachexia prevention via physical exercise: molecular mechanisms. *J. Cachexia. Sarcopenia Muscle* **4,** 111–24 (2013).
45. Puetz, T. W. & Herring, M. P. Differential effects of exercise on cancer-related fatigue during and following treatment: A meta-analysis. *Am. J. Prev. Med.* **43,** e1 (2012).
46. Mishra, S. I. *et al.* Exercise interventions on health-related quality of life for people with cancer during active treatment. *Cochrane database Syst. Rev.* **17,** CD008465 (2012).
47. Mishra, S. I. *et al.* Exercise interventions on health-related quality of life for cancer survivors. *Cochrane Database Syst. Rev.* **2012,** (2012).
48. Stene, G. B. *et al.* Effect of physical exercise on muscle mass and strength in cancer patients during treatment-A systematic review. *Crit. Rev. Oncol. Hematol.* **88,** 573–593 (2013).

49. Lira, F. S., Antunes, B. D. M. M., Seelaender, M. & Neto, J. C. R. The therapeutic potential of exercise to treat cachexia. *Curr. Opin. Support. Palliat. Care* **9,** 317–324 (2015).
50. Khamoui, A. V. *et al.* Aerobic and resistance training dependent skeletal muscle plasticity in the colon-26 murine model of cancer cachexia. *Metabolism* **65,** 685–698 (2016).
51. Ranjbar, K. *et al. Combined Exercise Training Positively Affects Muscle Wasting in Tumor-bearing Mice*. *Medicine & Science in Sports & Exercise* (2019). doi:10.1249/mss.0000000000001916
52. Denison, H. J., Cooper, C., Sayer, A. A. & Robinson, S. M. Prevention and optimal management of sarcopenia: A review of combined exercise and nutrition interventions to improve muscle outcomes in older people. *Clin. Interv. Aging* **10,** 859–869 (2015).
53. Shad, B. J., Wallis, G., van Loon, L. J. C. & Thompson, J. L. Exercise prescription for the older population: The interactions between physical activity, sedentary time, and adequate nutrition in maintaining musculoskeletal health. *Maturitas* **93,** 78–82 (2016).
54. Maddocks, M. *et al.* Practical multimodal care for cancer cachexia. *Curr. Opin. Support. Palliat. Care* **10,** 298–305 (2016).
55. Solheim, T. S. *et al.* A randomized phase II feasibility trial of a multimodal intervention for the management of cachexia in lung and pancreatic cancer. *J. Cachexia. Sarcopenia Muscle* **8,** 778–788 (2017).
56. Ericsson, A. C., Crim, M. J. & Franklin, C. L. A brief history of animal modeling. *Mo. Med.* **110,** 201–5 (2013).
57. Definition of animal model - NCI Dictionary of Cancer Terms - National Cancer Institute. Available at: https://www.cancer.gov/publications/dictionaries/cancer-terms/def/animal-model. (Accessed: 28th February 2019)
58. Russell, W. M. S. & Burch, R. L. *The principles of humane experimental technique.* (London: Methuen & Co. Ltd., 1959).
59. Mueller, T. C., Bachmann, J., Prokopchuk, O., Friess, H. & Martignoni, M. E. Molecular pathways leading to loss of skeletal muscle mass in cancer cachexia - can findings from animal models be translated to humans? *BMC Cancer* **16,** 75 (2015).
60. Ballaro, R., Costelli, P. & Penna, F. Animal models for cancer cachexia. *Curr. Opin. Support. Palliat. Care* 281–287 (2016). doi:10.1097/SPC.0000000000000233
61. Deboer, M. D. Animal models of anorexia and cachexia. *Expert Opin. Drug Discov.* **4,** 1145–1155 (2009).
62. Widner, D. B., Files, D. C., Weaver, K. E. & Shiozawa, Y. Preclinical and clinical studies on cancer-associated cachexia. *Front. Biol. (Beijing).* **13,** 11–18 (2018).
63. Vaitkus, J. A. & Celi, F. S. The role of adipose tissue in cancer-associated cachexia. *Exp. Biol. Med.* **242,** 473–481 (2017).
64. Bonetto, A. *et al.* Differential Bone Loss in Mouse Models of Colon Cancer Cachexia. *Front. Physiol.* **7,** 679 (2017).
65. Wilkinson, M. D. *et al.* The FAIR Guiding Principles for scientific data management and stewardship. *Sci. Data* **3,** 160018 (2016).
66. NWO. *Netherlands Code of Conduct for Research Integrity 2018*. (2018). doi:doi.org/10.17026/dans-2cj-nvwu

67. Common Terminology Criteria for Adverse Events (CTCAE) | Protocol Development | CTEP. Available at: https://ctep.cancer.gov/protocolDevelopment/electronic_applications/ctc.htm. (Accessed: 14th February 2019)
68. Takahashi, N. *et al.* Validation study of a new semi-automated software program for CT body composition analysis. *Abdom. Radiol.* **42,** 2369–2375 (2017).
69. Xiao, J. *et al.* Associations of pre-existing co-morbidities with skeletal muscle mass and radiodensity in patients with non-metastatic colorectal cancer. *J. Cachexia. Sarcopenia Muscle* **9,** 654–663 (2018).

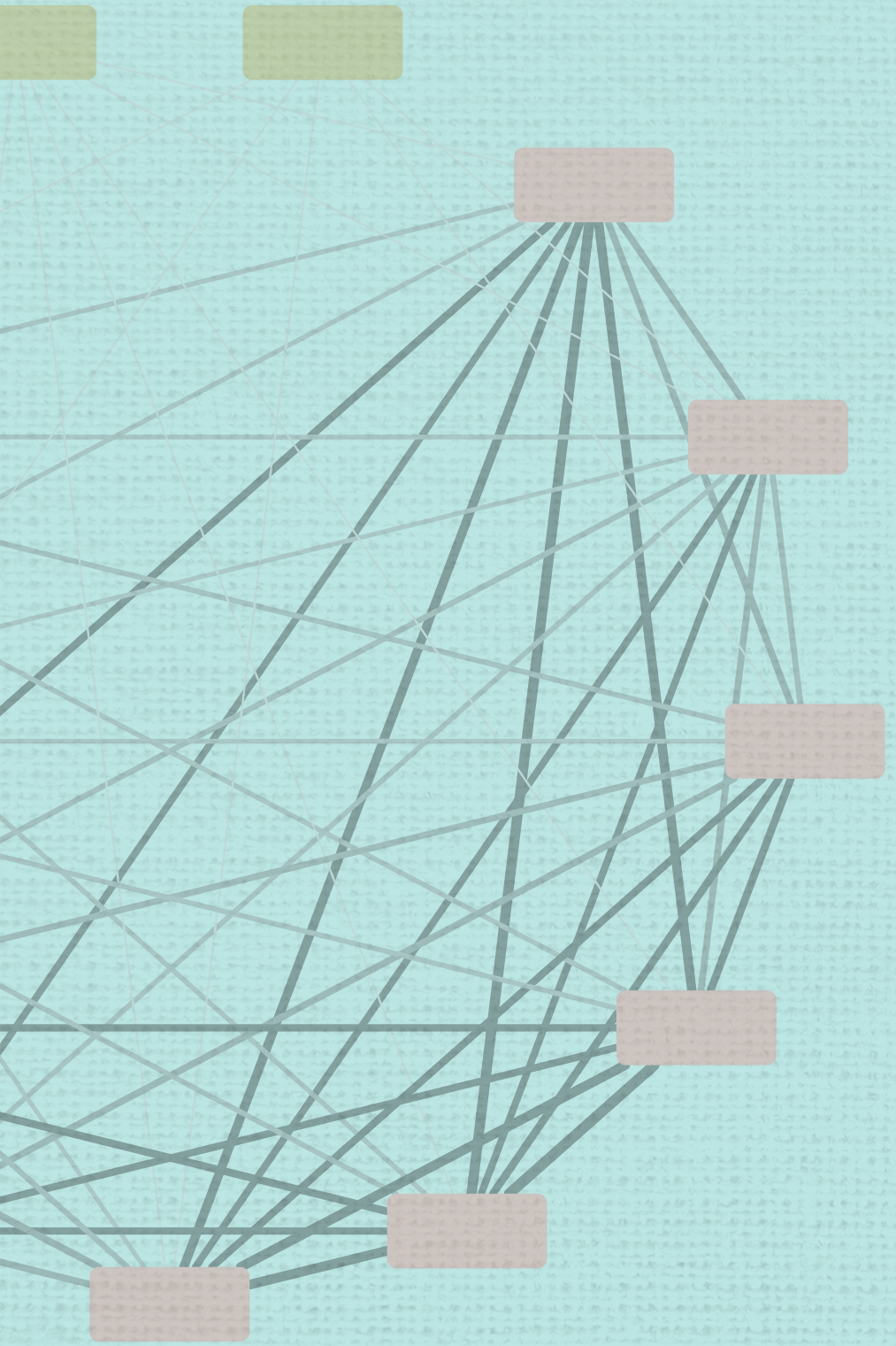

Summary

Cachexia is a common, serious and yet often under-recognised complication of cancer. Most obvious clinical manifestations of cachexia are loss of muscle mass, sometimes also including loss of fat mass and hence weight loss. This is driven by metabolic changes with or without a reduction in food intake, including elevated energy expenditure, excess catabolism and inflammation. Cachexia affects most patients with advanced stage cancer, with in some cancers more than 60% of all patients showing weight loss. Patients suffering from cachexia often also experience fatigue, muscle weakness and reduced response to cancer treatment. Conventional nutritional support is generally ineffective, the more so as anorexia often also develops in these patients. Together, these factors not only contribute to a reduced quality of life in these patients but are also assumed to be directly responsible for 20% of all cancer deaths. Thereby, aim of the current thesis was to get more insight into the processes driving this complex cachexia syndrome. Moreover, possible treatment targets and modalities were tested.

In view of the variation in degree and clinical manifestations of cancer cachexia, variations in body composition and relative amounts of lean or fat mass are commonly occurring. To investigate possible consequences for the pharmacokinetics of cancer medication, associations between body composition and side-effects of chemotherapeutic treatment were studied in chapter 2. This was performed in a cohort of colon cancer patients receiving a treatment regimen consisting of capacetabine and oxaliplatin. Most patients [90%] experienced some side-effect during their treatment. Reductions in the dose of oxaliplatin were most common, while capecitabine treatment was usually not reduced. In contradiction to literature, we found that the amount of muscle mass, both absolute and relative to fat mass, was not associated with side-effects. However, we did find that the amount of fat infiltration in muscle tissue was associated with having more side-effects of the chemotherapy. Fat infiltration in muscle is a marker of poor muscle health. Therefore, our findings suggest that in our study population, not muscle quantity, but muscle functional quality is associated with side-effects of chemotherapy treatment.

The complexity of the cachexia syndrome has thus far severely hampered the development of effective treatment regimens. General consensus exists that treatment should consist of a multi-modal program including nutrition, exercise and drugs. However, research on different treatment options in patients is difficult because of their situation and vulnerability. Therefore, animal studies are commonly used. In chapter 3 and 4, we studied effects of two treatment modalities for cachexia: nutrition (chapter 3) and training (chapter 4). To this end, we used the cancer cachexia model where C26 tumour cells are injected in the flank of a mouse to induce tumour development.

In chapter 3, we studied the effects of a specific nutritional combination, high in protein, leucine and fish-oil, on circulating calcium levels in the C26 model. We found that

the tumour increased calcium levels in the blood plasma. Moreover, plasma hypercalcemia was correlated with carcass mass and multiple organ masses. The specific nutritional combination was able to reduce the hypercalcemia. Subsequently, potential mechanisms underlying this effect were studied. Here, we focussed on the production of parathyroid hormone related protein (PTHrP) by the tumour cells that were used for the induction of cancer in the animals. PTHrP is a molecule well-known for its capacity of inducing hypercalcemia. We found that exposing the cells to the fish-oil component docosahexaenoic-acid (DHA) reduced their PTHrP production. Moreover, we also found that this was independent of cyclooxygenase-type 2 (COX-2), an enzyme involved in both DHA and PTHrP regulation. These results indicate that fish-oil, and specifically DHA, could be an important treatment component for reducing tumour-induced hypercalcemia.

In chapter 4, we investigated the possible effects of an easily accessible exercise treatment modality; whole body vibration training for a period of 19 days, C26 mice daily underwent 15 minutes of whole body vibration training. Our main finding was that in the tumour bearing group, training shifted the muscle transcriptome, measured using a micro array, towards a pattern comparable to that obtained in control mice. On *in-vivo* cachexia outcomes, we found that the vibration training was not able to reduce body weight loss or muscle loss. Moreover, minimal effects were found on muscle function of the *m. soleus.* Despite that no major visible effects on body composition were found, the shift in muscle transcriptome seems promising and more studies into whole body vibration training as treatment component for cachexia seem warranted.

In chapter 5, we studied to what extent the animal model that we used in chapter 3 and 4 mimics human cancer cachexia. This is important to assess the translatability of results from animal models to human patients. To do so, we compared publically available gene expression data, measured by micro-array or RNA-sequencing, in muscle tissue from different animal models with three human datasets. We found that there is no animal model outperforming other models in terms of similarity to the human datasets. Both on gene level and on pathway level, animal models not only displayed marked mutual and inter-study differences, but were also found to differ from human cachexia patients. Moreover, we found that on pathway level, different processes play different roles in different models. Unfortunately, due to the low number of human datasets, we were not able to draw firm conclusions based on this comparison. Therefore, upon appearance of additional well-described datasets, repetition of this comparison seems useful.

Within the field of cancer cachexia research, large amounts of data are increasingly being generated. Potential for future research is to focus more on sharing and integrating data. By doing so, more thorough insight can be gained in the complex mechanisms driving cachexia allowing the design of more specific and personalized treatment strategies.

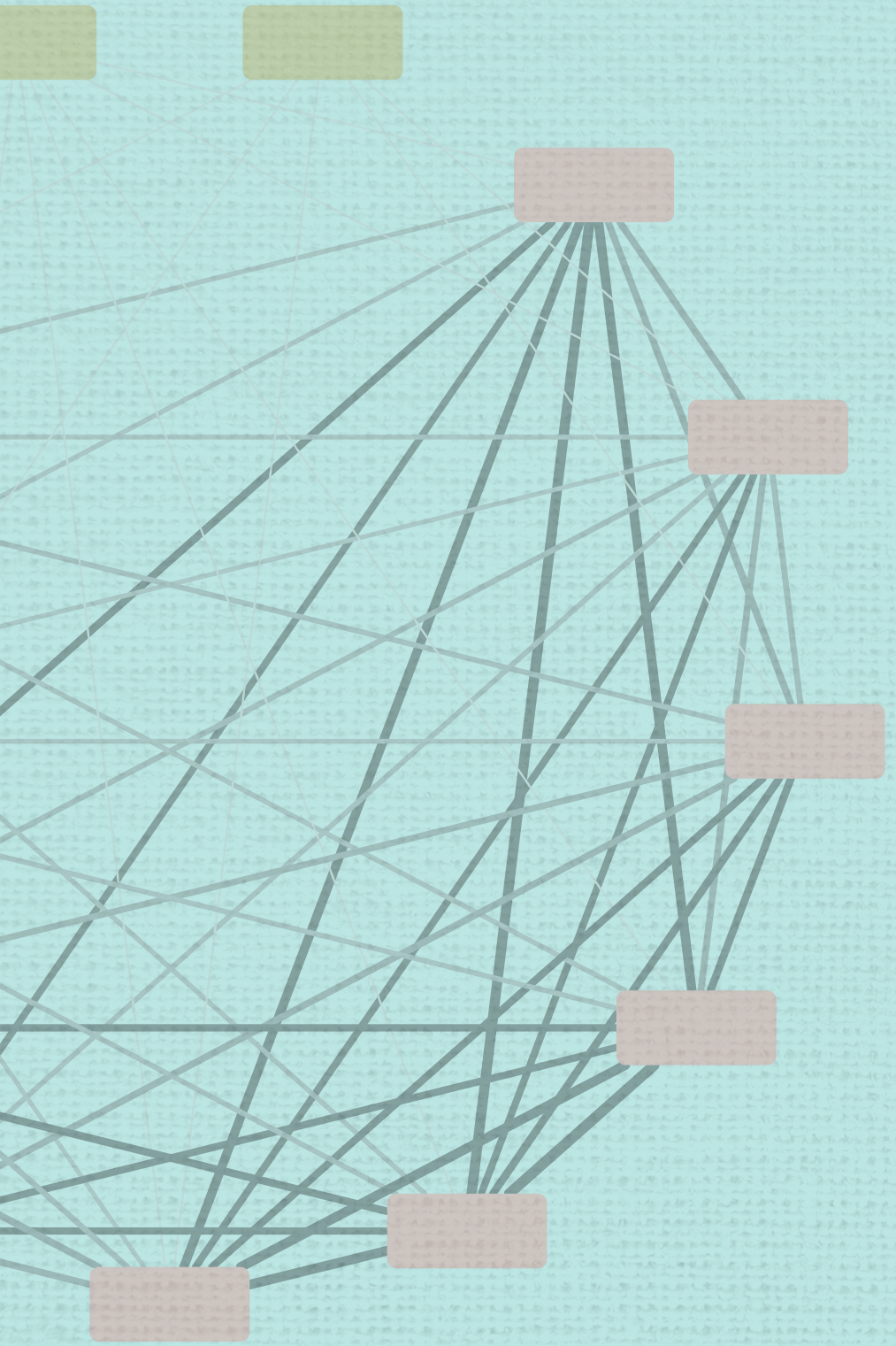

Acknowledgements

Na vijf en een half jaar is het dan eindelijk zo ver; mijn proefschrift is klaar! Vele e-mails, uren lezen, schrijven, lab werk, dierproeven, patiënten, uren coderen en meetings samengevat in een boekje. Cachexie is een complexe ziekte waar vele factoren een rol spelen en allerlei processen elkaar beïnvloeden. Voor het traject naar het vervolmaken van deze thesis was dat niet anders; een dierproef, een verhuizing op de WUR, mijn eerste kind, een humane trial, overleg met het ZGV, verhuizen naar een tijdelijke flat, overleg met Nutricia, een studie met publiek beschikbare data, nog een kind, een retrospectieve studie, verhuizen naar ons nieuwbouwhuis, een reorganisatie van de afdeling, overleg met TIFN, trouwen en een studie met data van een oude studie aangevuld met nieuwe labdata. In al deze processen heb ik hulp gekregen van heel veel mensen die ik hier graag wil bedanken.

Ten eerste wil ik al mijn begeleiders bedanken. **Klaske**, hartelijk dank voor je vertrouwen, de dagelijkse begeleiding en alle tijd en energie die je in mijn promotietraject hebt gestoken. Zonder jouw netwerk was dit breed opgezette project niet zo'n succes geweest. **Renate**, bedankt voor alle hulp bij het contact met het ziekenhuis voor de retrospectieve studie en het opzetten van de humane studie. **Ellen**, dank voor alle hulp bij het opzetten van de studies, het schrijven van de artikelen en je altijd prettige en opbouwende kritiek. **Renger**, jouw energie en enthousiasme heeft mij enorm geholpen dit project tot een succes te maken. De open en vertrouwde sfeer die jij weet te creëren in de vakgroep heb ik als zeer prettig ervaren.

Ook wil ik alle overige leden van de promotiecommissie bedanken. **Sander**, **Carla**, **Ramon** en **Richard**, bedankt dat jullie tijd wilden maken om mijn proefschrift te lezen en mijn verdediging bij te wonen.

Alle overige leden van de Nutrition and Pharmacology vakgroep, hartelijk dank voor jullie input op mijn werk. **Nikkie** en **Jvalini**, jullie hebben mij zeer goed op weg geholpen in de eerste stappen van mijn promotieonderzoek. **Jocelijn**, **Michiel** en **Ya**, dank voor alle input op mijn in vitro werk. **Wout**, dank voor jouw enthousiasme en je brede blik op de wetenschap. **Paulien**, ondanks de afstand heb ik toch erg veel aan jouw korte bezoeken aan Wageningen gehad om te sparren over het cachexie-onderzoek. **Ian** en **Tessa**, leuk om samen met jullie onder de vleugels van Renger te werken. Ik wens jullie nog veel succes in het afmaken van jullie promotie.

Iedereen die onderzoek doet naar spieren en mij regelmatig heeft vergezeld bij de muscle meetings hartelijk dank voor jullie hulp, betrokkenheid en input. **Mike**, **Pim**, **Rieneke**, **Marco**, **Lisette**, **Pol**, **Ellen**, allemaal nog veel succes verder met het belangrijke onderzoek naar spieropbouw en -afbraak!

Harm, hartelijk dank voor alle hulp bij de retrospectieve studie en het samen opzetten en schrijven van het retrospectieve paper. **Guido**, **Roland** en **Mark**, zonder jullie was het mij nooit gelukt om de genexpressie studie zo breed op te zetten. Hartelijk dank voor al jullie support!

Iedereen die aan de COLON-studie heeft gewerkt en mij heeft geholpen met de retrospectieve studie en het opzetten van de COMUNEX hartelijk dank! **Henriette**, zonder jouw hulp bij de METC-aanvraag en alle administratieve rompslomp die hierbij kwam kijken was de COMUNEX nooit goedgekeurd.

Dank ook voor alle hulp die ik vanuit het **ZGV** heb mogen ontvangen en de gastvrijheid voor het doen van onderzoek binnen het ziekenhuis. **Annebeth**, bedankt voor de hulp bij de retrospectieve studie. **Dik**, **Tjarda**, **Flip**, **Roland** en alle fysiotherapeuten die mij hebben geholpen met de COMUNEX, zonder jullie was deze studie nooit van de grond gekomen.

Vooral in het begin van mijn promotietraject heb ik erg veel gehad aan alle hulp en input vanuit **Nutricia**. **Yvette**, **Sjors**, **Bart**, **Joyce**, **Marion** en **Ardy**, heel erg bedankt voor alle hulp met de dierproef, het opzetten van de humane studie en de retrospectieve studie.

Alle kamergenootjes die mijn promotietraject in zowel De Valk als in het Helix wat aangenamer hebben gemaakt. Hartelijk dank voor alles! **Shoreh**, **Karin** en **Jenny**, dank voor de leuke tijd op de Valk met de altijd aanwezige zoetigheid en de sushi lunch! **Iris** en **Inge**, dank voor jullie gezelligheid op de kamer in het Helix. **Antwi**, thanks for all the nice talks about life, discussions about science and your always joyful and open presence!

Merel, **Maarten**, **Nadia**, **Carla**, **Frans**, **Bob** en **Saskia**. Hartelijk dank voor al jullie inspanning en hulp bij het verzamelen en analyseren van de data voor dit proefschrift. In het begeleiden van studenten heb ik altijd gezocht naar een mutual benefit en volgens mij is dat met jullie allemaal goed gelukt. Ik hoop dat jullie inzicht hebben gekregen in de leuke en minder leuke kanten van de wetenschap.

Natuurlijk wil ik ook mijn paranimfen hartelijk bedanken! **Mieke**, zonder de wekelijkse koffiemomentjes met jou had ik het niet vol gehouden. Iedere week samen spuien over hoe het allemaal beter moet was erg fijn. Maar ook jouw heerlijk nuchtere blik op zaken, je luisterende oor, oprechte interesse en coaching hebben mij erg geholpen! **Miranda**, jammer dat je pas zo laat in mijn promotie traject begonnen bent. Door de grote inhoudelijke overlap tussen onze promotietrajecten had ik aan jou voor het laatste stuk van mijn promotie nog een maatje om over het onderzoek te praten. Ook vond ik het fijn in jou iemand te vinden die het promoveren ook wat meer weet te relativeren; een promotieplek is ook gewoon een baan.

Al mijn nieuwe collega's van **Experience Data**, bedankt voor het warme bad waar ik in terecht ben gekomen. Ik voelde me meteen helemaal thuis in het bedrijf en zie erg uit naar de toekomst met jullie!

Guido (Weide), mijn bewegingswetenschappen-maatje! Bijna tegelijk gaan we nu promoveren. Jij net een weekje eerder dan ik. Waar ik de wetenschap de rug toe heb gekeerd ga jij wel verder als postdoc in Leuven. De wetenschap mag heel blij met jou zijn! Jouw doorzettingsvermogen en onvoorwaardelijke trouw zijn een groot goed. Vergeet niet om ook af en toe voor jezelf te kiezen.

Herman, **Inge**, **Anne**, **Naomi** en **Matt**, ik had me geen leukere schoonfamilie kunnen wensen! Ik voel me een volwaardig lid van de familie. Dank voor jullie support tijdens mijn promotietraject.

Pap, mam, dank voor alle liefde, aandacht en support. Jullie hebben mij altijd gesteund en ook voor ons klaar gestaan. Vele dagen gepland oppassen en vele dagen inspringen bij de opvang van Fieke en Pepijn als ze weer eens een kwaaltje van de crèche hadden meegenomen. Mede dankzij jullie hulp heb ik mijn promotietraject volgens plan en vooral binnen de tijd kunnen afronden.

Lieve **Laurie**, dank voor alle liefde afgelopen jaren! Ik vind het heerlijk om thuis te komen en over andere zaken dan werk te kunnen praten. Samen hebben we de afgelopen jaren veel meegemaakt. Trouwen, twee keer verhuizen en we hebben natuurlijk twee prachtige kindjes gekregen. Ik zou me geen leukere vrouw kunnen bedenken om dit allemaal mee te hebben meegemaakt! Ik heb super veel zin in de rest van onze toekomst samen!

Lieve **Fieke** en **Pepijn**, jullie kunnen dit nu nog niet lezen, maar jullie moet ik zeker ook bedanken. Promoveren is leuk, maar jullie zijn nog veel leuker! Jullie hebben ervoor gezorgd dat ik de hoofdzaken van de bijzaken kan scheiden en ik stress-vrij mijn promotietraject heb doorlopen.

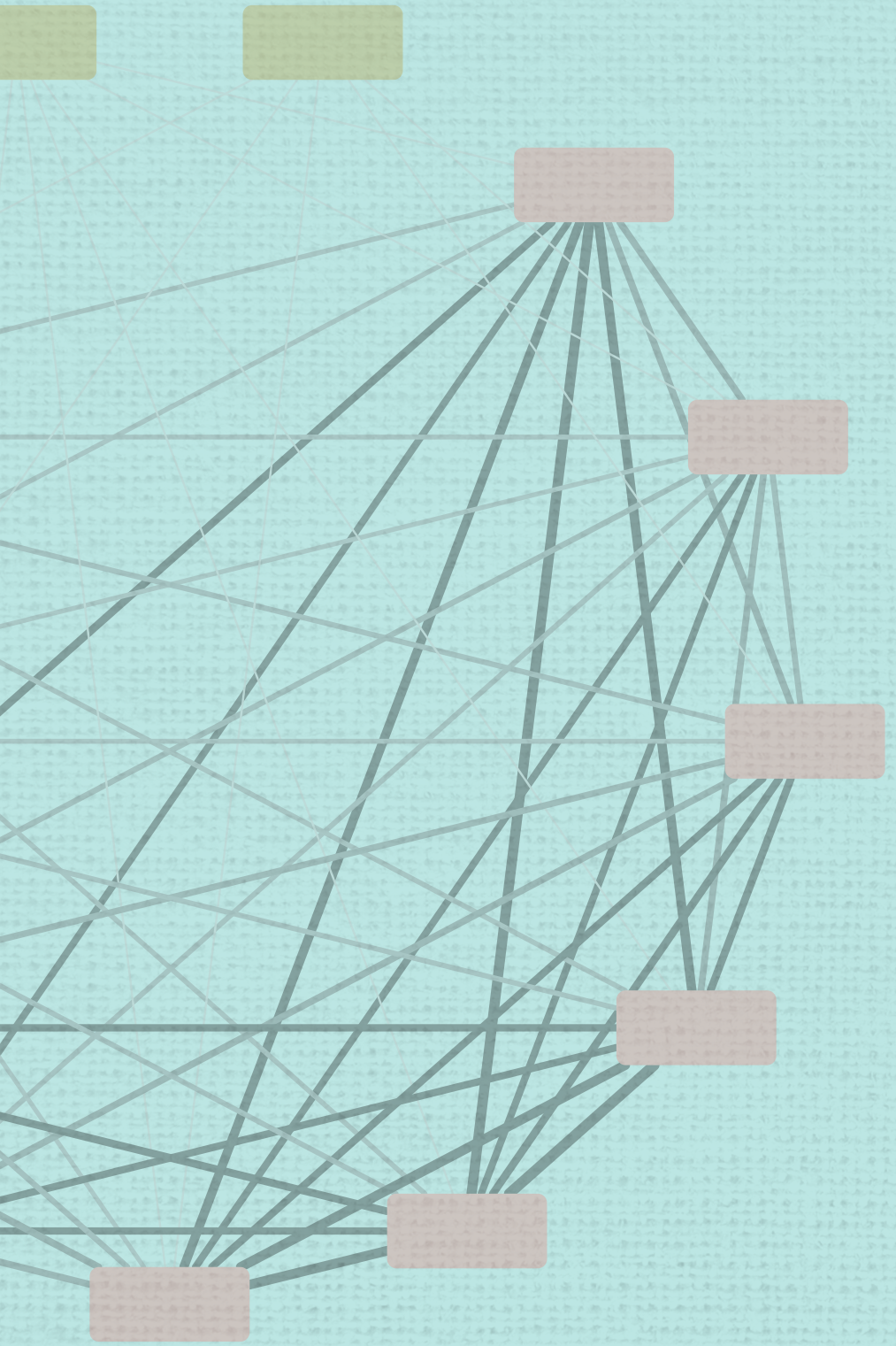

About the author

Biography

Rogier Leendert Charles Plas was born on the 18th of September 1987 in Amsterdam. He attended basic school in the Watergraafsmeer at the Watergraafsmeerse Schoolvereniging. In 1999, he started secondary school at the Barlaeus Gymnasium in Amsterdam. He combined the nature and health courses with extra courses in economics and modules in management and organisation and philosophy. During his time in secondary school he received a grant for the best profiel-werkstuk where he studied overweight and obesity in children. This is where his interest in human physique was already present. In 2006, after secondary school, Rogier moved to Utrecht to study chemistry. After one year he switched to studying Human Movement Sciences at the VU University in Amsterdam while still living in Utrecht. Between year one and two of the bachelor, he had a full time board position as treasurer of the Utrecht student sailing society Histos. During the third year of his bachelor, he did an internship where he studied the jumping capacity of a small primate (the common marmoset). After completion of the bachelor, Rogier continued the Research Master of Fundamental and Clinical Human Movement Sciences. There, his research was continued in the second year to further elucidate the extreme jumping performance of this small monkey. To do so, he studied the monkeys muscle characteristics both at the myology laboratory at the VU University and during a four month internship at the Manchester Metropolitan University. After completion of his master's degree, he briefly worked as a research assistant and assistant teacher at the VU University. His research during both bachelor and master intrigued Rogier to further study factors influencing muscle characteristics in both healthy and diseased state. Therefore, on the first of April 2014 (no joke) he started his PhD studying muscle wasting in cancer, also known as Cachexia. Working part-time and with a small contract extension, after almost five years, he completed his PhD of which the results are found in this thesis. On the first of April 2019 (again, no joke) he started a job as Data Scientist at Experience Data, a small data science consulting company in Utrecht.

List of Publications

Expected articles

Plas RLC, Van Dijk M, Dwarkasing JT, Van Gemerden F, Swarts HJM, Van Schothorst EM, Witkamp RF, Van Norren K. Whole-body-vibration training positively affects muscle transcriptome in C26 tumour bearing cachectic mice. *In preparation*

Plas RLC, Hooiveld G, Witkamp RF, Van Norren K. Relevance of cancer cachexia animal models – comparison of muscle whole genome gene expression in human and animal cachexia. *Submitted*

Published articles

Bobbert MF, **Plas RLC**, Weide G, Clairbois HEB, Hofman SO, Jaspers RT, Philippens IHCHM. Mechanical output in jumps of marmosets (Callithrix jacchus). *J Exp Biol* 2014;217:482–8.

Plas RLC, Degens H, Meijer JP, de Wit GMJ, Philippens IHCHM, Bobbert MF, Jaspers RT. Muscle contractile properties as an explanation of the higher mean power output in marmosets than humans during jumping. *J Exp Biol* 2015;218:2166–73.

Plas RLC, Norren K Van, Baar H Van, Aller C Van, Bakker M De, Botros N, Renger F. Side-effects related to adjuvant CAPOX treatment for colorectal cancer are associated with intermuscular fat area, not with total skeletal muscle or fat, a retrospective observational study. *J Cachexia, Sarcopenia Muscle - Clin Reports* 2018;3:2.

van der Ende M, Grefte S, **Plas R**, Meijerink J, Witkamp R, Keijer J, van Norren K. Mitochondrial dynamics in cancer-induced cachexia. *Biochim Biophys Acta - Rev Cancer* 2018;1870:137–50.

Plas RLC, Poland M, Faber J, Argiles J, Dijk M Van, Laviano A, Meijerink J, Witkamp RF, Helvoort A Van. A Diet Rich in Fish Oil and Leucine Ameliorates Hypercalcemia in Tumour-Induced Cachectic Mice. *Int J Mol Sci* 2019;20:1–12.

Overview of completed training activities

Discipline specific activities

- Laboratory Animal Science Course (Wageningen, 2014)
- World Congres Biomechanics (Boston, 2014)
- Dutch Nutritional Science Days (Deurne, 2014)
- Cachexia Conference (Paris, 2015)
- Cancer Cachexia Conference (Washington DC, 2016)
- Cachexia Conference (Rome, 2017)

General courses

- Advanced visualisation, integration and biological interpretation of -omics data (Wageningen, 2014)
- VLAG PhD week (Baarlo, 2014)
- Good Clinical Practice Course (Arnhem, 2014)
- Applied Statistics for VLAG (Wageningen, 2014)
- TIFN PhD day (Ede, 2015)
- Scientific Writing 2 (Wageningen, 2017)
- Big Data in the Life Sciences course (Wageningen, 2017)

Optional activities

- Preparation Research Proposal (Wageningen, 2014)
- TIFN expert meetings (Wageningen, 2014 – 2018)
- Weekly Nutrition and Pharmacology group meetings (Wageningen, 2014 – 2019)
- Muscle meetings (Wageningen, 2014 – 2018)
- MOOC: WageningenX: NUTR101x Introduction to Nutrition – Food for Health (Wageningen 2015)

Colophon

The research described in this thesis was financially supported by Wageningen University and Research, TI Food & Nutrition and Nutricia Research

Financial support from Wageningen University for the printing of this thesis is gratefully acknowledged.

Cover design by: Rogier Plas & Dennis Hendriks (Proefschriftmaken)

Layout: Rogier Plas

Printed by: Digiforce || Proefschriftmaken.nl